ABSTRACT

ENERGY BANDS, SURFACE STATES, AND RESONANT TRANSMISSION OF ELECTRONS IN FINITE ONE-DIMENSIONAL CRYSTALS

By

Willard M. Gersbacher, Jr.

The energies and wave functions of electrons in finite one-dimensional potentials designed to simulate various interesting physical situations have been calculated and are discussed. A general finite one-dimensional periodic potential was considered, and the form of the wave function in all regions of energy was established without recourse to the Bloch-Floquet theorem. Various types of potential terminations were considered, namely, step-function terminations at a potential minimum or maximum or at an arbitrary point in the end cell, and terminations by an arbitrary potential. The energy states (both band and surface) were calculated in each case and conditions were obtained which exhibit clearly how these states depend on the properties of the potential.

The band structure above the vacuum level was investigated by calculating the reflection coefficient for free electrons incident upon the periodic potential, for several types of terminations, and interesting relations between band-structures and tunneling were obtained. The resonant emission of electrons from metal

and non-metal surfaces covered with impurity layers was investigated for energies above the vacuum level by methods similar to those used in investigating the band structure.

In each area of investigation specific calculations were performed for Kronig-Penny type periodic potentials with appropriately selected parameters. The results of these calculations are summarized in a number of graphs.

ENERGY BANDS, SURFACE STATES, AND RESONANT TRANSMISSION OF ELECTRONS IN FINITE ONE-DIMENSIONAL CRYSTALS

By

Willard M. Gersbacher, Jr.

A THESIS

Submitted to
Michigan State University
in partial fulfillment of the requirements
for the degree of

DOCTOR OF PHILOSOPHY

Department of Physics

1970

To my wife and my parents

ACKNOWLEDGMENTS

I would like to thank Professor Truman O. Woodruff for suggesting the subject area of electronic properties of solids and for his help, encouragement, and patience throughout the course of this work.

For the financial support, I would like to thank the National Science Foundation and Michigan State University.

I would also like to thank Mrs. Frances Strachan for the help she has given in the typing of the final draft of the thesis.

Last, but not least, I would like to thank my wife, Victoria, for the typing and for the constant encouragement she has given me throughout.

TABLE OF CONTENTS

LIST OF TABLES

LIST OF FIGURES

INTRODUCTION

Progress in understanding surface phenomena has been slow, because physical and chemical processes at the surface are inherently more difficult to analyze than those in the bulk. The forces acting on the atoms at the surface are not symmetrical, as in the bulk, and consequently, the atoms are usually displaced from their ideal lattice positions. Moreover, just the fact that the surface constitutes an abrupt termination of the crystal lattice results in a deformation of the crystal potential -- its periodic nature is lost at the surface. This has far-reaching consequences for the electronic processes in the underlying region of the crystal close to the surface. At the same time, unsaturated forces from the surface atoms make them highly reactive towards various atoms outside the crystal. Thus, except when produced and maintained in a high-vacuum, the surface is covered by one or more layers of foreign matter, greatly increasing the complexity of an already difficult problem.

Although theoretical interest in electronic surface states has existed since the 1930's, little was accomplished because there was negligible technological motivation or opportunity for experimental confirmation. The great impetus for surface-state study came with the advent

of the transistor in the late 1940's. Since then further motivation has rapidly developed in conjunction with a variety of solid-state technologies.

Theoretical studies of the electrical properties of surfaces have progressed along two different lines. Tamm's[1] theoretical work, which treated a rather simplified model, was extended by Shockley[2] and by other workers to cover more general situations. It was shown that in covalent crystals, surface states may be associated with the unfilled orbitals or dangling bonds of the surface atoms, which may trap an electron at the surface. The historical development and a summary of the various theoretical techniques used to calculate surface states is given quite completely by Davison and Levine[3]. Suffice it to say that most of the calculations since 1950 have used a LCAO (or MO) type approach which was first introduced by Goodwin[4] in the late 1930's.

The second approach to this problem has been essentially phenomenological. Its aim was to determine the characteristics of the surface states by fitting a few specified parameters of the theory to experiment. The theory was completely analogous to that of bulk impurity states. This approach has proved extremely fruitful in characterizing the surface of several crystals, such as germanium and silicon. However, the correspondence is

still small between the experimentally observed surface states and the theoretically proposed Tamm or Shockley states.

It is the purpose of this paper to establish a better understanding of the Tamm- and Shockley-type surface states by showing specifically what parameters these states depend on, and how these states change as the parameters which specify the periodic potential are varied. Since most calculations which have been performed to date deal only with semi-infinite crystals, many interesting effects which are peculiar to finite crystals have been neglected; consequently, investigation of some of these effects seems appropriate. It was thought better to perform simplified exact calculations relating to several different questions concerning finite crystals and using several different types of boundary conditions in each case rather than to carry out a lengthy approximate calculation designed to illuminate only one aspect of real crystals. For simplicity, the one-electron scheme is used throughout, although it is probable that surface polarons and many-body interactions between surface states can occur. The justification for using this approximate scheme is that practically all the new concepts which have been introduced into physics through solid-state theory,

such as energy bands, effective mass, and Brilluoin zones, have been obtained via the one-electron approximation. However, what one achieves in simplicity of calculation by using this scheme one pays for with certain ambiguities which would not otherwise arise.

In the one-electron approximation, one attempts to represent all the various forces acting on a single electron by a single static field acting independently on each electron. This one field includes both the interactions between electrons and those between ions. The one electron Schrodinger equation, then, may be written as

$$\left[-\frac{\hbar^2}{2m}\nabla^2 + V_n(\underline{k},\underline{r})\right]\psi_n(\underline{k},\underline{r}) = E_n(\underline{k})\,\psi_n(\underline{k},\underline{r}).$$

The significance of the potential in this equation has been the subject of much study. In the one-electron scheme one assumes the existence of such an average potential acting on each electron. From the fact that (in the Born-Oppenheimer approximation)[5] the interaction potential has the periodicity of the lattice, one infers that V_n (k,r) has the same periodicity. What is usually done is to pick a physically plausible potential for each state and solve the one-electron problem. It is common practice to assume the same potential for all electron states (i.e. $V_n(k,r) = V(r)$). The accuracy of this approximation is at present

not known. Also, when a V (r) is determined in an ad hoc fashion it is clear that only those results which are reasonably insensitive to the choice can be trusted. Thus, one expects only qualitative agreement between calculation and experiment.

The technique used in this paper is based on the so-called cell-matching procedure. In this technique, the assumed crystal periodic potential is divided into cells, a cell being one period of the periodic potential, and solutions of Schrodinger's equation are found in each cell. By connecting the solutions in each cell continuously to those in the next cell, a wave function is constructed which is across the part of the crystal in which the potential is perfectly periodic. This wave function is then matched to the solution of Schrodinger's equation in the surface region to form a wave function for the crystal as a whole.

To solve any problem by this procedure in three dimensions is quite difficult, since the wave function must be matched continuously from cell to cell at an infinite number of points on the cell boundaries. The LCAO (or MO) methods are better suited for this type of problem, although they are not conceptually as clear. Since the interest here will be in clarifying various qualitative questions concerning finite crystals and not in quantitative results, only one-dimensional situations will be

considered. Although this limitation may lead to neglect of many interesting effects, it is believed that most of the results obtained will have important analogs in three dimensions.

In Section I, the wave function for the periodic part of the crystal potential is constructed for any value of energy without recourse to the Bloch-Floquet theorem. Section II establishes the conditions under which surface states may exist for the Tamm and Shockley type potential terminations. Section III shows how to apply the principles discussed in Section II to the Kronig-Penney periodic potential with Tamm- and Shockley-type terminations. In Section IV, the effects of termination at an arbitrary point in the end cell are considered. Section V deals with the band structure above the vacuum level by investigating the diffraction of normally incident free electrons from the surface of a finite periodic potential. Section VI deals with a related phenomenon: resonant electron emission from crystals covered with several layers of adsorbed foreign atoms.

SECTION I

DETERMINATION OF THE FORM OF THE WAVE FUNCTIONS AND ENERGY BANDS FOR A FINITE PERIODIC POTENTIAL

A suitable starting point for the calculation of the energy bands and wave functions for a finite crystal, is described in an article by James[6]. In this article, James gives a particularly clear and elementary derivation of the band structure of permitted energy levels for an infinite crystal. Although he considers only infinite crystals, he discusses the properties of all solutions of the Schrodinger equation, including those which do not satisfy the infinite-crystal boundary conditions, namely, the solution in the forbidden bands. He also introduces a new parameter $\sigma(E)$, which, like the effective momentum $p(E)$, depends upon and partially characterizes the periodic potential. The essential reason for using James' results is that they may easily be applied to the case of finite crystals. This is because, unlike most derivations of the form of the wave functions for periodic potentials, James does not rely on the Bloch-Floquet theorem, which was derived for the case of an infinitely extended periodic potential. The manner in which the wave functions are constructed leaves no doubt

as to the form of the wave functions in all regions of energy.

We shall, in summarizing and extending this work, make the necessary modifications for the finite crystal. Since we are modifying James' results, we shall give an explanation of the various steps of James' derivation which must be changed, and refer the reader to the article when the analysis for the infinite crystal can be directly carried over to the finite crystal. The results which follow are valid for a general one-dimensional crystal, containing a finite number of atoms each of which is represented by a potential well whose shape is symmetrical about the center of the atom but is otherwise arbitrary. The specification of a potential which is symmetrical about the center of the atom is for mathematical convenience rather than a necessity since the results which follow may be altered to include potentials which can not be so defined.[7]

We consider the time independent Schrodinger equation for a particle of mass m with energy E in a periodic potential V(x),

$$-\frac{\hbar^2}{2m}\frac{d^2}{dx^2}\psi(x) + V(x)\psi(x) = E\psi(x), \qquad (1.1)$$

where V(x) is periodic with period a, and is defined only

for the range $0 \leq x \leq Na$ by

$$V(x) = V(\bar{x} + na) \quad , \quad \begin{cases} n = 0, 1, \ldots, N-1, \\ 0 \leq \bar{x} \leq a. \end{cases} \qquad (1.2)$$

In the region where $x > Na$ and $x < 0$, we shall, for the moment, leave the potential unspecified. The range of x will be sub-divided into periods or cells of length a, such that in the n-th cell

$$na \leq x \leq (n+1)a \quad , \quad n = 0, 1, \ldots, N-1. \qquad (1.3)$$

We choose the origin of our coordinate system so that the potential in each cell is symmetrical about the center of the cell.

We now fix our attention on the zeroth cell $0 \leq x \leq a$, and on a particular E. Since Schrodinger's equation is of second order, it will have two linearly independent solutions. For the potential as defined above, the solutions considered are two real functions which we shall call $g(E;x)$ and $u(E;x)$. The specification of $g(E;x)$ and $u(E;x)$ is completed by requiring them to be symmetric and antisymmetric, respectively, about the center of the cell. That is,

$$g_0(E) \equiv g(E;0) = g(E;a), \tag{1.4a}$$

$$g_0'(E) \equiv g'(E;0) = -g'(E;a), \tag{1.4b}$$

$$u_0(E) \equiv u(E;0) = -u(E;a), \tag{1.4c}$$

$$u_0'(E) \equiv u'(E;0) = u'(E;a). \tag{1.4d}$$

For convenience, we shall normalize these functions so that

$$\begin{aligned} g(E;a/2) &= 1 \ , \ g'(E;a/2) = 0 \ , \\ u(E;a/2) &= 0 \ , \ u'(E;a/2) = 1 \ . \end{aligned} \tag{1.5}$$

Since solutions to Schrodinger's equation have a constant Wronskian, we then have, for any x,

$$\begin{aligned} W\{g(E;x), u(E;x)\} &= 1 \ , \\ &= g(E;x)u'(E;x) - g'(E;x)u(E;x). \end{aligned} \tag{1.6}$$

It should be recalled that a necessary condition for the linear independence of a set of solutions is that their Wronskian be non-zero. This fact will be used later.

These functions need only be defined for the range $0 \leq x \leq a$. Since the potential has the same form in every

cell, g(E;x-na) and u(E;x-na) will be the independent solutions in the nth cell. Within each cell, an arbitrary solution ψ_n of the wave equation can be expressed as an appropriate linear combination of the corresponding cell solutions:

$$\psi_n(x) = \alpha_n g(E;x-na) + \beta_n u(E;x-na), \qquad (1.7)$$
$$\begin{cases} na \le x \le (n+1)a, \\ n = 0, 1, 2, \cdots, N-1. \end{cases}$$

These cell wave functions and their derivatives could now be matched at the boundaries of each cell to form a continuous wave function for the entire crystal. However, the coefficients of our independent solutions depend on the cell index and vary from cell to cell in a complicated manner, making interpretation of the form of the wave function difficult. This difficulty of interpretation has been eliminated by James, who defines a new set of linearly independent cell solutions. Each of these new solutions is itself a linear combination of g(E;x) and u(E;x), the combination in each case being such that the new solutions are linearly independent. He defines these so-called self-matching solutions so that the dependence on the cell index is incorporated in each independent solution in such a way as to make each independent solution in the n-th cell connect smoothly on to the same independent solution in the next cell. With

the aid of the following definitions[8]

$$\rho \equiv \rho(E) = (g_0'/g_0)/(u_0'/u_0), \tag{1.8a}$$

$$\sigma_\pm \equiv \sigma_\pm(E) = \mp (u_0'/u_0)\,\rho^{\frac{1}{2}}, \tag{1.8b}$$

$$\gamma_\pm \equiv \gamma_\pm(E) = \left(\frac{1 \pm \rho^{\frac{1}{2}}}{1 \mp \rho^{\frac{1}{2}}}\right), \tag{1.8c}$$

$$f_\pm(E;X) = \frac{1}{(1 \mp \rho^{\frac{1}{2}})}\left(\frac{g(E;x)}{g_0} \mp \frac{u(E;x)}{u_0}\rho^{\frac{1}{2}}\right), \tag{1.8d}$$

James is able to write the independent solutions as

$$\psi_\pm(x) = \gamma_\pm^n f_\pm(E;X-na), \begin{cases} na \le X \le (n+1)a, \\ n = 0, 1, \ldots, N-1. \end{cases} \tag{1.9}$$

The significance of $\sigma_\pm$, $\gamma_\pm$ is made clear by the relations

$$\sigma_\pm = \frac{f_\pm'(E;0)}{f_\pm(E;0)} = \frac{f_\pm'(E;a)}{f_\pm(E;a)}, \tag{1.10}$$

$$\gamma_\pm = \frac{f_\pm(E;a)}{f_\pm(E;0)}. \tag{1.11}$$

It should be noted that the quantity $-(u_0'/u_0)\,|\rho|^{\frac{1}{2}}$ may be thought of as an effective wave number since it reduces in the free electron limit to the wave number $k = \sqrt{2mE/\hbar^2}$.

The general solution to Schrodinger's equation will be a linear combination of these two linearly independent solutions,

$$\psi(x) = C_+\psi_+(x) + C_-\psi_-(x), \qquad (1.12)$$

where now C_+ and C_- are constants independent of the cell index. The nature of $\psi_+(x)$ and $\psi_-(x)$ will depend to a large degree on the value of $\rho(E)$. To obtain an idea of how $\rho(E)$ will vary, it is necessary to examine $g_o(E)$, $g'_o(E)$, $u_o(E)$, $u'_o(E)$.

For very low values of E ($E < V_{min}$) the solutions g(x), u(x) are damped and we must have g_o, $u'_o > 0$, and g'_o, $u_o < 0$. As E increases, g(x) and u(x) become oscillatory, and then oscillate with decreasing wavelength; it follows that g_o, g'_o, u_o, u'_o, oscillate between positive and negative values, as E increases. According to James, the order in which the quantities under consideration vanish is

$$g_o', (g_o, u_o'), (g_o', u_o), (g_o, u_o'), (g_o', u_o), \ldots . \qquad (1.13)$$

The order (within a parenthesis) of the zeroes of g_o and u_o' or of g_o' and u_o is not fixed, but varies with the character of the potential considered. These zeroes may in fact coincide. The order in which these quantities go to zero has

important consequences for the existence of surface states, as we shall see in the next section.

It follows from the above considerations that ρ varies from $-\infty$ to $+\infty$, depending on the values of g_o, g_o', u_o, u_o'. A typical plot of ρ versue E is shown in Figure 1.1. Notice that the form which ρ takes allows a natural separation of the graph into three regions, depending on whether $\rho < 0$, $0 < \rho < 1$, or $\rho > 1$. It should be noted that this graph depends only upon the values of g_o, g_o', u_o, u_o'; that is, the graph depends <u>only</u> upon the potential in one cell, and does not depend upon the number of cells or the type of termination at either end of the crystal. As we shall see below, this plot determines what we shall call the band structure of the cell. The term band structure, as used here, refers to the structure of this plot of ρ versus E for a single cell solution. The fact that several identical cells are joined together means that the band structure is constant across the identical cells. Thus, instead of associating a band structure with a periodic potential, we can in fact associate a band structure with one cell. The case of a periodic potential can then be treated as a special case of combining the individual cell band structures.

We now investigate the dependence of the ψ's on ρ in the various regions of interest. For each case, the

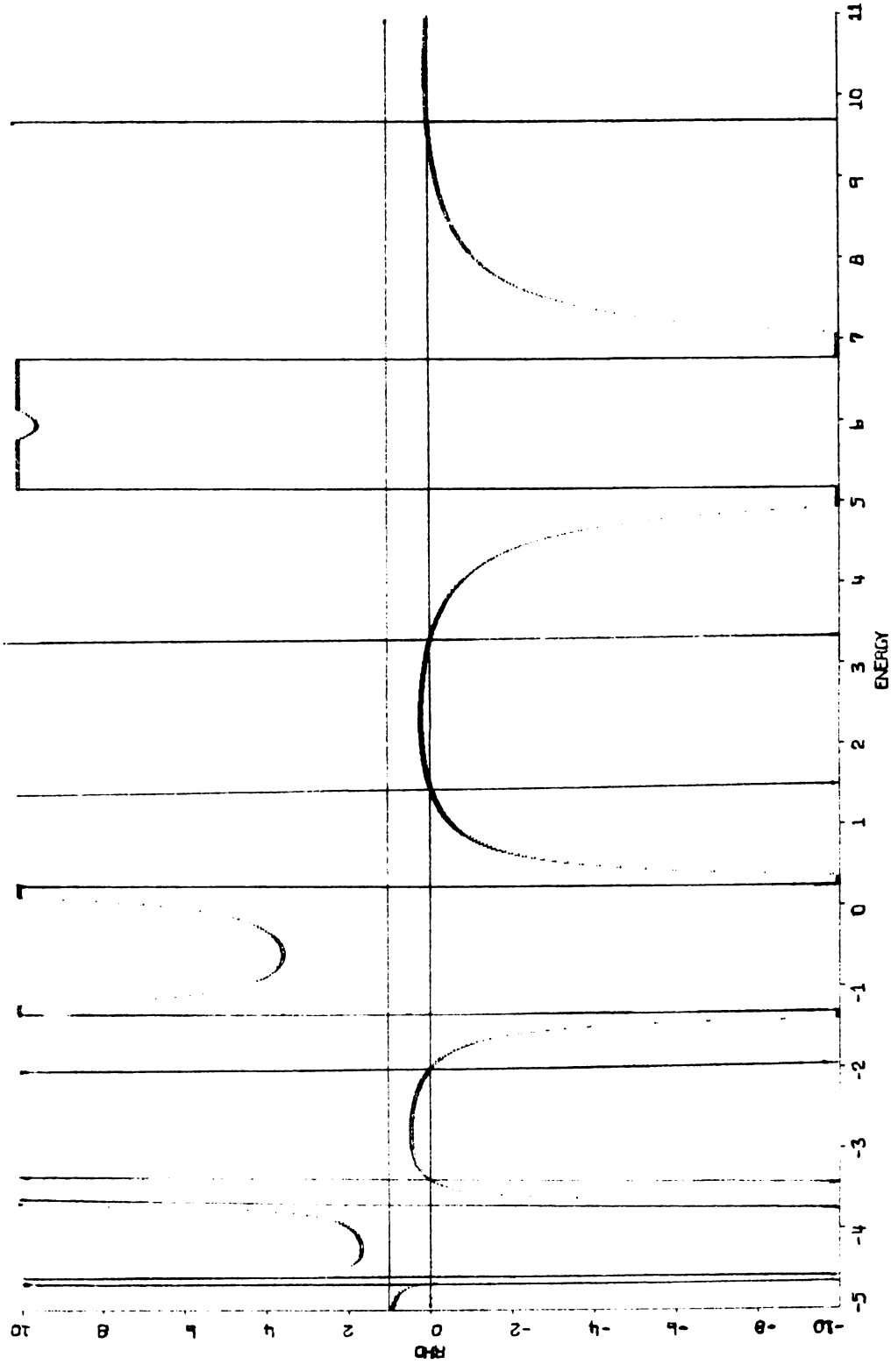

Figure 1.1. Determination of the energy band regions.

range of x and the value of n will be specified by

$$na \leq x \leq (n+1)a, \quad n = 0, 1, 2, \ldots, N-1.$$

Case 1. $\rho = \pm\infty$.

In this case, r_+ and r_- are equal to -1, $\sigma_+ = \sigma_- = 0$ if $u_0' = 0$, and $\sigma_+ = \sigma_- = \pm\infty$ if $g_0 = 0$. Because of the normalization, it is necessary to construct two new independent solutions, which remain finite:

$$\psi_1(x) = \left(\frac{\psi_+(x) + \psi_-(x)}{2}\right), \quad \psi_2(x) = \left(\frac{\psi_+(x) - \psi_-(x)}{2\sigma}\right). \tag{1.14}$$

Letting u_0' go to zero in these combinations, we obtain in the limit

$$\psi_1(x) = (-1)^n \frac{u(x-na)}{u_0}, \tag{1.15a}$$

$$\psi_2(x) = (-1)^n\left[(2n+1)g_0 u(x-na) - u_0 g(x-na)\right]. \tag{1.15b}$$

For $g_0 = 0$, we find,

$$\psi_1(x) = (-1)^n\left[(2n+1)u_0' g(x-na) - g_0' u(x-na)\right], \tag{1.16a}$$

$$\psi_2(x) = (-1)^n \frac{g(x-na)}{g_0'}. \tag{1.16b}$$

In both cases, one of the solutions repeats itself exactly in each cell, except for a sign change, and the other solution increases linearly in amplitude as x increases.

Case 2. $\rho < 0$.

In this case, $\rho^{\frac{1}{2}}$ is imaginary and $f_{\pm}$, $\psi_{\pm}$ are complex. We may define

$$\rho^{\frac{1}{2}} = \pm i\,|\rho|^{\frac{1}{2}}. \tag{1.17}$$

Let us for the moment use the positive sign but keep in mind that the negative sign is also acceptable. Then

$$r_+ = \left(\frac{1 + i\,|\rho|^{\frac{1}{2}}}{1 - i\,|\rho|^{\frac{1}{2}}}\right) , \quad r_- = \left(\frac{1 - i\,|\rho|^{\frac{1}{2}}}{1 + i\,|\rho|^{\frac{1}{2}}}\right). \tag{1.18}$$

Since $r_+^* = r_-$, $r_-^* = r_+$ and $r_+ r_- = 1$, we may <u>define</u> a constant k by the relations,

$$r_+ = e^{ika} \quad , \quad r_- = e^{-ika}. \tag{1.19}$$

Then, characterizing our wave functions by k, we have

$$\psi_{+k}(x) = e^{ikna} f_+(E; x - na), \tag{1.20a}$$

$$\psi_{-k}(x) = e^{-ikna} f_{-}(E; x-na). \qquad (1.20b)$$

We may define two new functions by

$$P_{+k}(x) = e^{-ik(x-na)} f_{+}(E; x-na), \qquad (1.21a)$$

$$P_{-k}(x) = e^{ik(x-na)} f_{-}(E; x-na). \qquad (1.21b)$$

It may easily be verified that

$$P_{+k}(x+a) = P_{+k}(x), \quad P_{-k}(x+a) = P_{-k}(x). \qquad (1.22)$$

Therefore, we may rewrite our independent solutions as

$$\psi_{+k}(x) = e^{ikx} P_{+k}(x), \qquad (1.23a)$$

$$\psi_{-k}(x) = e^{-ikx} P_{-k}(x), \qquad (1.23b)$$

where $P_{+k}(x)$, $P_{-k}(x)$ are periodic functions with period a. Now we see that if the sign of $\rho^{\pm}$ is chosen negative, one need only change ψ_{+k} to ψ_{-k} and ψ_{-k} to ψ_{+k}. These solutions are of the familiar Bloch form and do not change in magnitude from cell to cell. They may, however, change by a complex phase factor.

Case 3. $\rho = 0$.

In this case, $r_+ = r_- = 1$, $\sigma_+ = \sigma_- = 0$ if $g'_0 = 0$, and $\sigma_+ = \sigma_- = \pm\infty$ if $u_0 = 0$. Constructing new solutions in the same way as for Case 1, we have for $g'_0 = 0$:

$$\psi_1(x) = \frac{g(x-na)}{g_0}, \tag{1.24a}$$

$$\psi_2(x) = g_0 u(x-na) - (2n+1) u_0 g(x-na). \tag{1.24b}$$

Similarly, for $u_0 = 0$, we obtain:

$$\psi_1(x) = u'_0 g(x-na) - (2n+1) g'_0 u(x-na), \tag{1.25a}$$

$$\psi_2(x) = \frac{u(x-na)}{u'_0}. \tag{1.25b}$$

These solutions behave in the same way as do those for Case 1 except that these solutions do not have a sign change in going from cell to cell.

Case 4. $0 < \rho < 1$.

In this case, $\rho^{\frac{1}{2}}$, $r_\pm$, $f_\pm$, $\psi_\pm$ are all real. Since $0 < r_- < 1$, $1 < r_+ < +\infty$ and $r_+ r_- = 1$, we may define a positive constant K by the relations

$$r_+ = e^{ka}, \quad r_- = e^{-ka}. \tag{1.26}$$

Then,

$$\psi_{+k}(x) = e^{kna} f_+(E; x-na), \qquad (1.27a)$$

$$\psi_{-k}(x) = e^{-kna} f_-(E; x-na). \qquad (1.27b)$$

In the same way as for $\rho < 0$, we define periodic functions $P_{+K}(x)$ and $P_{-K}(x)$ by

$$P_{+k}(x) = e^{-k(x-na)} f_+(E; x-na), \qquad (1.28a)$$

$$P_{-k}(x) = e^{+k(x-na)} f_-(E; x-na), \qquad (1.28b)$$

where $P_{\pm k}(x+a) = P_{\pm k}(x)$ as may be verified. Then our two independent functions are

$$\psi_{+k}(x) = e^{kx} P_{+k}(x), \qquad (1.29a)$$

$$\psi_{-k}(x) = e^{-kx} P_{-k}(x). \qquad (1.29b)$$

ψ_{+k} increases exponentially in magnitude with increasing x, while ψ_{-k} decreases exponentially.

It should be noted that the case $\rho = 1$ never occurs since this would imply that $g_0'/g_0 = u_0'/u_0$ or $g_0 u_0' - g_0' u_0 = 0$, which would mean that g(x)

and u(x) are not linearly independent.

Case 5. $\rho > 1$.

In this case $-1 < r_- < 0$, $-\infty < r < -1$, and $f_\pm$, $\psi_\pm$, $\rho^{\pm}$ are all real. In view of the ranges of r_+ and r_- and the relation $r_+ r_- = 1$, it is convenient to define a constant K by

$$r_+ = -e^{+ka}, \quad r_- = -e^{-ka}. \tag{1.30}$$

Then

$$\psi_{+k}(x) = (-1)^n e^{nka} f_+(E; x-na), \tag{1.30a}$$

$$\psi_{-k}(x) = (-1)^n e^{-nka} f_-(E; x-na). \tag{1.30b}$$

Defining new functions

$$G_{+k}(x) = (-1)^n e^{-k(x-na)} f_+(E; x-na), \tag{1.31a}$$

$$G_{-k}(x) = (-1)^n e^{+k(x-na)} f_-(E; x-na), \tag{1.31b}$$

it is easily seen that

$$G_{\pm k}(x+a) = -G_{\pm k}(x), \quad G_{\pm k}(x+2a) = G_{\pm}(x), \tag{1.32}$$

so that the $G_{\pm\, K}(x)$ are periodic functions with period 2a.

We then have as our independent solutions

$$\psi_{+k}(x) = e^{kx} G_{+k}(x), \tag{1.33a}$$

$$\psi_{-k}(x) = e^{-kx} G_{-k}(x). \tag{1.33b}$$

The magnitudes of ψ_{+k} and ψ_{-k} behave as in Case 4.

For purposes of clarity in later sections, we shall refer to energy regions in which the wave function is of the form

$$\psi(x) = C_{+k} e^{ikx} P_{+k}(x) + C_{-k} e^{-ikx} P_{-k}(x), \tag{1.34a}$$

as pass bands (P.B.) and energy regions in which the wave function is of the form

$$\psi(x) = C_{+k} e^{kx} P_{+k}(x) + C_{-k} e^{-kx} P_{-k}(x), \tag{1.34b}$$

$$\psi(x) = C_{+k} e^{kx} G_{+k}(x) + C_{-k} e^{-kx} G_{-k}(x) \tag{1.34c}$$

as attenuation bands (A.B.).

SECTION II

TERMINATION OF THE PERIODIC POTENTIAL - DETERMINATION OF THE CONDITIONS FOR BAND AND SURFACE STATES

We shall now consider various boundary conditions which may be imposed at either end of the periodic potential. The type of boundary condition we wish to impose will, of course, depend upon the specific physical phenomena we are trying to represent. For example, near the surface the atoms do not have symmetrical forces acting on them as in the bulk. This results in a deviation from perfect periodicity, which may take several different forms. One of these deviations might be an increase in a basic lattice translation, the closer to the surface the atom is situated. Another deviation might be total reconstruction of the several layers of atoms near the surface into a different type of structure from the bulk. Several other types of deviations might occur, and in general we have to consider the specific type of bonding and the lowest energy state of the system to decide which type of deviation will occur. We might also consider the dirty-surface case which arises when the unsaturated forces or dangling bonds of the surface atoms tend to attract foreign atoms which may be

floating around outside the crystal. This usually results in 4 or 5 layers of foreign atoms being deposited on the surface before the bonds are saturated and requires consideration of interfaces between crystals with different periodic potentials.

We shall start with the simplest boundary conditions possible and try to understand most of the phenomena which occur for this case. We shall also outline a procedure for the computation of more complicated terminations. This method is straightforward enough so that further calculations using it could be made without any major difficulties.

The simplest way in which to terminate the periodic potential is by a step function at either end. (Incidentally, the relative smallness of the surface dipole contribution to the work function bears witness that this type of termination may not be too seriously in error in many cases[9].) For the present, consider the termination to be made either at a potential maximum or at a potential minimum (see Figure 3.1). The first type of termination is commonly referred to as Shockley-type[10] whereas the second type of termination is referred to as Tamm-type[11]. These classifications are named for the authors who first showed that these type of potential terminations could have surface energy states associated with them. The Shockley-type potential termination is generally applied to covalent

crystals where the surface perturbations are small whereas the Tamm-type termination is thought to be valid in cases where the surface perturbations are large. The Shockley termination is usually thought to have more physical validity; it corresponds to terminating the crystal between two atoms. Both types of terminations allow us to divide the periodic potential into cells in which the potential is symmetric about the center of each cell. The Shockley-type termination yields a cell with a potential minimum at the center whereas the Tamm-type has a potential maximum there.

For either case, we go about solving for the energy states by matching the wave functions in all regions at their respective boundaries to form a smoothly varying function of position. This matching, of course, will only be possible for particular values of the energy, and it is our purpose to find those energies which do allow a continuous wave function. These energies will be our eigenvalues. The band structure (i.e. the regions of energy in which the wave functions are either running waves of constant amplitude or exponentially increasing and decreasing waves) is determined completely by the periodic potential. The exact position of the eigenstate in this band structure will be determined by energy conditions which are derived below.

For energies less than or equal to the lesser of V_1 and V_2, we set up the matching conditions as follows: For

$x \leq 0$, the solution of the Schrodinger equation yields

$$\psi(x) = A e^{K_1 x} \quad , \; K_1 = \sqrt{\frac{2m}{\hbar^2}(V_1 - E)}, \tag{2.1}$$

where we have used the condition that ψ go to zero at $-\infty$. For $0 \leq x \leq Na$, we have five forms of the wave function which the solution of Schrodinger's equation takes, depending upon the region of energy. In all cases, the general solution will be a linear combination of the independent solutions with constant coefficients which must be determined by the matching conditions. Let us for the present discuss in detail only the case of the running waves and then list the other cases, since the procedure is the same in all cases. Then for Case 2, $\rho < 0$,

$$\psi(x) = C_{+k}\psi_{+k}(x) + C_{-k}\psi_{-k}(x), \tag{2.2a}$$

$$\psi_{\pm k}(x) = e^{\pm ikx} P_{\pm k}(x). \tag{2.2b}$$

For $x \geq Na$, we have

$$\psi(x) = \mathcal{B} e^{-K_2(x-Na)} \quad , \; K_2 = \sqrt{\frac{2m}{\hbar^2}(V_2 - E)}. \tag{2.3}$$

Continuity of the wave function and its derivative, or alternately continuity of the logarithmic derivative at

x = 0, requires

$$K_1 = \left(\frac{C_{+k}\sigma_{+k} + C_{-k}\sigma_{-k}}{C_{+k} + C_{-k}}\right),$$

$$= \sigma_+\left(\frac{C_{+k} - C_{-k}}{C_{+k} + C_{-k}}\right), \tag{2.4}$$

where we have used

$$\psi'_{+k}\Big]_{x=0} = \sigma_+ \quad , \quad \psi'_{-k}\Big]_{x=0} = \sigma_-, \tag{2.5}$$

$$\psi_{+k}\Big]_{x=0} = 1 \quad , \quad \psi_{-k}\Big]_{x=0} = 1,$$

$$\sigma_+ = -\sigma_- .$$

Similarly, at x = Na, we have

$$-K_2 = \sigma_+\left(\frac{C_{+k}e^{ikNa} - C_{-k}e^{-ikNa}}{C_{+k}e^{ikNa} + C_{-k}e^{-ikNa}}\right), \tag{2.6}$$

where again we have used the properties of the wave function

$$\psi'_{+k}\Big]_{x=Na} = \sigma_+ e^{ikNa} \quad , \quad \psi_{-k}\Big]_{x=Na} = \sigma_- e^{-ikNa},$$

$$\psi_{+k}\Big]_{x=Na} = e^{ikNa} \quad , \quad \psi_{-k}\Big]_{x=Na} = e^{-ikNa}. \tag{2.7}$$

Dividing Eq. (2.4) by Eq. (2.6), multiplying out the quantities and grouping terms, we obtain the quadratic equation

in C_{+k} and C_{-k}:

$$C_{+k}^2 e^{ikNa}(K_2+K_1) - 2i(K_2-K_1)\sin kNa\, C_{+k}C_{-k} - C_{-k}^2 e^{-ikNa}(K_1+K_2) = 0. \quad (2.8)$$

Dividing through by $(K_1+K_2)e^{ikNa}$ and solving for C_{+k} in terms of C_{-k}, we have

$$C_{+k} = \left[i\left(\frac{K_2-K_1}{K_2+K_1}\right)\sin kNa \pm \sqrt{1-\left(\frac{K_2-K_1}{K_2+K_1}\right)^2 \sin^2 kNa}\right] \cdot e^{-ikNa} C_{-k}. \quad (2.9)$$

Now $-1 \leq \left(\frac{K_2-K_1}{K_2+K_1}\right) \leq +1$ and K_1, K_2 are always positive so we may define a phase angle ϕ by the relation

$$\sin\phi = \left(\frac{K_2-K_1}{K_2+K_1}\right)\sin kNa \quad (2.10)$$

Then, Eq. (2.4) becomes

$$C_{+k} = [\pm\cos\phi + i\sin\phi]\, e^{-ikNa} C_{-k} \quad (2.10a)$$

or

$$C_{+k} = \pm e^{ikNa \pm i\phi} C_{-k}. \quad (2.10b)$$

We may now substitute back into the Eq. (2.4) or (2.6) to obtain the conditions for matching. Substitution into (2.4) yields the two conditions

$$K_1 = -i\sigma_4 \tan\left(\frac{kNa-\phi}{2}\right), \qquad (2.11a)$$

$$K_1 = i\sigma_4 \cot\left(\frac{kNa+\phi}{2}\right). \qquad (2.11b)$$

$$\sigma_4 = -i\frac{u_0'}{u_0}|\rho|^{\frac{1}{2}},$$

If we had used Eq. (2.6), we would have obtained

$$K_2 = -i\sigma_4 \tan\left(\frac{kNa+\phi}{2}\right), \qquad (2.12a)$$

$$K_2 = i\sigma_4 \cot\left(\frac{kNa-\phi}{2}\right). \qquad (2.12b)$$

Both sets of equations give equivalent energies when the equality is satisfied. We shall, for convenience, use the first set of conditions. Both sets reduce to the same set when $V_1 = V_2$ since the phase angle goes to zero.
For the other four regions, the matching conditions are listed below.

Case 1: $\rho = \pm\infty$, $g_0 u_0' = 0$.

$$\left(\frac{K_1+K_2}{2}\right) = N\left(\frac{u_0'}{u_0}\right), \quad g_0 = 0. \qquad (2.13)$$

$$2\left(\frac{K_1 K_2}{K_1+K_2}\right) = \frac{1}{N}\left(\frac{g_0'}{g_0}\right), \quad u_0' = 0. \tag{2.14}$$

Case 3: $\rho = 0$, $g_0' u_0 = 0$.

$$\left(\frac{K_1+K_2}{2}\right) = N\left(\frac{g_0'}{g_0}\right), \quad u_0 = 0. \tag{2.15}$$

$$2\left(\frac{K_1 K_2}{K_1+K_2}\right) = \frac{1}{N}\left(\frac{u_0'}{u_0}\right), \quad g_0' = 0. \tag{2.16}$$

Case 4: $0 < \rho < 1$.

$$K_1 = -\sigma_+ \tanh\left(\frac{KNa-\Phi}{2}\right), \tag{2.17a}$$

$$K_1 = -\sigma_+ \coth\left(\frac{KNa+\Phi}{2}\right), \tag{2.17b}$$

where

$$K = -\frac{1}{a}\log\left(\frac{1-\rho^{\frac{1}{2}}}{1+\rho^{\frac{1}{2}}}\right), \tag{2.18a}$$

$$\sigma_+ = -\frac{u_0'}{u_0}\rho^{\frac{1}{2}} \tag{2.18b}$$

$$\sinh\Phi = \left(\frac{K_2-K_1}{K_2+K_1}\right)\sinh KNa. \tag{2.18c}$$

Case 5: $\rho > 1$.

$$K_1 = -\sigma_+ \tanh\left(\frac{KNa - \Phi}{2}\right), \qquad (2.19a)$$

$$K_1 = -\sigma_+ \coth\left(\frac{KNa + \Phi}{2}\right), \qquad (2.19b)$$

where

$$K = -\frac{1}{a}\log\left(\frac{\rho^{\frac{1}{2}} - 1}{\rho^{\frac{1}{2}} + 1}\right), \qquad (2.20)$$

and σ_+ , $\sinh \Phi$ are defined as in Case 4.

These matching conditions are transcendental equations and cannot be solved explicitly for the energy of matching. The correct energy eigenvalues can be found by a graphical method. The left-hand side of a particular matching condition is plotted as a function of energy on the same graph as the right-hand side of the matching condition. The points at which the curves of the left and right hand sides cross yield satisfaction of the boundary conditions, and consequently give the energy eigenvalues. The regions in which the curves cross will determine the character of the wave functions. The boundaries of these regions, as noted in Section I, are determined by the zeros of $g'_o(E)$, $g_o(E)$, $u'_o(E)$, $u_o(E)$. It is important to note in what order these functions go to zero as the energy increases because this order determines whether conditions are favorable

or not for surface states to occur. Consequently, it is instructive to follow the matching conditions as a function of energy for a particular sequence in which g'_o, g_o, u'_o, u_o go to zero to obtain insight into what conditions determine whether a surface state might occur.

For simplicity, we consider the case where $V_1 = V_2$ so that $K_1 = K_2$ and $\phi = \Phi = 0$.

Let us first consider the case of the zeroes occurring in the following order with increasing energy.

$$g_o', g_o, u_o', u_o, g_o', g_o, u_o', u_o, \ldots \qquad (2.21)$$

A qualitative graph of $-(u_o'/u_o)|\rho|^{\frac{1}{2}}$ is given for this case in Figure 2.1. Notice that a discontinuity in the slope occurs at $g'_o = 0$.

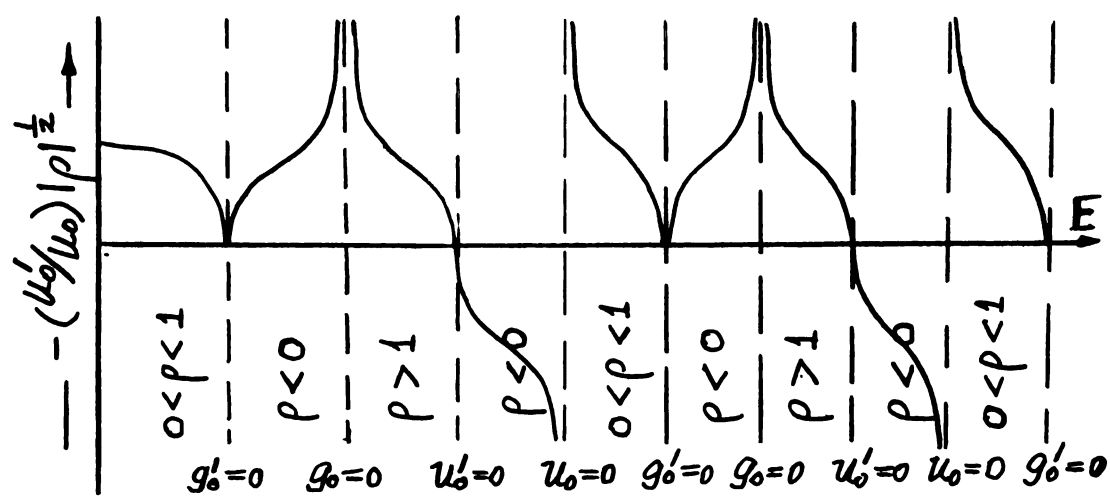

Figure 2.1. Effective wave number versus energy - Case 1.

The above characteristics are those for the reduced zone scheme where we have limited k to the range $0 \leq k \leq \pi/a$. If we had taken the sign on $|\rho|^{\frac{1}{2}}$ to be positive for the odd-numbered bands and negative for the even-numbered bands, we would have obtained completely positive values for the graph above with discontinuities in the slope occurring at $u'_0 = 0$ also. In such a case, an energy versus k plot would be in the extended zone scheme.

The left-hand side of each of the matching conditions given by Eqs. 2.11-2.20 is $K_1 = \sqrt{(2m/\hbar^2)(V_1 - E)}$, and when plotted as a function of energy is just half of a parabola with its axis along the E coordinate. It is positive for all values of energy. The right-hand side of the matching conditions will have alternating regions in which we must use the appropriate formulae.

The first region, corresponding to the energy at the bottom of the potential well, is an attenuation band $0 < \rho < 1$. In this region, $-(u'_0/u_0)|\rho|^{\frac{1}{2}}$ is positive, as are $\tanh(KNa/2)$ and $\coth(KNa/2)$, so that

$$-\left(-\frac{u'_0}{u_0}\rho^{\frac{1}{2}}\right)\tanh\left(\frac{KNa}{2}\right) < 0, \qquad (2.22a)$$

$$-\left(-\frac{u'_0}{u_0}\rho^{\frac{1}{2}}\right)\coth\left(\frac{KNa}{2}\right) < 0. \qquad (2.22b)$$

As the energy increases to the zone boundary where $g_o' = 0$, K approaches zero, as does $-(u_o'/u_o)|\rho|^{\frac{1}{2}}$. Therefore, the product $-\frac{u_o'}{u_o}|\rho|^{\frac{1}{2}}\tanh(\frac{KNa}{2})$ goes to zero while the product $-\frac{u_o'}{u_o}|\rho|^{\frac{1}{2}} \cdot \coth(\frac{KNa}{2})$ approaches the limit $-(-\frac{u_o'}{u_o})/N < 0$. This last limit is a result of the fact that $-(u_o'/u_o)|\rho|^{\frac{1}{2}}$ goes to zero at the same rate as $\coth(\frac{KNa}{2})$ goes to infinity so that a finite limit is achieved at $g_o' = 0$. Both functions are less than zero for the whole region so that no crossing with the K_1 curve is possible. At $g_o' = 0$, we have $\rho = 0$, $k = 0$ so that $-\frac{u_o'}{u_o}|\rho|^{\frac{1}{2}}\tan(\frac{kNa}{2})$ is zero and $-(-\frac{u_o'}{u_o}|\rho|^{\frac{1}{2}}\cot(\frac{kNa}{2}))$ has the value $-(-u_o'/u_o)/N$, providing a smooth connection into the next region of a pass band. From the $g_o' = 0$ boundary to the $g_o = 0$ boundary, ρ varies from 0 to $-\infty$, and consequently, k varies from 0 to π/a. $-(u_o'/u_o)|\rho|^{\frac{1}{2}}$ is positive in this region. $-\cot(\frac{kNa}{2})$ is just $\tan(\frac{kNa}{2} - \frac{\pi}{2})$ so that both functions have the same form, one being shifted by $\pi/2$. Both functions have periods of π within which they vary from $-\infty$ to $+\infty$. Now, as k varies from 0 to π/a, $\tan(kNa/2)$ goes through N/2 periods so that it passes through any positive number N/2 times if N is even and (N+1)/2 times if N is odd. $-\cot(\frac{kNa}{2})$ also goes through N/2 periods and goes through any positive number N/2 times if N is even and (N-1)/2 times if N is odd. Multiplication of $\tan(kNa/2)$ and $-\cot(kNa/2)$ by $-(u_o'/u_o)|\rho|^{\frac{1}{2}}$ changes the slope of these functions,

but is is true that the total number of intersections with K_1 will be N, and consequently there will be N eigenvalues. As the boundary $g_o = 0$ is approached, $-\frac{u_o'}{u_o}|\rho|^{\frac{1}{2}}\tan(\frac{kNa}{2})$ goes to the value $-(-\frac{u_o'}{u_o})N < 0$ if N is even and $\pm\infty$ if N is odd. Likewise, $-(-\frac{u_o'}{u_o}|\rho|^{\frac{1}{2}})\cot\frac{kNa}{2}$ goes to $\pm\infty$ if N is even and $-(-\frac{u_o'}{u_o})N < 0$ if N is odd. At $g_o = 0$, we connect on to an attenuation band where $\rho > 1$. On the boundary, $-(-\frac{u_o'}{u_o}|\rho|^{\frac{1}{2}})\tanh(\frac{kNa}{2})$ is equal to $-(-\frac{u_o'}{u_o})N$ and $-(-\frac{u_o'}{u_o}|\rho|^{\frac{1}{2}})\coth(\frac{kNa}{2})$ is equal to $\pm\infty$. As the energy increases in going to the next boundary $u_o' = 0$, $-(-\frac{u_o'}{u_o}|\rho|^{\frac{1}{2}})\tanh(\frac{kNa}{2})$ increases to zero and $-(-\frac{u_o'}{u_o}|\rho|^{\frac{1}{2}})\coth(\frac{kNa}{2})$ increases from $-\infty$ to the value $\frac{g_o'}{Ng_o} < 0$. The two functions are both negative for the whole region so that no crossings are possible. At $u_o' = 0$, $\rho = -\infty$, $k = \pi/a$, and $-(u_o'/u_o)|\rho|^{\frac{1}{2}}$ is zero, going negative in the next region of a pass band. Since k varies from π/a to 0 with increasing energy, the behavior of $\tan(\frac{kNa}{2})$ and $-\cot(\frac{kNa}{2})$ is the reverse of that found in the first band. However, since $-\frac{u_o'}{u_o}|\rho|^{\frac{1}{2}}$ is negative for this region, the products $(-\frac{u_o'}{u_o}|\rho|^{\frac{1}{2}})\cdot\tan(\frac{kNa}{2})$ and $-(-\frac{u_o'}{u_o}|\rho|^{\frac{1}{2}})\cot(\frac{kNa}{2})$ yield the same form for the functions as in the first band. At $u_o' = 0$, we have $(-\frac{u_o'}{u_o}|\rho|^{\frac{1}{2}})\cdot\tan(kNa/2) = 0$ if N is even and $\frac{g_o'}{Ng_o} < 0$ if N is odd while $-(-\frac{u_o}{u_o}|\rho|^{\frac{1}{2}})\cot(\frac{kNa}{2})$ is equal to g_o'/Ng_o if N is even and zero if N is odd. In going from $u_o' = 0$ to $u_o = 0$, we again have a total of N crossings of the K_1 curve. At $u_o = 0$, $-\frac{u_o'}{u_o}|\rho|^{\frac{1}{2}}\tan(\frac{kNa}{2})$ goes to $N\frac{g_o'}{g_o} < 0$ and $-(-\frac{u_o'}{u_o}|\rho|^{\frac{1}{2}})\cot(\frac{kNa}{2})$

goes to $\pm \infty$. These functions connect on to the forbidden band boundary conditions (for $0 < \rho < 1$) at $u_o = 0$: $-\left(-\frac{u_o'}{u_o}|\rho|^{\frac{1}{2}}\right)\tanh\left(\frac{KNa}{2}\right) = N\frac{g_o'}{g_o}$ and $-\left(-\frac{u_o'}{u_o}|\rho|^{\frac{1}{2}}\right)\coth\left(\frac{KNa}{2}\right)$ $= \pm \infty$. Continuing across this region to the boundary $g_o' = 0$, $-\left(-\frac{u_o'}{u_o}|\rho|^{\frac{1}{2}}\right)\tanh\left(\frac{KNa}{2}\right)$ increases to zero while $-\left(-\frac{u_o'}{u_o}|\rho|^{\frac{1}{2}}\right)\cdot\coth\left(\frac{KNa}{2}\right)$ goes to $-(-u_o'/u_o)/N<0$. Again both functions are entirely negative in this region so that no crossings of K_1 are possible. At $g_o' = 0$, we are again back to the same type of band as considered before. As may be seen by the above arguements, for the sequence of zeros of the functions g_o', g_o, u_o' and u_o considered, no surface states are possible.

We now consider the case when the order in which g_o', g_o, u_o', u_o go to zero deviates from the order given above. For example, suppose the order is given by

$$g_o', g_o, u_o', u_o, g_o', (u_o', g_o), u_o, g_o', \cdots \quad (2.23)$$

In this case, the order of the functions in parenthesis, u_o' and g_o, is reversed. A qualitative graph of $-(u_o'/u_o)|\rho|^{\frac{1}{2}}$ is given below in Figure 2.2. Comparison of this graph with that of the previously considered sequence shows that the main result of switching the order of g_o, u_o' is to cause $-(u_o'/u_o)|\rho|^{\frac{1}{2}}$ to be zero on the upper band edge at $u_o' = 0$, at which point it goes negative in the region $\rho > 1$.

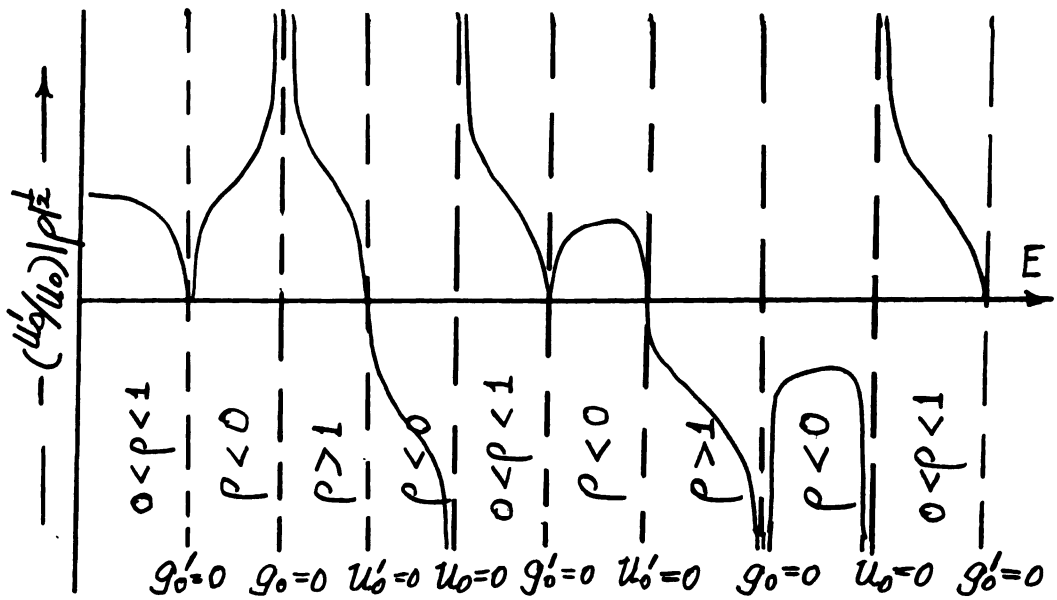

Figure 2.2. Effective wave number versus energy - Case 2.

At $g_0 = 0$, $-(u_0'/u_0)|\rho|^{\frac{1}{2}}$ is equal to - ∞ at which point it increases to some negative value before going to negative infinity again at the upper band edge $u_0 = 0$. The essential feature to notice is that the form of $-(u_0'/u_0)|\rho|^{\frac{1}{2}}$ is altered in the two band regions adjacent to the attenuation region in which it goes negative. In the lower band, between $g_0' = 0$ and $u_0' = 0$, $-\left(\frac{u_0'}{u_0}|\rho|^{\frac{1}{2}}\right)\tan\left(\frac{kNa}{2}\right)$ will go through N/2 periods if N is even or odd achieving the value of 0 at $u_0' = 0$ if N is even and $\frac{1}{N}\left(\frac{g_0'}{g_0}\right) > 0$ if N is odd. Notice that the ratio g_0'/g_0 is greater than zero in contrast to the previous situation. For N odd, the magnitude of the product $\frac{1}{N}\left(\frac{g_0'}{g_0}\right)$ will determine whether the crossing

of K_1 occurs in a pass-band or in an attenuation band. For N small and the potential weak, the value $\frac{1}{N}(g_e'/g_o) > K_1$, and the crossing will occur in a pass band region. For N large, the ratio g_e'/g_o, which depends only on the periodic potential, remains the same but is reduced by a large number N so that $\frac{1}{N}(g_e'/g_o) < K_1$, and no crossing occurs in the pass-band region. The function $-(-\frac{u_o'}{u_o}|\rho|^{\frac{1}{2}})\cot(\frac{kNa}{2})$ behaves in a similar way, attaining the value of $\frac{1}{N}(g_o'/g_o)$ > 0 if N is even and 0 if N is odd. Thus the number of band states which occur will be either N if $\frac{1}{N}(g_o'/g_o) > K_1$ or N-1 if $\frac{1}{N}(g_o'/g_o) < K_1$. At $u_o' = 0$, $-(-\frac{u_o'}{u_o}|\rho|^{\frac{1}{2}})\tanh(\frac{kNa}{2})$ = 0 and $-(-\frac{u_o'}{u_o}|\rho|^{\frac{1}{2}})\coth(\frac{kNa}{2}) = \frac{1}{N}(g_o'/g_o)$. In going from $u_o' = 0$ to $g_o = 0$, $-(-\frac{u_o'}{u_o}|\rho|^{\frac{1}{2}})\tanh(\frac{kNa}{2})$ increases to the value $N(u_o'/u_o) > 0$ and $-(-\frac{u_o'}{u_o}|\rho|^{\frac{1}{2}})\coth(\frac{kNa}{2})$ goes to + ∞. Again, if N is small such that $N(\frac{u_o'}{u_o}) < K_1$, then no crossings will occur, but if N is large such that $N(u_o'/u_o) > K_1$, we obtain crossing in the attenuation band. It should be pointed out that an intermediate case with $\frac{1}{N}(g_o'/g_o) > K_1$ and $N(u_o'/u_o) > K_1$ may occur, in which case there is only one crossing in the forbidden band. For N large, such that $\frac{1}{N}(g_o'/g_o) < K_1$ and $N(\frac{u_o'}{u_o}) > K_1$, we obtain two crossing in the forbidden band. By analogy with the band considered previously, the allowed band bordering this attenuation band from above will have N allowed states if $N(\frac{u_o'}{u_o}) < K_1$ and N-1 states if $N(\frac{u_o'}{u_o}) > K_1$. We may

summarize the results of the above reasoning by the following table. (The function written above each column is to indicate at what energy the conditions are to be evaluated.)

Table 2.1. Existence conditions for Surface States - Case 1.

$u_0' = 0$	$g_0 = 0$	
$\frac{1}{N}\left(\frac{g_0'}{g_0}\right) > K_1$	$N\left(\frac{u_0'}{u_0}\right) < K_1$	No surface states
$\frac{1}{N}\left(\frac{g_0'}{g_0}\right) < K_1$	$N\left(\frac{u_0'}{u_0}\right) < K_1$	One surface state coming from lower band
$\frac{1}{N}\left(\frac{g_0'}{g_0}\right) > K_1$	$N\left(\frac{u_0'}{u_0}\right) > K_1$	One surface state coming from upper band
$\frac{1}{N}\left(\frac{g_0'}{g_0}\right) < K_1$	$N\left(\frac{u_0'}{u_0}\right) > K_1$	2 surface states from upper and lower bands

We see that for large N, one of the pass-band states from the two adjacent pass-bands moves into the attenuation band to form two surface states.

The situation is similar when the zeroes of u_0, g_0' are interchanged; that is, for

$$g_0', g_0, u_0', (g_0', u_0), \ldots \qquad (2.24)$$

In this case we may represent the conditions for surface state occurrence as

Table 2.2. Existence conditions for Surface States - Case 2.

$g_0' = 0$ $\quad u_0 = 0$

$\frac{1}{N}\left(\frac{u_0'}{u_0}\right) > K_1$	$N\left(\frac{g_0'}{g_0}\right) < K_1$	No surface states
$\frac{1}{N}\left(\frac{u_0'}{u_0}\right) < K_1$	$N\left(\frac{g_0'}{g_0}\right) < K_1$	One surface state from lower band
$\frac{1}{N}\left(\frac{u_0'}{u_0}\right) > K_1$	$N\left(\frac{g_0'}{g_0}\right) > K_1$	One surface state from upper band
$\frac{1}{N}\left(\frac{u_0'}{u_0}\right) < K_1$	$N\left(\frac{g_0'}{g_0}\right) > K_1$	2 surface states from upper and lower bands

Thus, we see that a necessary condition for the possible occurrence of surface states is that the band edges cross. When this condition is fulfilled, the actual occurrence depends upon the number of atoms considered and on the strength of the potential.

The effect of unequal terminations (i.e. $V_1 \neq V_2$) at either end of the crystal is to spread the energy levels. However, this effect is not large since the difference between V_1 and V_2 is manifested in K_1, K_2 which vary only slowly with changes in V_1 and V_2.

For a periodic potential terminated at an arbitrary

point in the end cell by a step function, the formalism which we are using is not the most convenient. However, the matching calculations may be done in the same manner as above, matching the wave function and its derivative at the termination point to obtain a contiruous wave function. This procedure is carried out in Section IV for a Kronig-Penney[12] type periodic potential and the results are examined. It is found that this type of termination gives rise to many other surface states besides the ones considered above.

For arbitrary terminations of the crystal potential, it is necessary to use iterative techniques to integrate the Schrodinger equation. For the region of the crystal in which the crystal is perfectly periodic, we know the wave function and its derivative at all points. At the point where the potential starts to deviate from perfect periodicity, we may iterate through the arbitrarily varying potential to a point outside the crystal where the potential is constant. In this region, the wave function must have the exponential decay form, $e^{-K|X|}$, so that we may match this to form a continuous wave function in all regions. This method may also be used to connect two different types of periodic potentials by a region of non-periodic potential. In this way, a wide variety of problems may by dealt with, with few changes in the

calculational apparatus necessary to change from consideration of one phenomenon to another.

Another application which can be made of this method is to the calculation of the reflection and transmission coefficient through several identical barriers. This topic will be discussed in Sections V and VI.

SECTION III

TERMINATION OF A KRONIG-PENNEY POTENTIAL

In order to obtain a better understanding of the principles discussed in Section II, we next consider the Tamm- and Shockley-type terminations of a Kronig-Penney[13] type potential, as shown in Figure 3.1. By the Kronig-Penney type potential, we mean an array of a finite number of rectangular well potentials. The reason for choosing this type of potential is that it leads to a Schrodinger equation which can be solved easily, and the energy band structure associated with it is similar in many respects to that of a real crystal. Two important features which serve to illustrate this point are the existence of points of contact between different allowed bands (a special type of band crossing) and the behavior of the band structure as the energy approaches infinity; namely, the attenuation band gaps go to zero. Maue,[14] and later Statz,[15] and Koutecky,[16] have derived conditions for the crossing of bands. In these papers it is shown that crossing occurs for potentials which require large numbers of Fourier components to represent them, with some of the components being

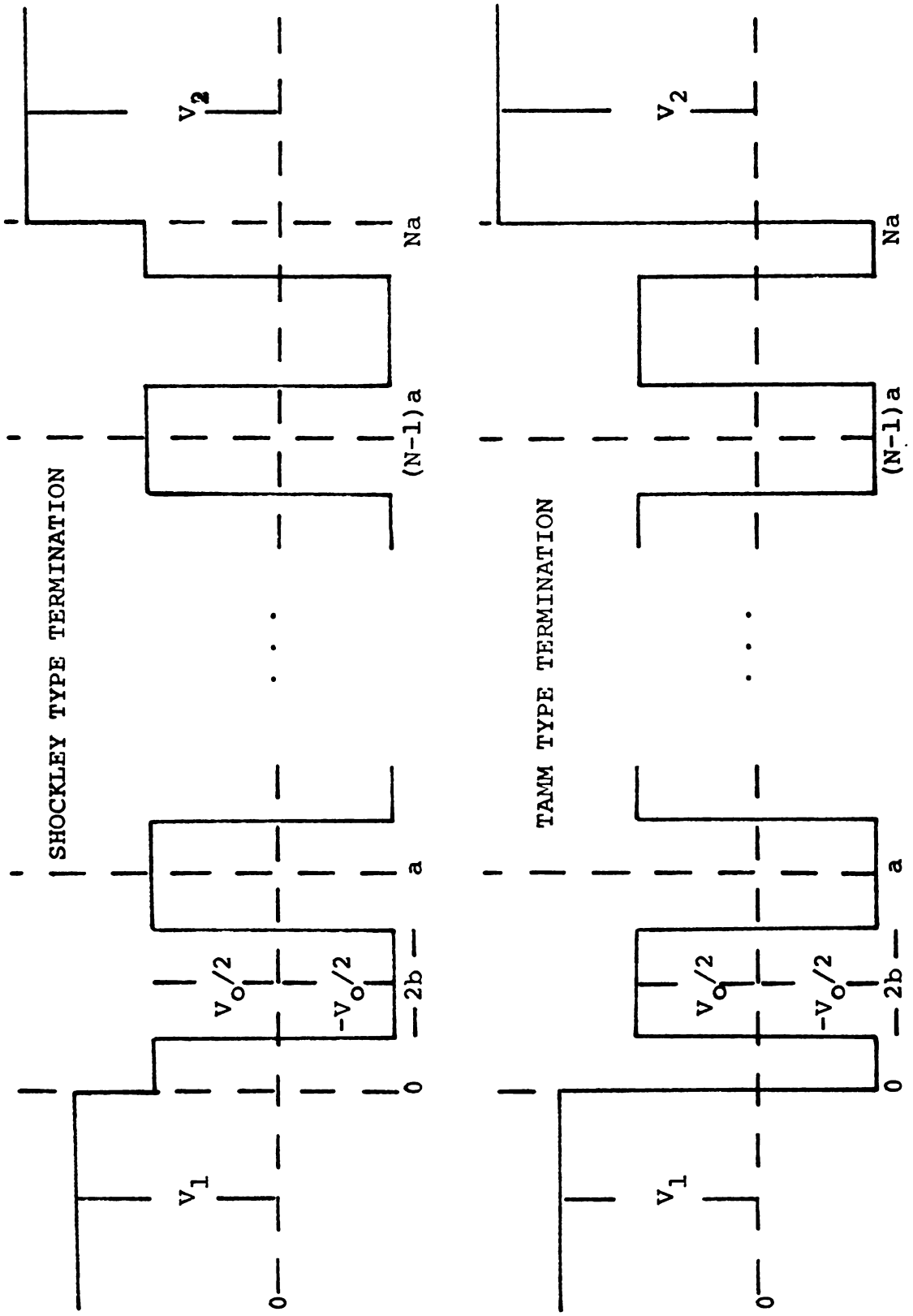

Figure 3.1. Shockley- and Tamm- type potential terminations.

negative. Since a rectangular well potential abounds in harmonics, as does a real potential, we expect the Kronig-Penny model to be a useful model of a real potential.

A. SHOCKLEY-TYPE TERMINATION

We begin by considering the Shockley-type termination. Dividing the periodic potential into cells yield a cell with a potential minimum at the center.

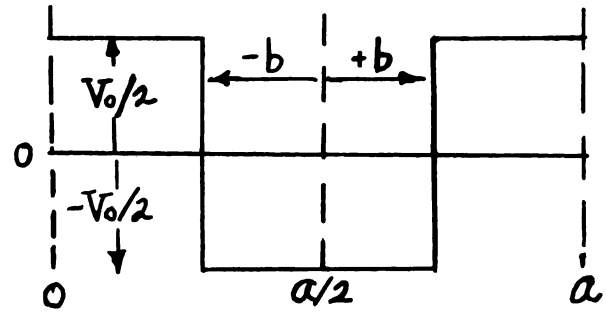

In the region, $a/2-b \leq x \leq a/2+b$, the Schrodinger equation has two linearly independent solutions,

$$g(x) = \cos k(x-a/2), \qquad k=\sqrt{\frac{2m}{\hbar^2}(E+V_0/2)}; \tag{3.1a}$$

$$u(x) = \frac{\sin k(x-a/2)}{k}. \tag{3.1b}$$

Note that

$$g(a/2)=1 \quad , \quad g'(a/2)=0, \tag{3.2a}$$

$$u(a/2)=0 \quad , \quad u'(a/2)=1. \tag{3.2b}$$

If we now connect these solutions individually to the

solutions of Schrodinger's equation in the region $o \leq x \leq a/2-b$, we obtain for $E<V_o/2$, the values of $g(x)$, $g'(x)$, $u(x)$, $u'(x)$ on the left cell boundary:

$$g_o = \cos kb \cosh K(a/2-b) - \frac{k}{K}\sin kb \sinh K(a/2-b), \quad (3.4a)$$

$$g_o' = -K\cos kb \sinh K(a/2-b) + k \sin kb \cosh K(a/2-b), \quad (3.4b)$$

$$u_o = \frac{1}{k}\cos kb \sinh K(a/2-b) - \frac{1}{K}\sin kb \cosh K(a/2-b), \quad (3.4c)$$

$$u_o' = \cos kb \cosh K(a/2-b) + \frac{K}{k}\sin kb \sinh K(a/2-b), \quad (3.4d)$$

$$K = \sqrt{\frac{2m}{\hbar^2}(V_o/2 - E)}.$$

For $E = V_o/2$, and $E>V_o/2$, we must connect in a similar way to obtain expressions for g_o', g_o, u_o', u_o. To determine the pass bands and attenuation bands, it is necessary to make a plot of ρ versus E, where ρ has been defined in Section I as

$$\rho = (g_o'/g_o)/(u_o'/u_o). \quad (3.5)$$

Such a plot was described in Section I. The exact positions of the band edges (i.e. energies at which one of the quantities g_o', g_o, u_o', u_o equals zero) will depend on a, b, V_o. To obtain a qualitative idea of what effects these parameters will have on the band structures, we may make energy versus potential depth plots for several values

of the well width and the lattice constant a. Such plots are shown in Figures 3.2, 3.3, and 3.4. Figure 3.2 has a well width of 0.75a, while Figure 3.3 has a width of 0.5a, and Figure 3.4 has a width of 0.25a. These graphs were obtained by making a ρ versus E plot for a given a, b, V_o to obtain the points where g_o', g_o, u_o', u_o, go to zero (i.e. the band structure). The parameter V_o was then changed incrementally and another ρ versus E plot was made. In this way, the dependence of the band structure on V_o was obtained for a given a, b. Allen[17] has obtained similar but more detailed graphs, varying the constant b for 12 values, for the Kronig-Penney type potential, and the reader should refer to his article for more detail.

> Note: In all graphs contained in this thesis, we shall use units in which $\hbar^2/2m = 1$. To this end we choose our unit of length to be angstrom and our unit of energy to be $(1.97)^2 = 3.88$ electron volts. This energy unit will be denoted by E.U. hereafter.

For the above mentioned figures, note that for large values of the potential V_o, the pass-band regions are very narrow, corresponding to the tight binding of electrons to the constituent wells or atoms. For large energies E, the effect of the potential is not "felt" as much, allowing the pass-band to widen. As we decrease the strength of the potential, the pass-bands widen allowing some of the band edges or boundaries to cross or just make contact.

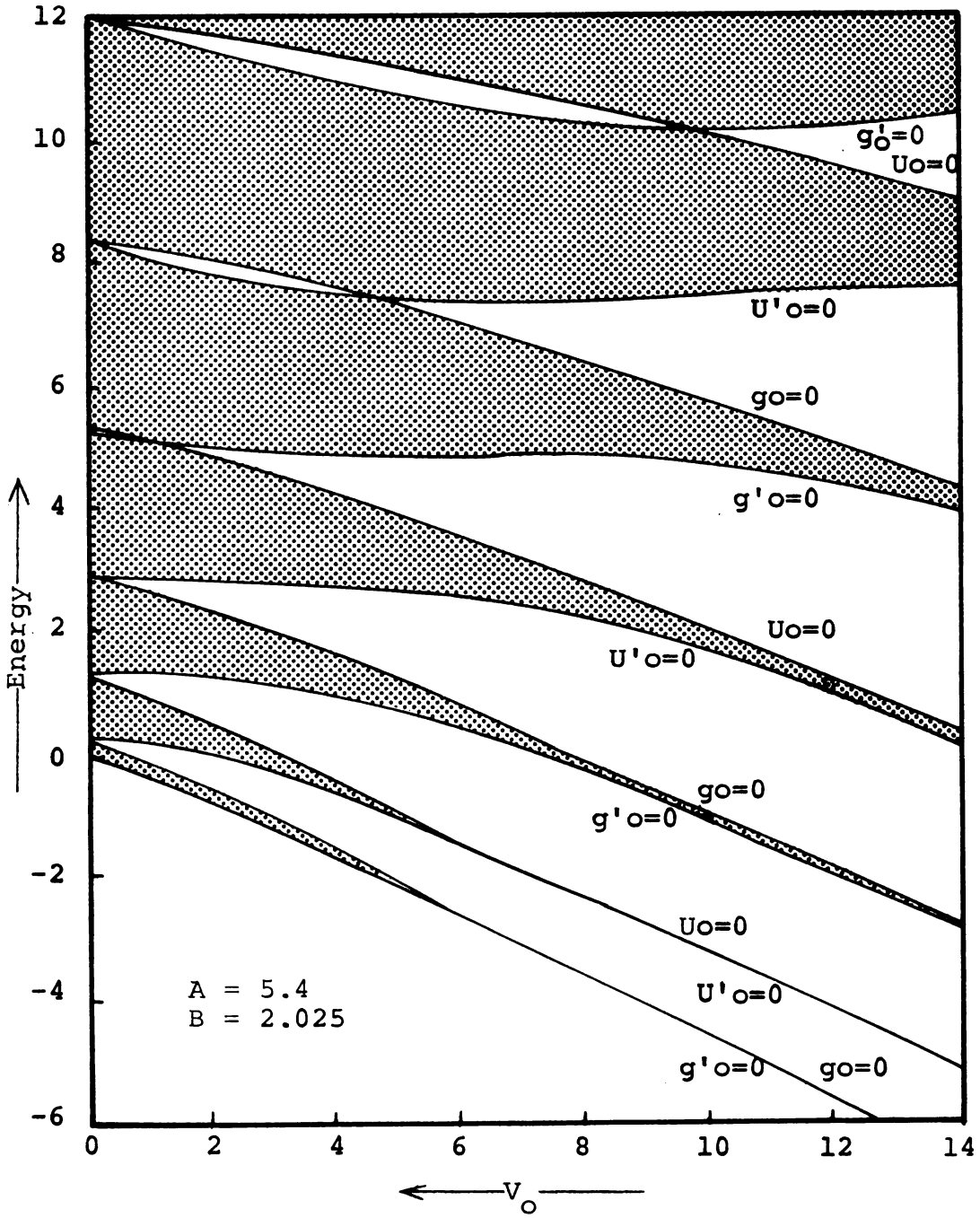

Figure 3.2 Band structure as a function of well depth for a Kronig-Penney potential with 2b= 0.75a.

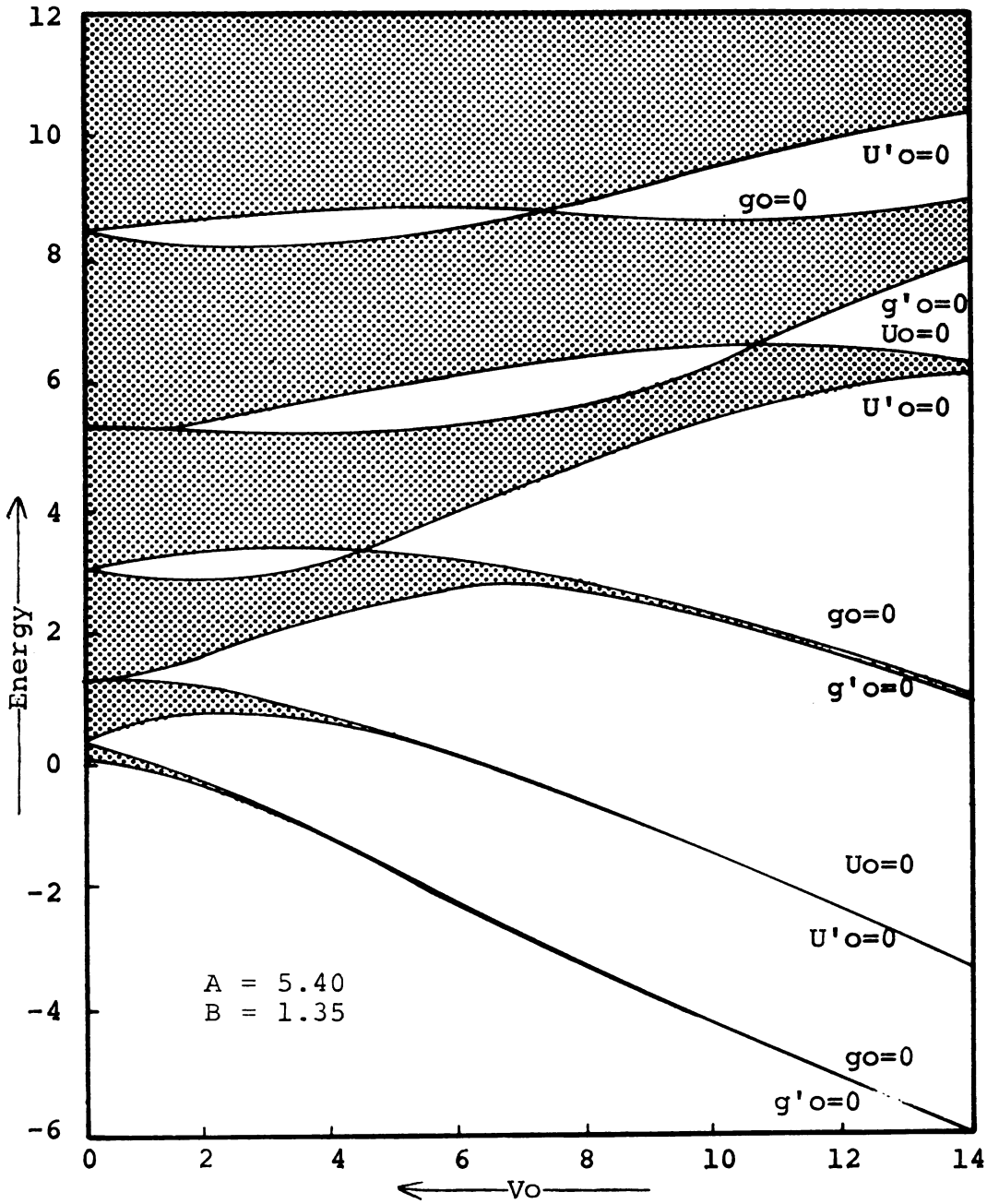

Figure 3.3 Band structure as a function of well depth for a Kronig-Penney potential with 2b= 0.50a.

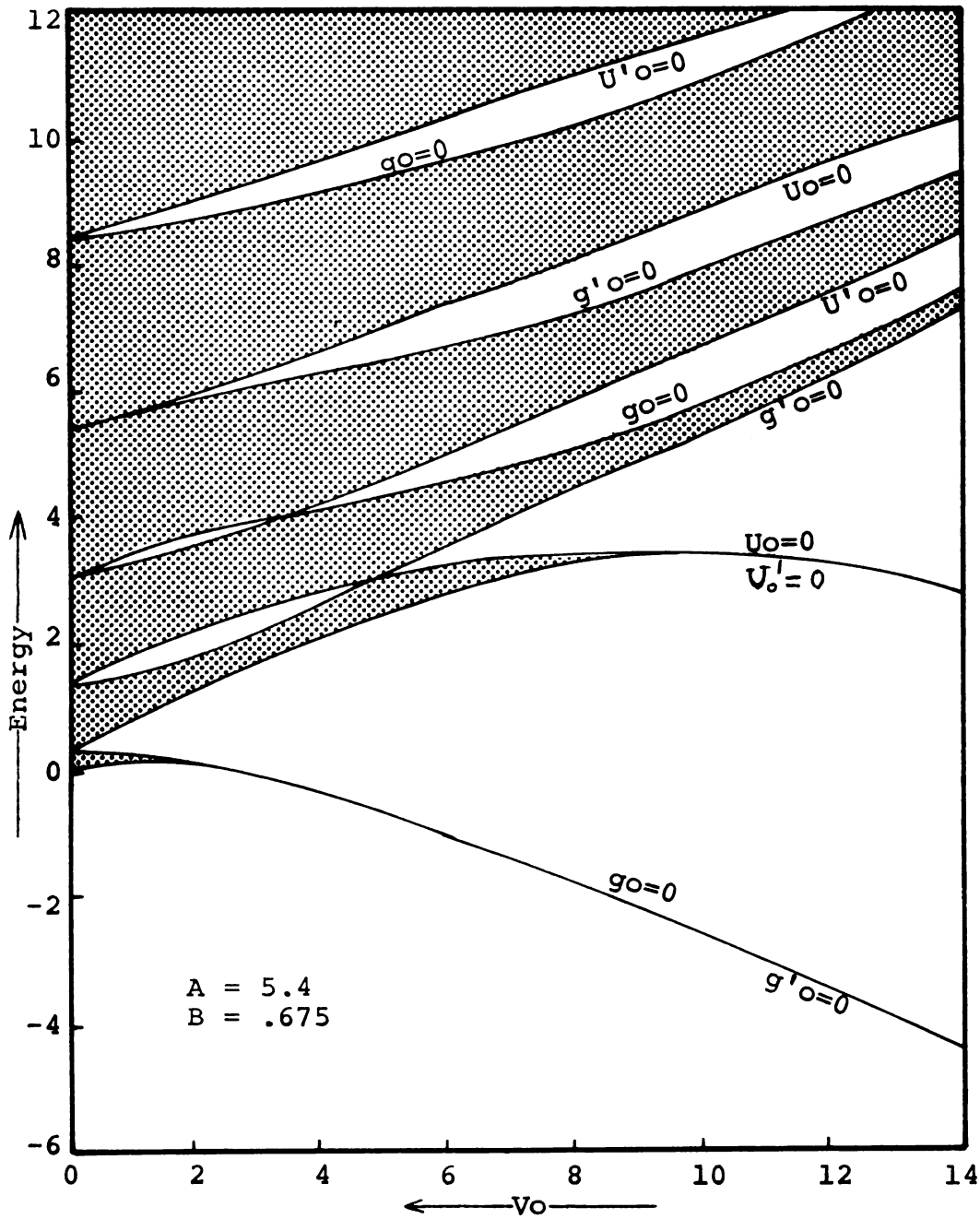

Figure 3.4 Band structure as a function of well depth for a Kronig-Penney potential with 2b= 0.25a.

This is best illustrated in Figure 3.3 in which the upper band edge of the third pass-band edge crosses with the lower band edge of the fourth pass-band, the upper band edge of the fourth pass-band crosses with the lower band edge of the fifth pass-band, and the upper band edge of the fifth pass-band just touches the lower band edge of the sixth pass-band. For the tight binding situation, the band edges are determined by the sequence of zeroes,

$$g_0', g_0, u_0', u_0, g_0', g_0, u_0', u_0, \ldots . \quad (3.6)$$

As we saw in Section II, this sequence of zeroes does not allow the emergence of surface states. As the potential is decreased, the bands which cross have an attenuation region between them, which is favorable for the appearance of states. The points at which the bands cross can be shown to occur only for $E > V_0/2$.[18] By consideration of the equations for g_0', g_0, u_0', u_0, one can show that the crossing points are given by

$$\left.\begin{aligned} E_{cross} &= \frac{n^2\pi^2}{8b^2} + \frac{m^2\pi^2}{8(a/2-b)^2} \\ V_{0cross} &= \frac{n^2\pi^2}{4b^2} - \frac{m^2\pi^2}{4(a/2-b)^2} \end{aligned}\right\} V_{0cross} > 0. \quad (3.7)$$

where n, m are integers. It should be noted that the appearance of band crossing only for $E > V_0/2$ is not

peculiar to our model potential but can be proved to hold for any arbitrary periodic one-dimensional potential.[19] (This does not hold for three dimensional crystals.) Since the value of the vacuum level energy is of the order of 20 eV for most real solids,[20] we see that to obtain surface states V_o must be weak enough to allow band crossings within this range, and consequently, surface states of the Shockley type would be expected to appear for nearly free electrons. We note also in passing that the width of the attenuation regions does not decrease monotonically with increasing energy but varies in width due to the crossings. However, on the average, the width will go to zero as the energy goes to infinity. As V_o goes to zero, the attenuation band-widths go to zero yielding a continuous pass-band region, or a free electron region.

To proceed, we consider specific values for a, b, V_o. As a reasonable approximation for a real crystal, we let V_o have the magnitude of the first Fourier component of the O.P.W. potential for silicon[21] along the (111) direction and take $V_1 = V_2 = V_{ooo}$, the average potential for silicon. Along this direction, Si has a lattice constant of approximately 5.4 A^o. The well width will be taken to be equal to the barrier width. For the present, we shall limit ourselves to four cells. Thus

$$V_1 = V_2 = 25\,eV = 6.5\,E.U., \quad (3.8a)$$

$$V_o = 13.2\,eV = 3.4\,E.U., \quad (3.8b)$$

$$a = 5.4\,A^\circ \quad (3.8c)$$

$$b = 1.35\,A^\circ \quad (3.8d)$$

$$N = 4 \quad (3.8e)$$

A plot of ρ versus energy is given in Figure 3.5. Notice that the lowest pass-band is very narrow, of the order of .02 E.U. in width. The attenuation-band above this pass-band is large, of the order of 1.75 E.U. or about 6.8 eV, which is much too large a gap, the experimentally observed gap for Si being about 1.2 eV. However, one of the difficulties associated with the choice of a potential in the one-electron approximation is that the Fermi energy is not unambiguously known.[22] By inspection of the widths of the attenuation energy widths up to the value of the vacuum, 6.5 E.U., we see that a width which is of the same order of magnitude as 1.2 eV would be that width occurring between 5 E.U. and 6 E.U..

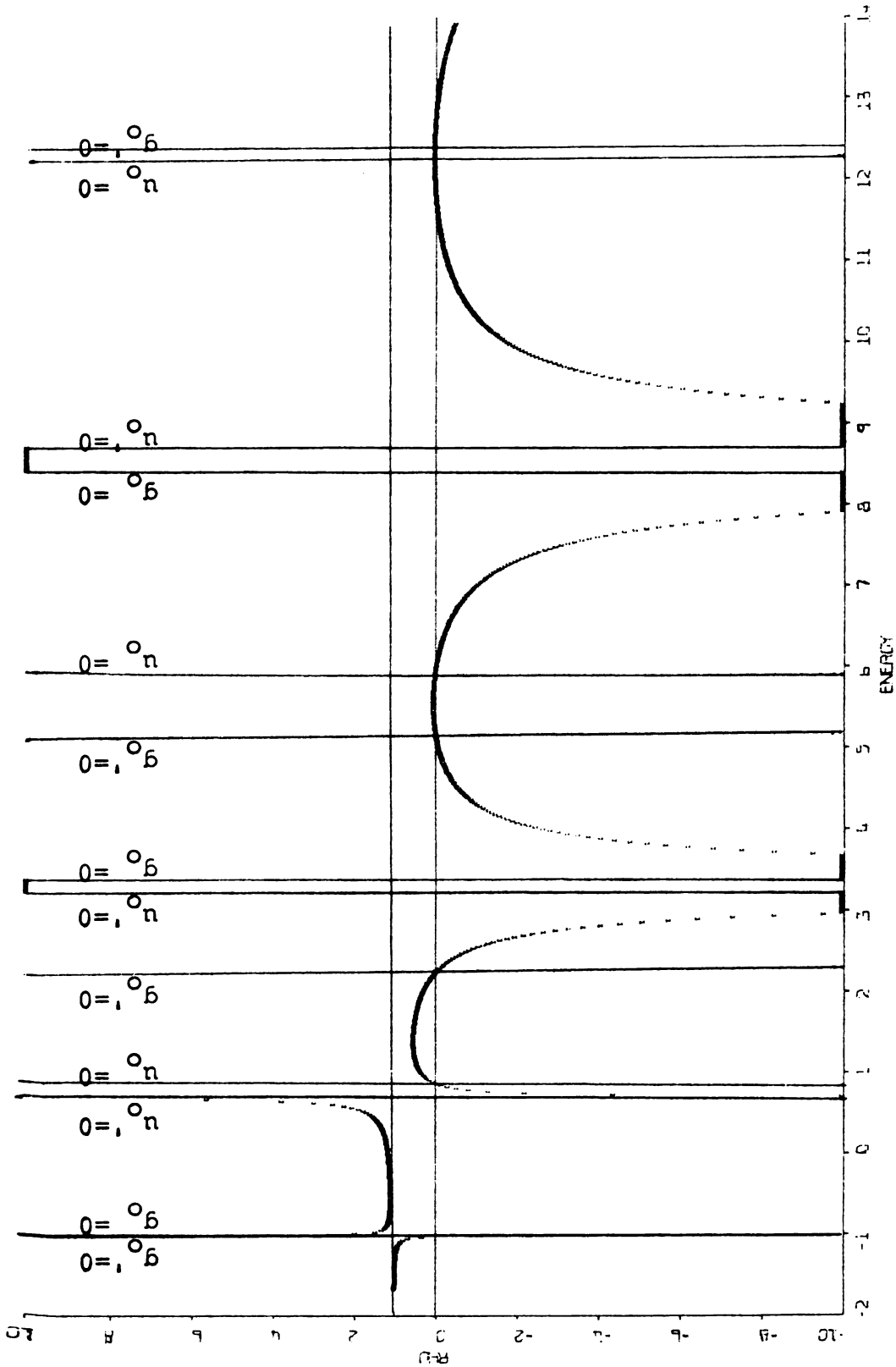

Figure 3.5. Determination of pass bands and attenuation bands.

If the Fermi energy were assigned to this region, the work function would be of the correct order of magnitude as would the attenuation band width. However, this width is still rather wide. This discrepency may be accounted for by the fact that, while we are using an O.P.W. potential, we are not orthogonalizing our wave functions to the core wave functions, so this potential is incorrect for our wave functions. Antoncik[23] has shown that this orthogonalization may be taken into account by subtracting an effective potential from the O.P.W. potential, the effective potential being calculated from the core wave functions. The sum of the two potentials is known as the pseudo-potential. The valence and conduction wave functions may then be calculated without an orthogonalization procedure. For our purposes, we assume that the O.P.W. potential is reduced in magnitude (i.e. V_o is reduced). By inspection of Figure 3.3, we see that if V_o is reduced to about 2.4 E.U., the attenuation width between 5 E.U. and 6 E.U. becomes about 1.2 eV which is approximately the energy gap observed.

Since this calculation is for illustrative purposes only, we shall use the value of $V_o = 3.4$ E.U. in the calculations which follow, being satisfied that we are in the correct range.

Using the boundary conditions derived in Section

II, (Eqs. 2.11-2.20) we plot the left hand side of these equations on the same graph as the right hand side to obtain Figure 3.6. The vertical lines indicate band edges. The solid curve is just the left hand side of the boundary conditions, $K_1 = \sqrt{\frac{2m}{\hbar^2}(V_1 - E)}$. The dotted curves are the two functions on the right hand side of the boundary conditions. The crossing of the K_1 curve and the dotted curves determines the eigenvalues. This procedure for finding eigenvalues is exactly analogous to the method of finding eigenvalues for an electron in a box with finite ends. Notice that in Figure 3.6, the band edges are determined by the sequence of zeros of g_o', g_o, u_o', u_o in the order,

$$g_o', g_o, u_o', u_o, g_o', (u_o', g_o), (g_o', u_o). \quad (3.9)$$

From the considerations of Section II, we expect to find surface states occurring between ($u_o' = 0$, $g_o = 0$) and between ($g_o' = 0$, $u_o = 0$). This is indeed the case. A pass-band state from the third pass-band has moved into the attenuation region. The number of cells is not great enough or the potential is not strong enough to move the upper pass-band state down into the attenuation-band, so there is only one surface state. The same situation applies for the next higher attenuation region,

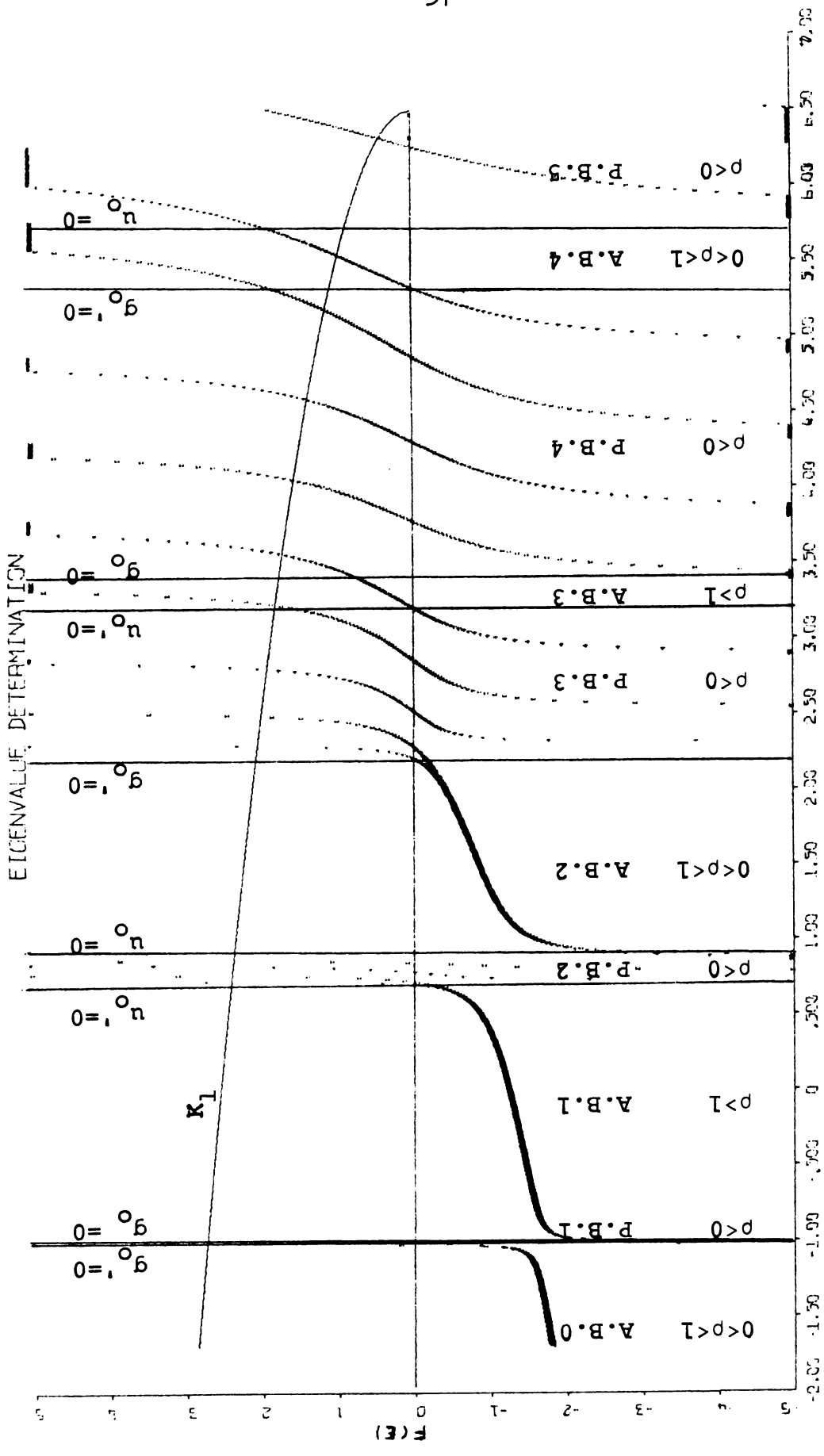

Figure 3.6. Determination of the eigenvalues for the Shockley type termination. The crossing of the K_1 curve with a dotted curve determines an eigenvalue.

except that now for the partial pass-band (which would be pass-band 5 if V_1, V_2 were large enough to include the whole pass-band) one of the pass-band states has moved down into the attenuation region. Note also the effect of varying V_1 or V_2. Since the dotted curves do not depend on V_1 or V_2 (if $V_1 = V_2$), we can vary $K_1 = \sqrt{\frac{2m}{\hbar^2}(V_1 - E)}$ to see that increasing and decreasing V_1 raises and lowers the crossing points and consequently the energy eigenvalues. Since K_1 depends on the square root of V_1, we do not expect the energy crossing points to change very much as V_1 is varied except for energies near the vacuum level.

An energy versus (k and K) plot in the reduced-zone scheme is shown in Figure 3.7. The horizontal lines indicate the band edges. The solid curves are the E versus k plots in the pass bands whereas the dashed curves are the E versus K plots in the attenuation regions. To be entirely correct, we should have plotted E versus K along the imaginary axis perpendicular to the real values of k. This would then yield a band structure with pass bands connected by imaginary loops across the attenuation bands. These imaginary loops are referred to by Heine[24] as "real lines", their exact meaning coming from the analytic continuation of k in E(k) into the complex plane with only real values for

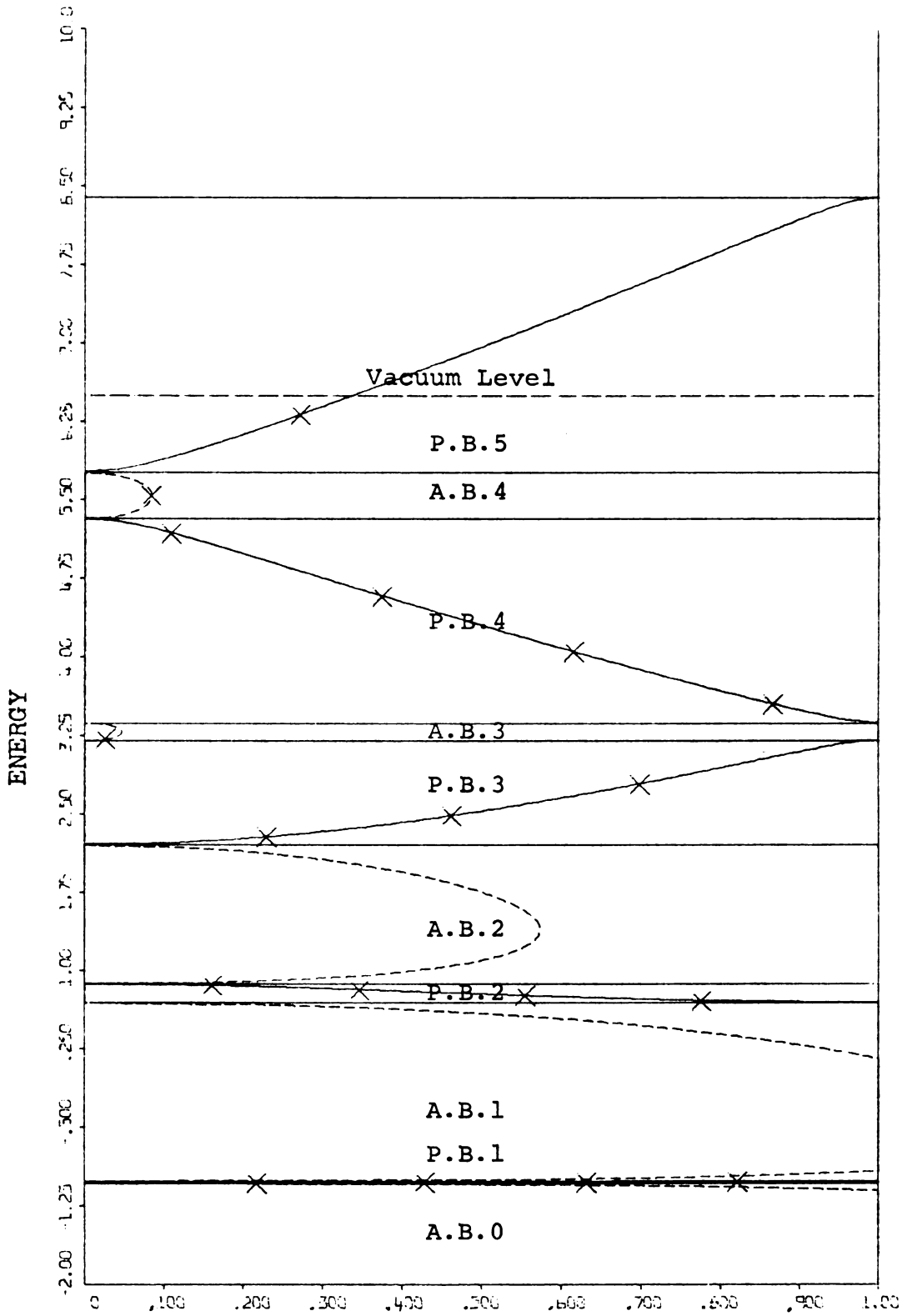

Figure 3.7. Energy versus (k and K). The X's denote eigenvalues which were determined in Figure 3.6 (Shockley).

E considered. The X's represent the eigenvalues as determined from Figure 3.6. Notice that in attenuation band 3, the value of K is very small so that our wave function in this region is not attenuated very strongly going into the interior of the crystal. In attenuation band 4, the value of K is larger but is still not large enough to attenuate the wave function strongly.

Figures 3.8 (a-e) are plots of the wave functions. The pass-band functions are labeled as $\psi_{\alpha,\beta}$ where α is the pass-band index, and β is the index of k_β in the pass-band (e.g. $\psi_{1,1}$ denotes pass-band 1, the lowest k value labeled k_1). The surface wave functions are denoted by $\{\psi_{\gamma,\delta}\} \sim \psi_{\alpha,\beta}$ where $\{\ \}$ indicates a surface wave function, γ indicates the attenuation-band, the numbering starting above the first pass-band, and δ indicates the label on K_δ ($\delta = 1$ or 2). The symbolic notation $\sim \psi_{\alpha,\beta}$ is to indicate which pass band function has moved into the attenuation gap. Notice that the wave functions are just modulated box wave functions (i.e. modulated solutions to the problem of an electron in a box). The surface wave functions are hardly attenuated at all, as was to be expected from the small attenuation constant K. In fact, since the value of K is proportional to the band width,[25] we do not expect to obtain appreciable attenuation for

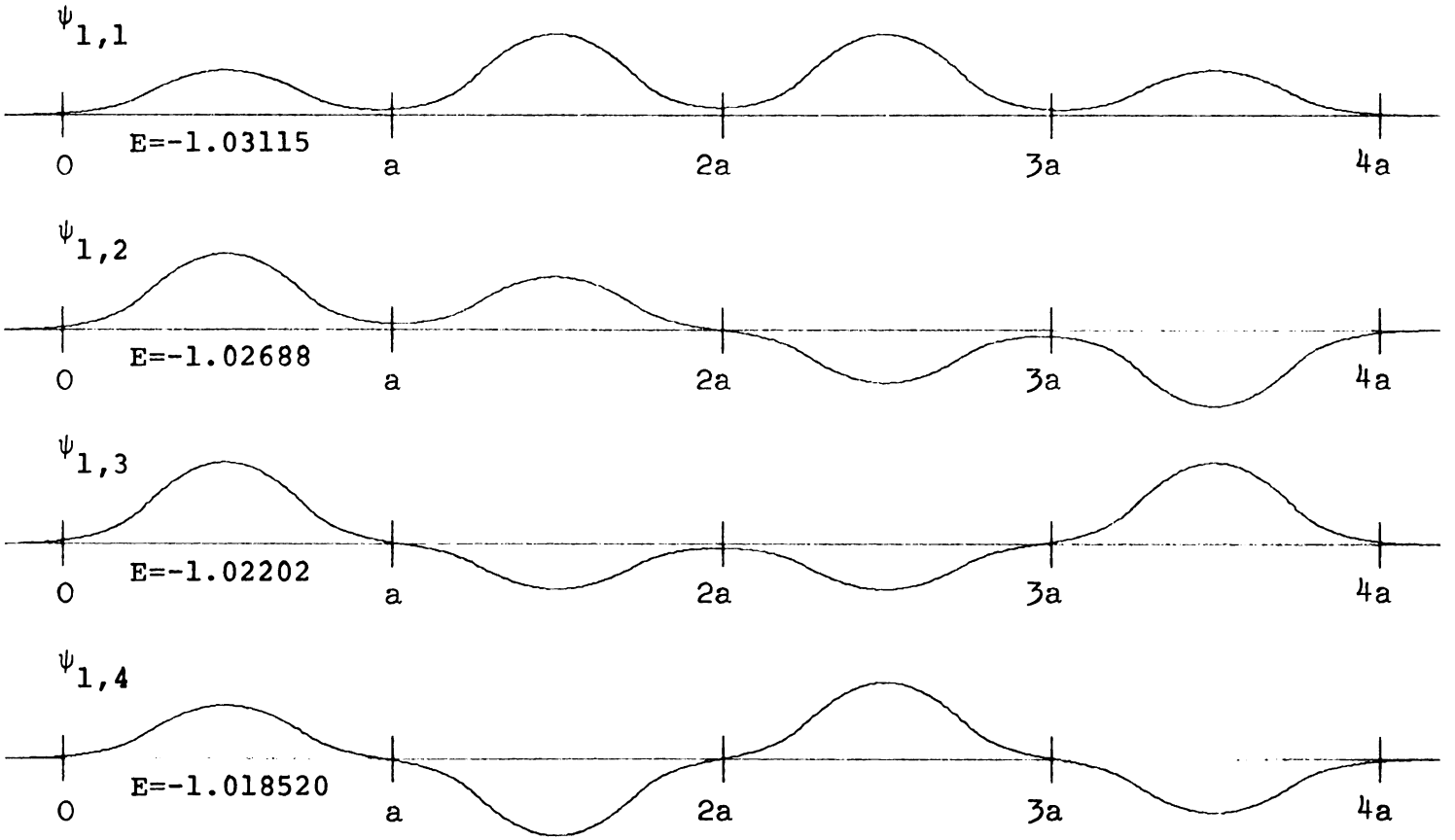

Figure 3.8a. Eigenfunctions for the first pass band (Shockley).

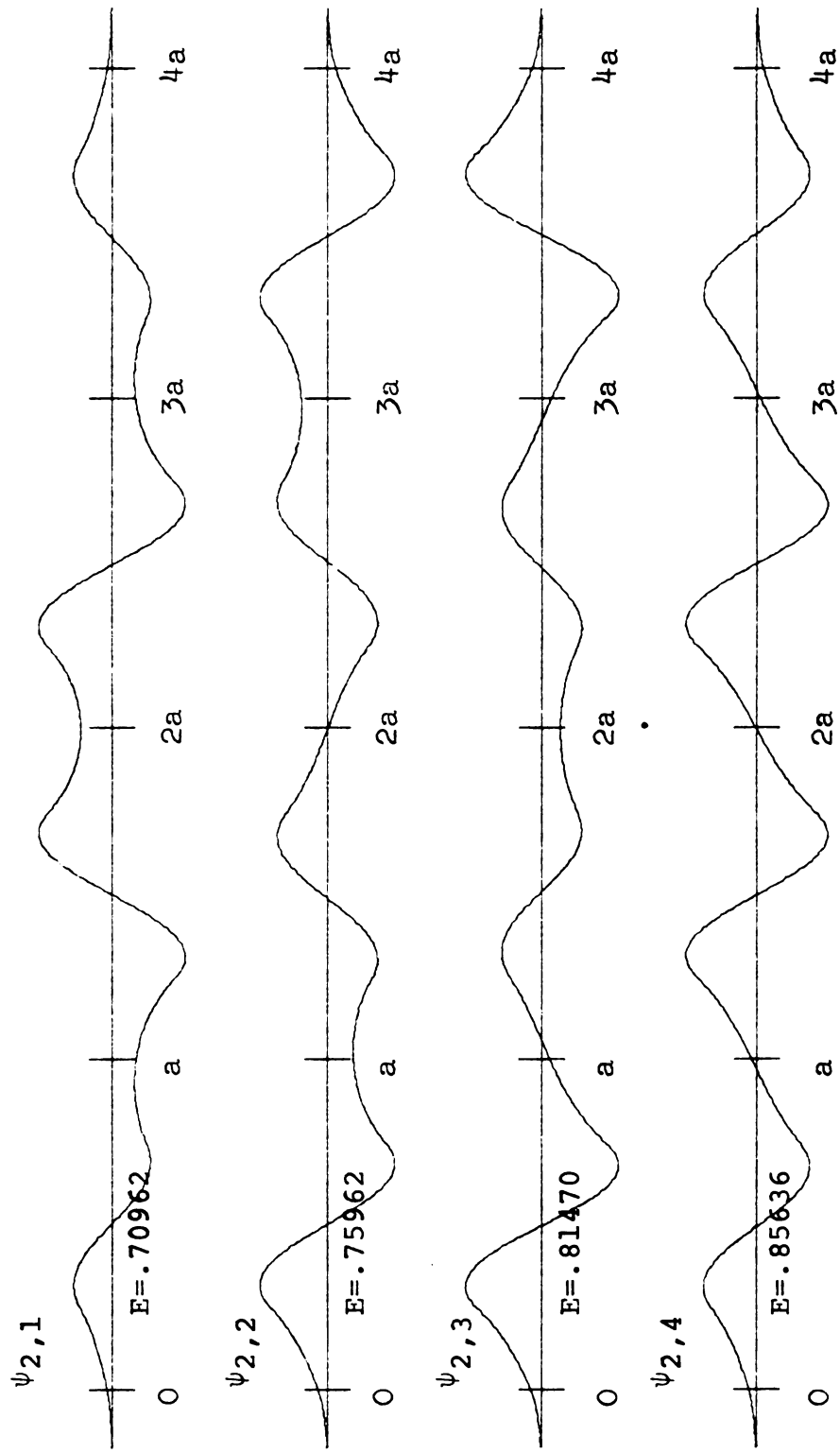

Figure 3.8b. Eigenfunctions for the second pass band (Shockley).

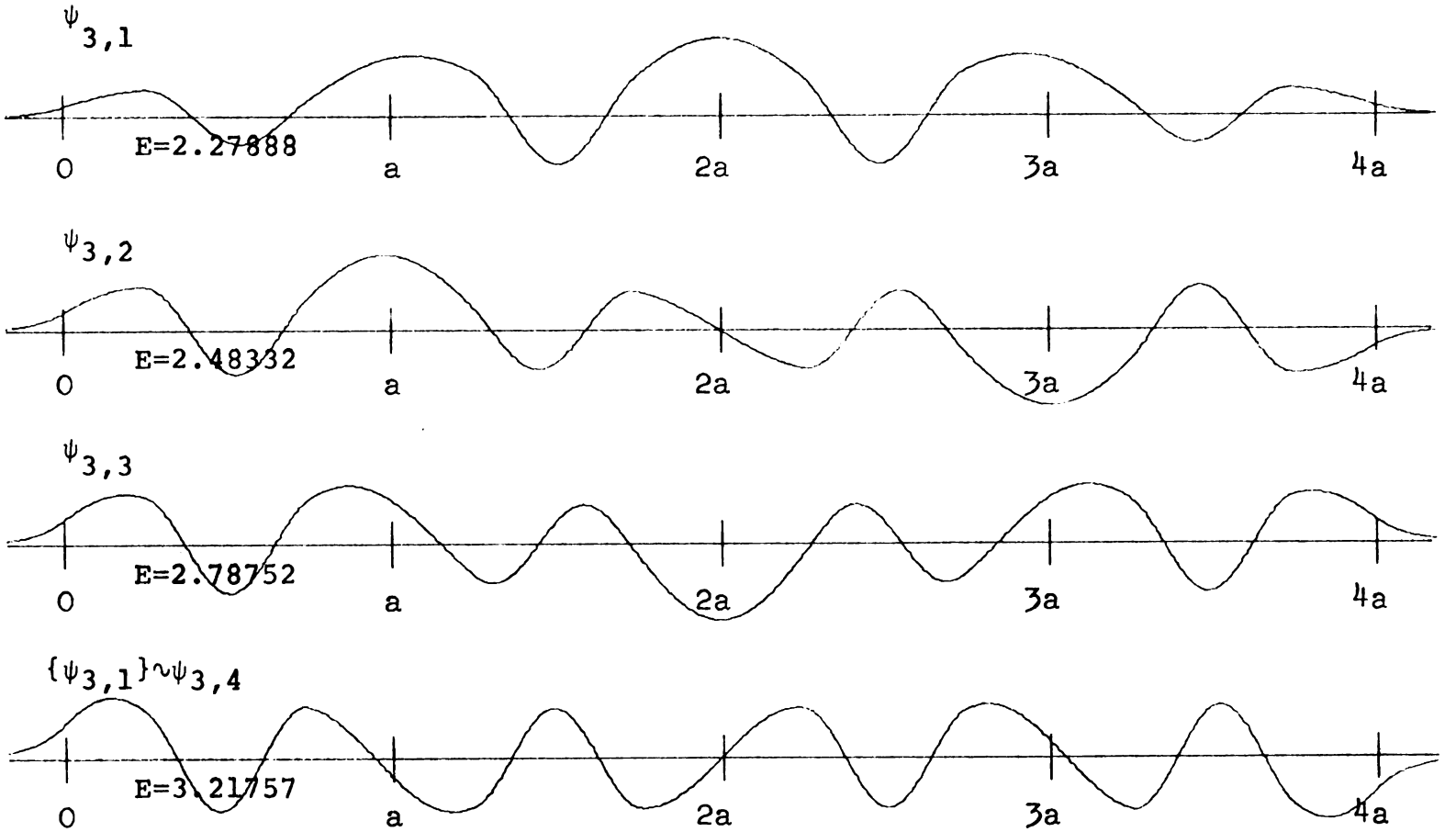

Figure 3.8c. Eigenfunctions for the third pass band and surface state eigenfunction which has emerged into the third attenuation band from the top of the third pass band (Shockley).

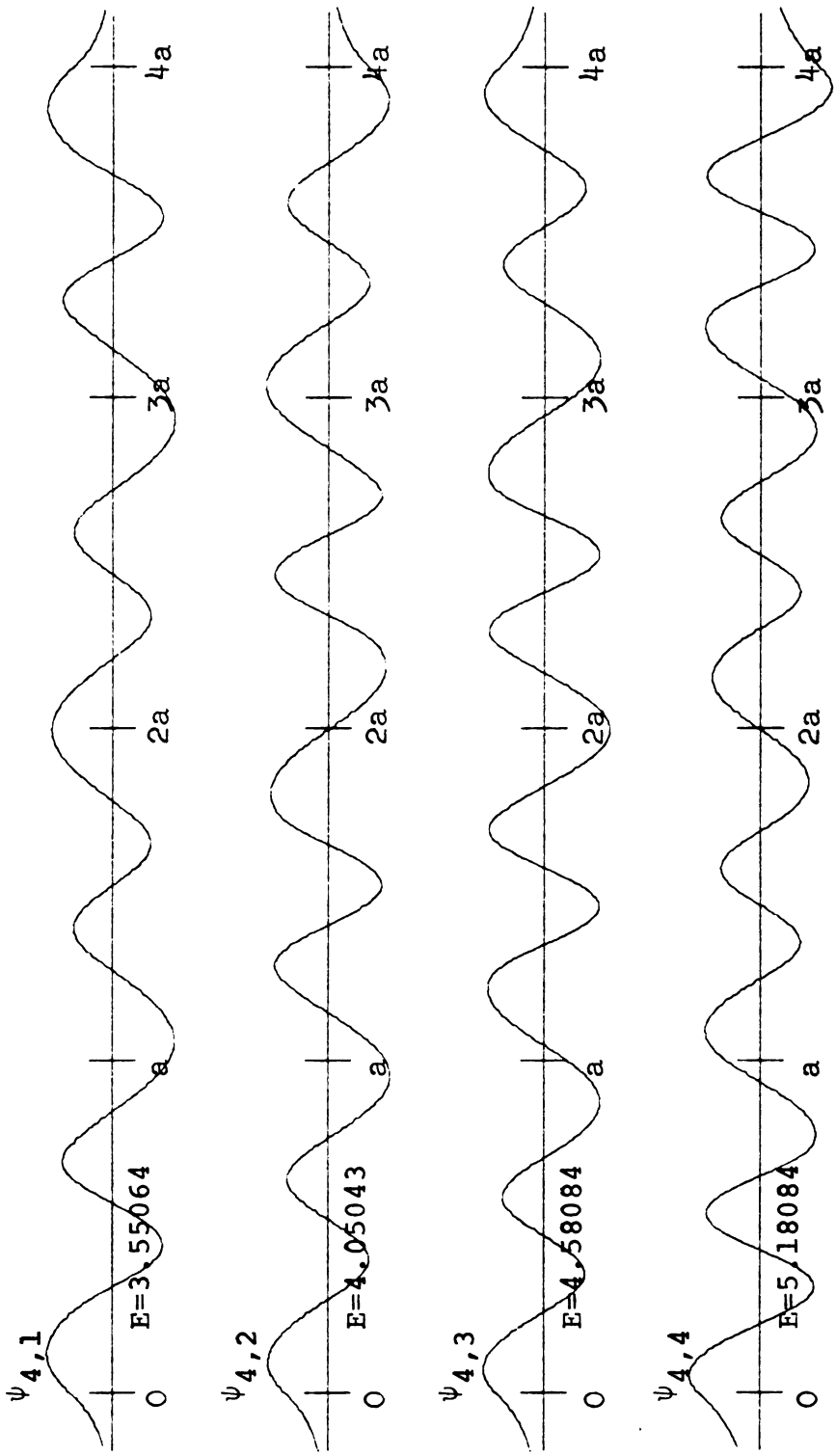

Figure 3.8d. Eigenfunctions for the fourth pass band (Shockley).

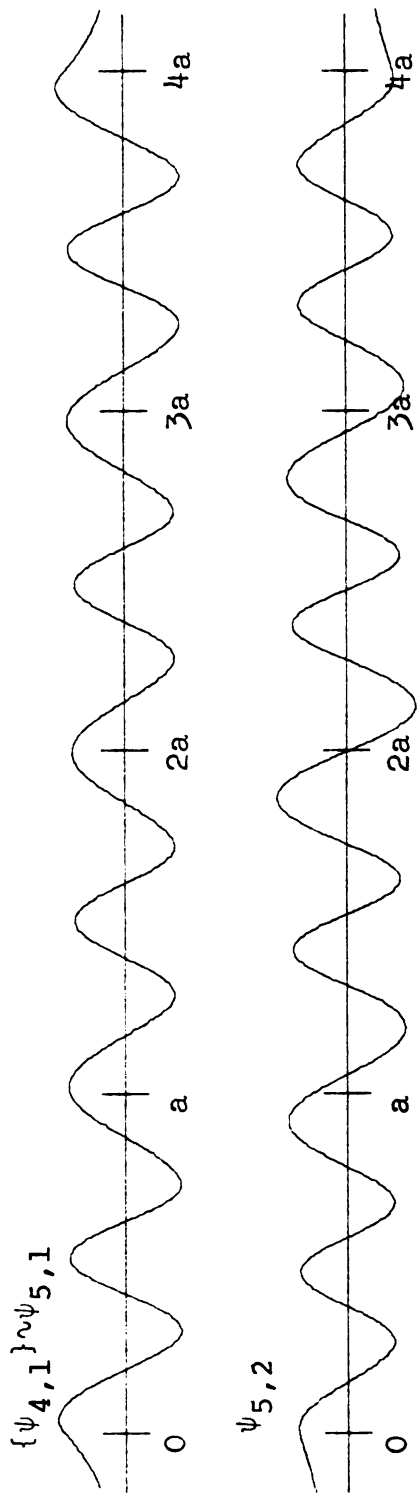

Figure 3.8e. Surface state eigenfunction which has emerged into the fourth attenuation band from the bottom of the fifth pass band and eigenfunction of the fifth partial pass band (Shockley).

less than 5 cells. To obtain a feeling for the way in which the surface wave functions behave for larger crystals, the surface states were calculated for attenuation bands 3 and 4 with N = 20. In this case, N is large enough to pull into the attenuation regions two pass-band states from the upper and lower pass-bands. The results are plotted in Figures 3.9 (a,b). Notice particularly the attenuation in Figure 3.9b where the K constant is larger.

The location of the surface state energies in the attenuation region is not the middle of the gap as was found by Shockley,[26] (a result quoted by several other authors). In fact, their location in the gap depends on the potential considered, the height of the vacuum level, and the number of cells. For the parameters considered in this example, we may observe the dependence of the surface state eigenvalues on the value of N for the two attenuation bands in which surface states occur. A plot of the surface state energy versus N is given in Figures 3.10 (a,b). The points on these graphs are not connected by a smooth line because the variation of the energy eigenvalues for fractional values of N is quite complicated, as will be shown in Section IV. It is evident from these graphs, that the surface states do not occur in the middle of the gaps, and that for N be-

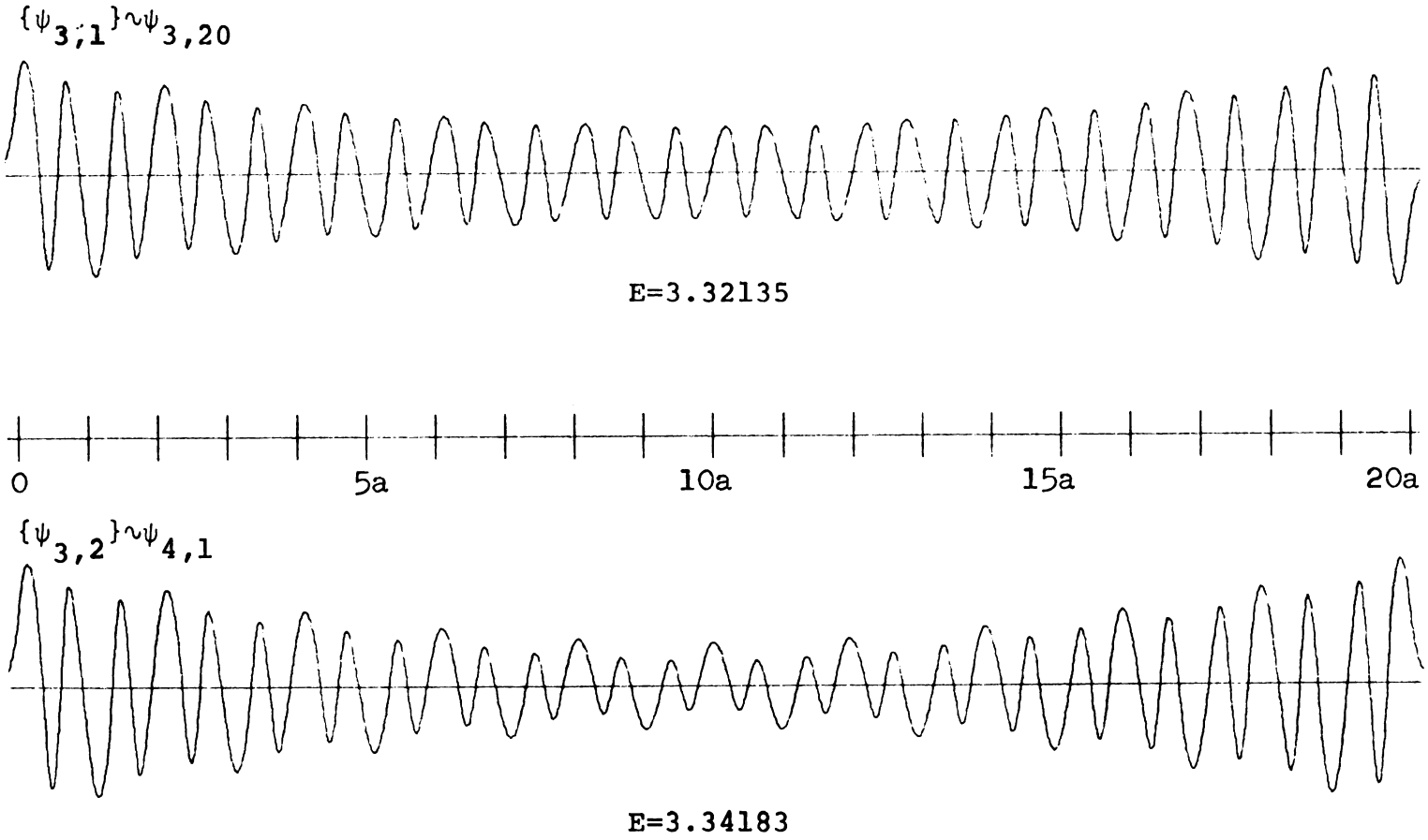

Figure 3.9a. Surface state eigenfunctions in the third attenuation band. The eigenstates for the top of the third and the bottom of the fourth pass bands have moved into the third attenuation band to form two surface states (Shockley).

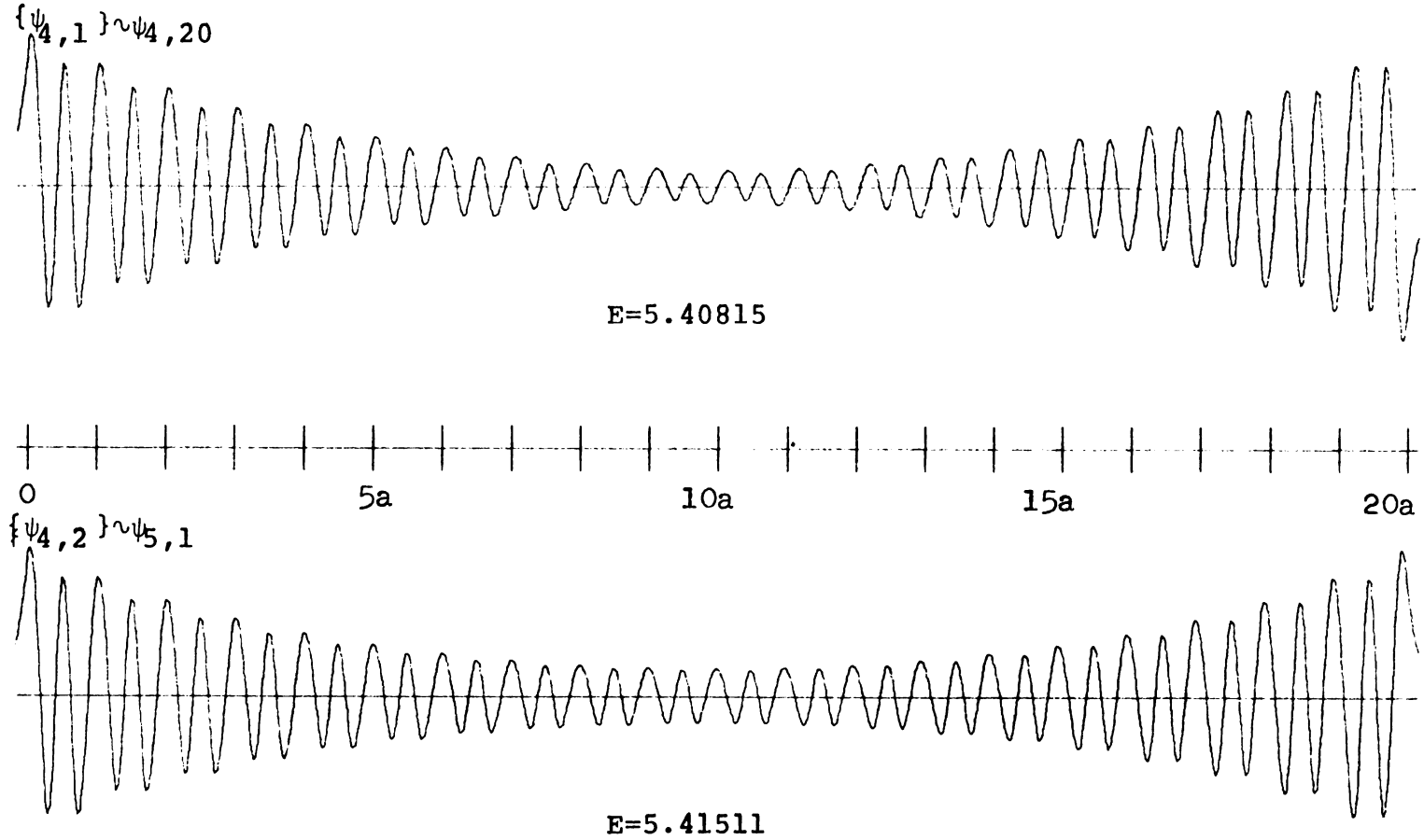

Figure 3.9b. Surface state eigenfunctions in the fourth attenuation band. The eigenstates for the top of the fourth and the bottom of the fifth pass bands have moved into the fourth attenuation band to form two surface states (Shockley).

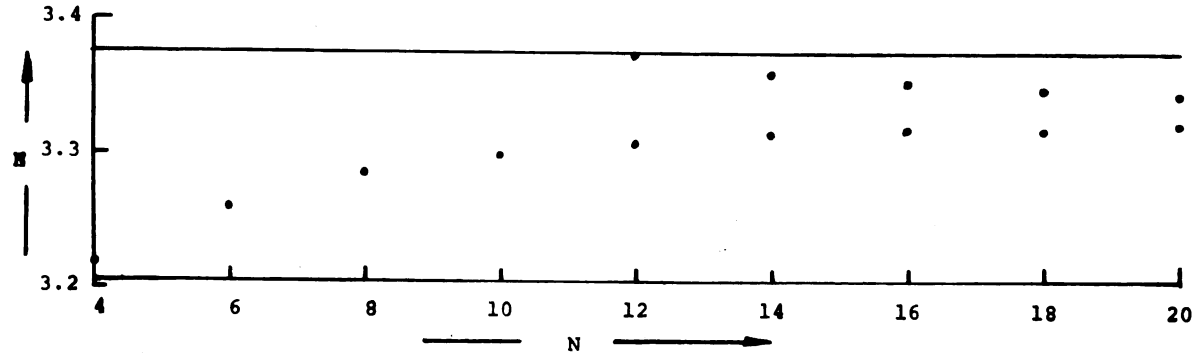

Figure 3.10a Surface state eigenvalues for the third attenuation band versus the number of cells.

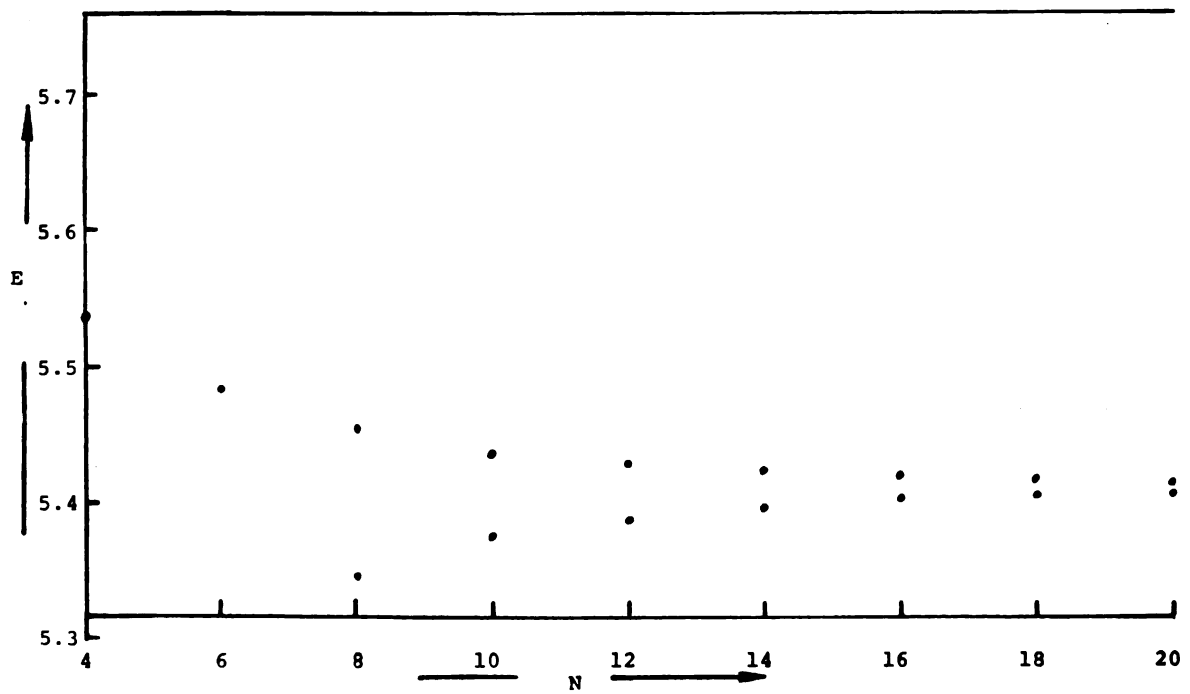

Figure 3.10b Surface state eigenvalues for the fourth attenuation band versus the number of cells.

coming very large, the two states approach a common asymtote. That is, they both approach the same energy. The rate at which they approach each other is dependent on the K constant; the more attenuated the wave function, the faster the states will come together with increasing N. It is clear from the above that this behavior may be explained quite simply.

Since the surface cells are terminated symmetrically, an electron which spends most of its time near the surface (in a surface state) and does not interact with the other surface state will have the same energy on either end of the crystal, for very large crystals. In other words, the electron on the right edge does not "feel" the electron on the left edge because of the localization. As the crystal is made smaller, the electrons begin to "see" one another and their interaction splits the degeneracy in the energy levels, in analogy to splitting of the atomic energy levels into bands when the atoms are brought together. For the surfaces very close together, the interaction is great enough to push one state completely out of the attenuation-band and change it into a pass-band state.

B. TAMM-TYPE TERMINATION

For the Tamm-type termination, for comparison, we shall use the same parameters a, b, V_o, V_1, V_2, N, as

we used for the Shockley-type termination. The cell for this case has a potential maximum at the center as shown below.

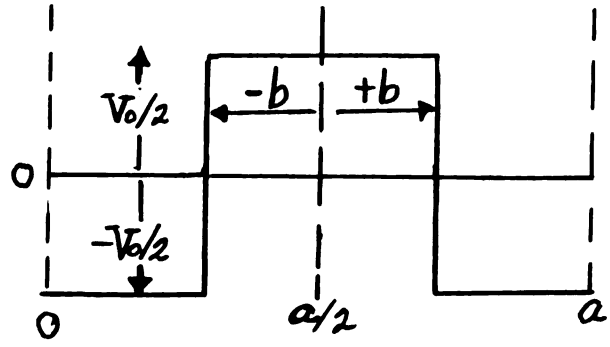

Proceeding as before, we may write down the solutions to Schrodinger's equation for $a/2-b \leq x \leq a/2+b$, $E < V_o/2$, as

$$g(x) = \cosh k(x-a/2), \qquad (3.10a)$$

$$k = \sqrt{\frac{2m}{\hbar^2}(V_o/2 - E)},$$

$$u(x) = \frac{\sinh k(x-a/2)}{k}. \qquad (3.10b)$$

Connecting these solutions to the solutions in the region $0 \leq x \leq a/2-b$ yields the expressions on the left edge of the cell of

$$g_o = \cosh kb \cos k(a/2-b) + \frac{K}{k}\sinh kb \sin k(a/2-b), \qquad (3.11a)$$

$$g_o' = k\cosh kb \sin k(a/2-b) - K\sinh kb \cos k(a/2-b), \qquad (3.11b)$$

$$u_o = -\frac{1}{K}\sinh Kb\cos k(\tfrac{a}{2}-b) - \frac{1}{k}\cosh Kb\sin k(\tfrac{a}{2}-b), \quad (3.11c)$$

$$u_o' = \cosh Kb\cos k(\tfrac{a}{2}-b) - \frac{k}{K}\sinh Kb\sin k(\tfrac{a}{2}-b), \quad (3.11d)$$

$$k = \sqrt{\tfrac{2m}{\hbar^2}(E+V_o/2)}.$$

For $E = V_o/2$, $E > V_o/2$, we connect to the appropriate functions. With the parameters chosen earlier, a/2 is equal to 2b, so that the functions g_o', g_o, u_o', u_o, for the Tamm-type termination may be related to the same parameters for the Shockley-type termination. Thus we see by inspection of the two sets of equations that

SHOCKLEY		TAMM	
g_o'	=	g_o',	(3.12)
g_o,	=	u_o',	
u_o'	=	g_o	
u_o	=	u_o	

This may be illustrated by reflecting Figure 3.3 across the $V_o = 0$ vertical axis as shown in Figure 3.11. The band edges are labeled to clearly indicate which function determines the boundary. For small values of V_o, the sequence of functions is given by

$$g_o,(u_o',g_o),u_o,g_o',g_o,u_o',(g_o',u_o),(u_o',g_o). \quad (3.13)$$

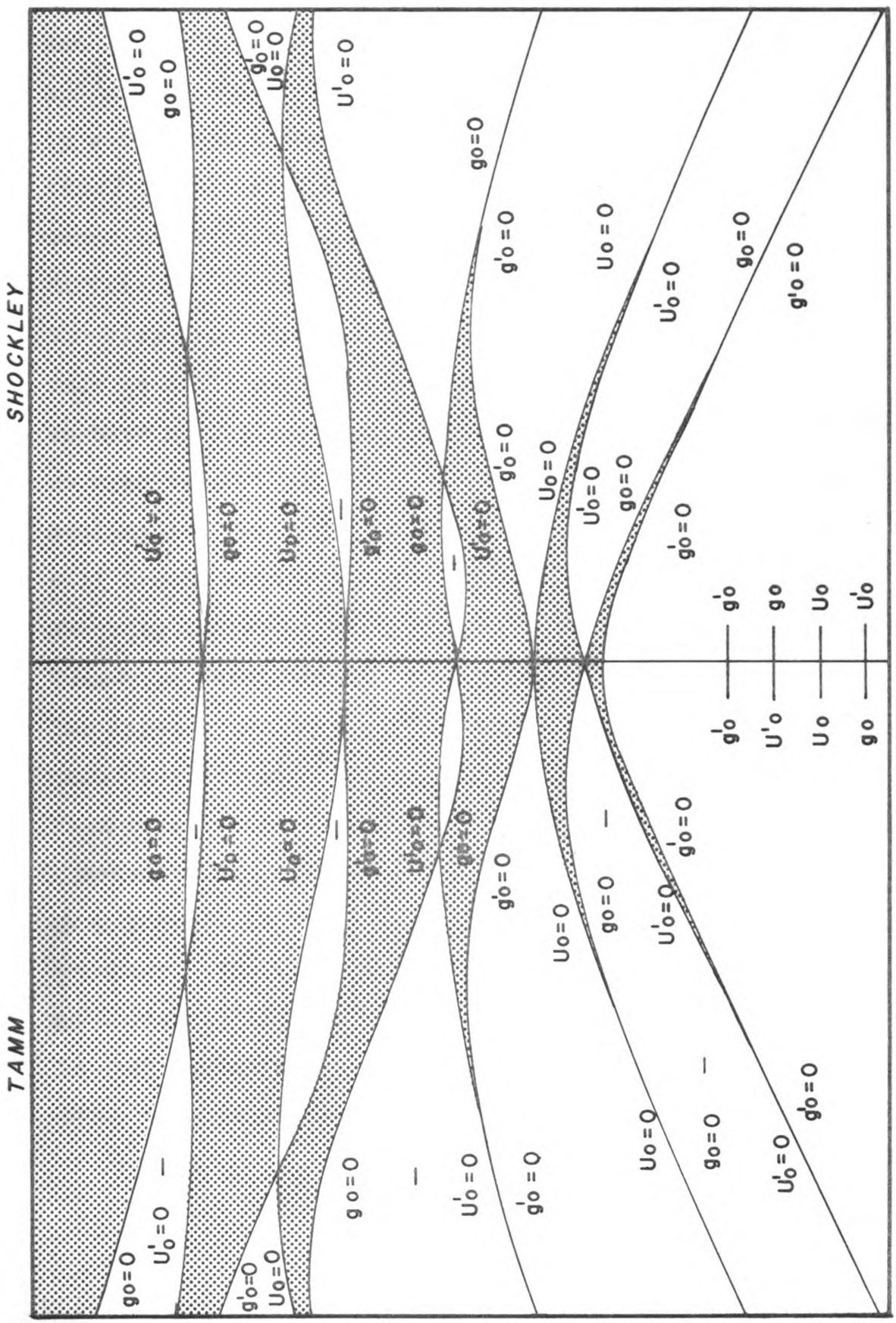

Figure 3.11 Comparison of Tamm and Shockley band structures.

By previous considerations, we expect to find surface states between ($u_o' = 0$, $g_o = 0$), ($g_o' = 0$, $u_o = 0$), and ($u_o' = 0$, $g_o = 0$). Note also that some crossing and uncrossing of the band edges has occurred at $V_o = 0$ in going from a Shockley-type termination to a Tamm-type termination. As V_o increases, some of the bands again cross to yield a tight-binding situation. The main difference between this Tamm-type termination and the Shockley-type termination is that for the tight-binding case we still have surface states in the Tamm case but we have no surface states for the Shockley case. Actually, as used by most authors (and in this paper so far), the designation Tamm-type termination is a misnomer. This will become more evident later. Suffice it to say that Shockley states as well as Tamm states may occur for the Tamm-type termination. We shall distinquish between the two types of states by the fact that Shockley-type states occur between pass-bands which have crossed once whereas Tamm-type states occur between pass-bands which have crossed twice. The Shockley-type states occur only for weak potentials and disappear as the potential becomes stronger. The Tamm-type states occur only for strong potentials. Another characteristic which can be used to distinguish the two types of states is the degree to which they penetrate into the crystal, or in other words,

their localization. The Shockley-type surface state has a large attenuation length, being able to penetrate rather far into the crystal, as surface states go. The Tamm-type surface state, on the other hand, is quite localized and is appreciable only in the first cell near the surface. Both types of states may occur at the same time for weak potentials. This is because for low energies, close to or below the maximum of the periodic potential, the electron feels the effect of the potential quite strongly and thus is essentially tightly bound. For higher energies, the effect of the potential upon the electron is much less, allowing the electron to behave like an almost free electron. Thus when both types of states occur, we expect to find the Tamm-type states occurring at very low energies whereas we expect the Shockley-type to occur near the vacuum level.

Proceeding as we did with the Shockley-type termination, we apply the boundary conditions for the Tamm-type termination to determine the eigenvalues. Figure 3.12 illustrates the graphical procedure. This figure should be compared with Figure 3.6 for the Shockley case. Although it is not evident from the graph, the crossing of the K_1 curve in the attenuation band region between ($u_o' = 0$, $g_o = 0$) is actually two crossings, one curve superimposed on the other. These two eigenstates are

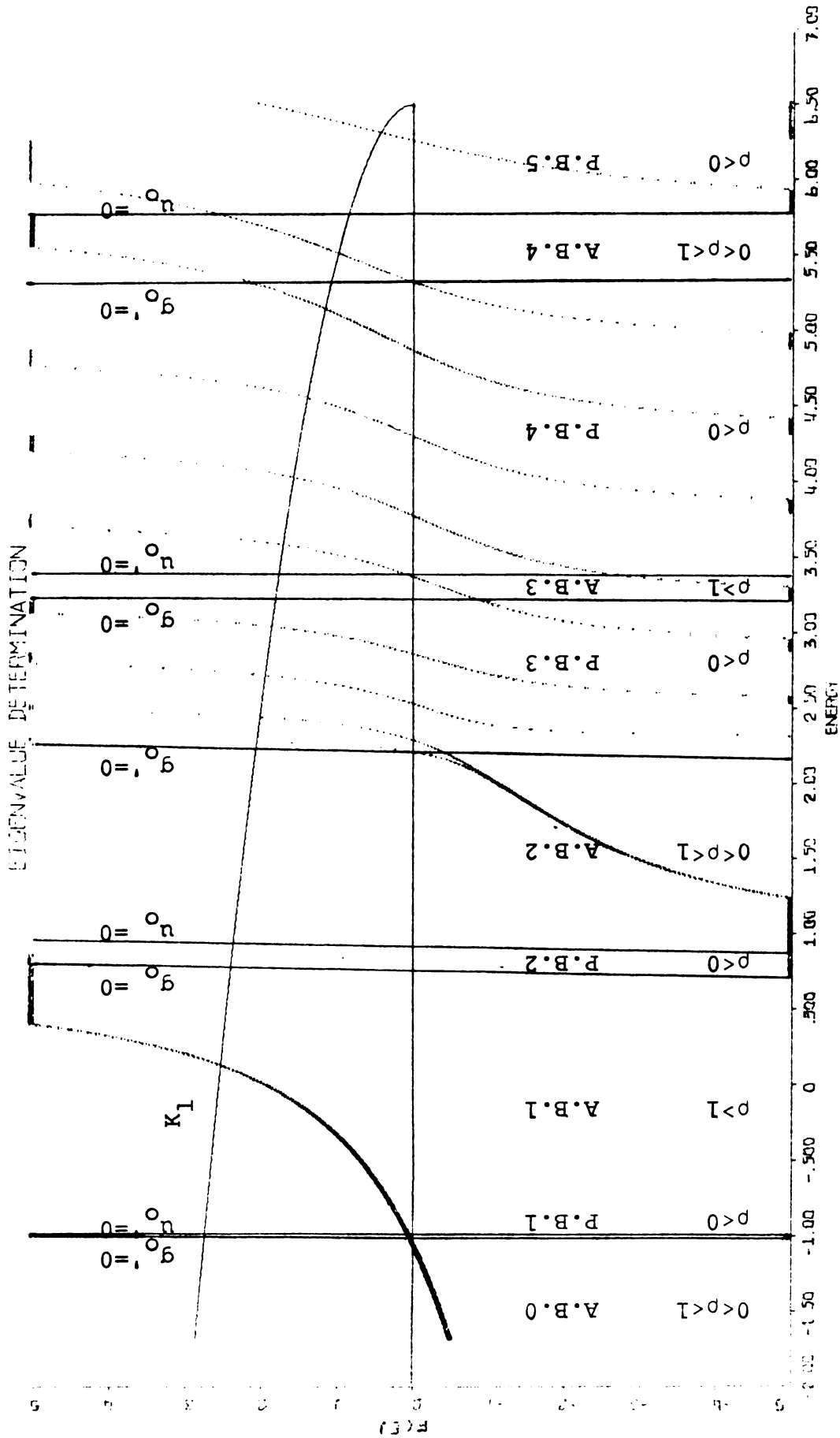

Figure 3.12. Determination of the eigenvalues for the Tamm type termination. The crossing of the K_1 curve with a dotted curve determines an eigenvalue.

of the Tamm-type since they occur for very low energies. The surface state occurring between ($g_o' = 0$, $u_o = 0$) is exactly analogous to the surface state found for the Shockley-type termination. The same considerations which determine whether there will be 0, 1, or 2 states in this gap may be applied to this situation.

An energy versus (k and K) graph is shown in Figure 3.13. This graph should be compared with Figure 3.7; note the differences and the similarity. In attenuation band 1, note that the value of K in this range is actually off the scale of the graph and was not plotted outside the limits shown. However, the X's (there are two X's, one superimposed upon the other) are positioned at the point where the K curve would go if it had been plotted on a larger scale. The X's of course represent the eigenvalues obtained from Figure 3.12. The pass-band states in pass-band 4 and 5 and the surface state in attenuation-band 4 are approximately the same for both Tamm- and Shockley-type terminations. The surface state in attenuation band 4 has approximately the same magnitude of attenuation (i.e. K) as that of the Shockley-type termination state calculated earlier, and we expect the same general behavior of the wave function going into the crystal. However, the two states occurring in attenuation-band 1 have a very large attenuation constant K and should

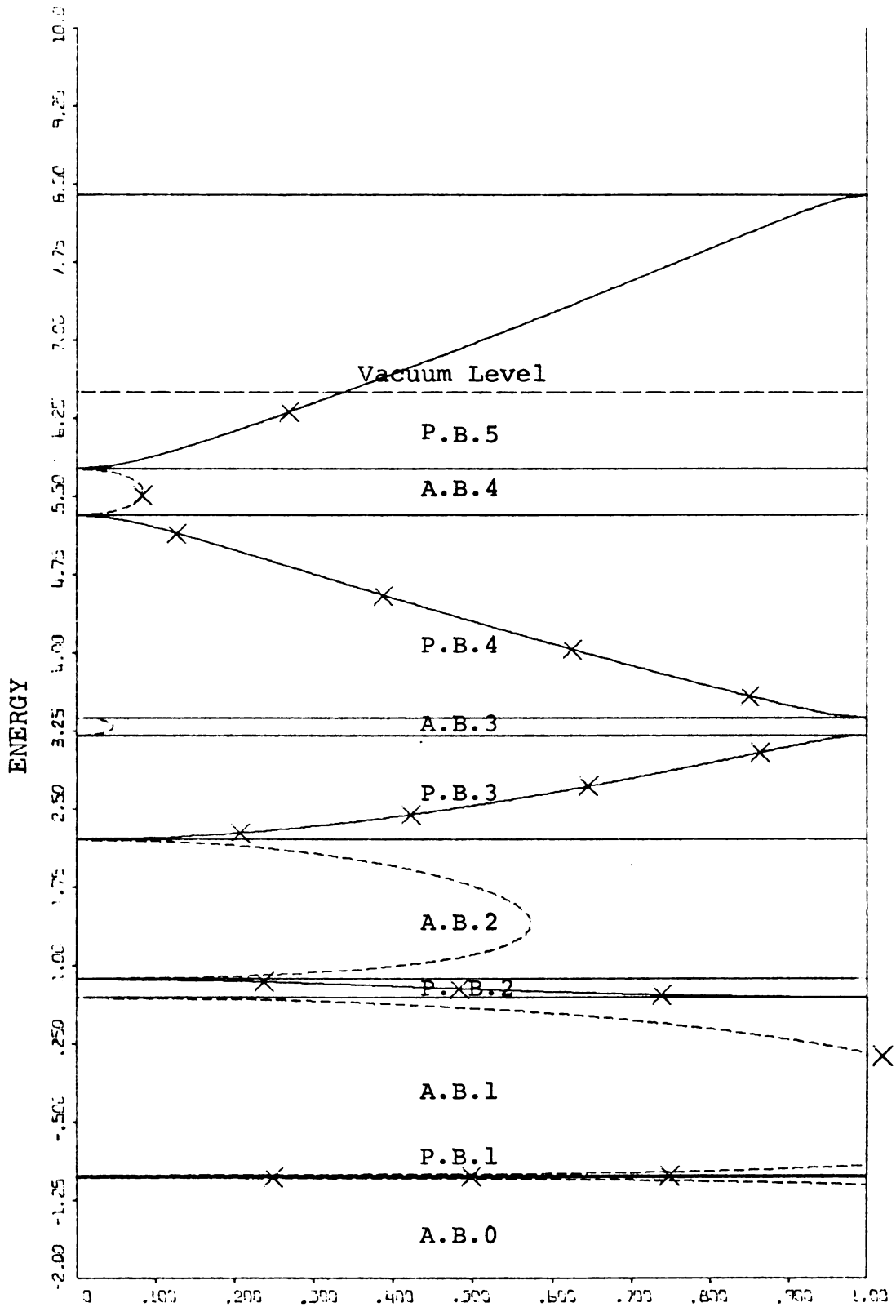

Figure 3.13. Energy versus (k and K). The X's denote eigenvalues which were determined in Figure 3.12 (Tamm).

be highly localized near the surface.

Figures 3.14 (a-e) are plots of the wave functions for the energy eigenvalues obtained above. These wave functions should be compared with Figures 3.8 (a-e) for the Shockley-type termination. Note particularly the Tamm-type states which are plotted at the bottom of Figure 3.14a and at the top of Figure 3.14b. They are quite localized at the surface and in fact extend further outside the crystal than the other surface states considered. Note also the energies at which each occurs. They indeed lie practically at the same energy due to the large attenuation and consequent lack of interaction. This result has been discussed earlier for the Shockley-type surface states except that in that case a larger crystal was required to establish it. Figure 3.15 is a plot of the surface state wave functions in the 4-th attenuation band for 20 cells. As may be seen by comparison with Figure 3.9b, the differences between the states are small and hence the designation of Shockley-type states for both sets.

Finally, we should comment that the procedure outlined for finding the energy states by the graphical method of plotting various quantities was only for illustrative purposes. The actual computations were performed on a CDC 6500 computer, with the processes

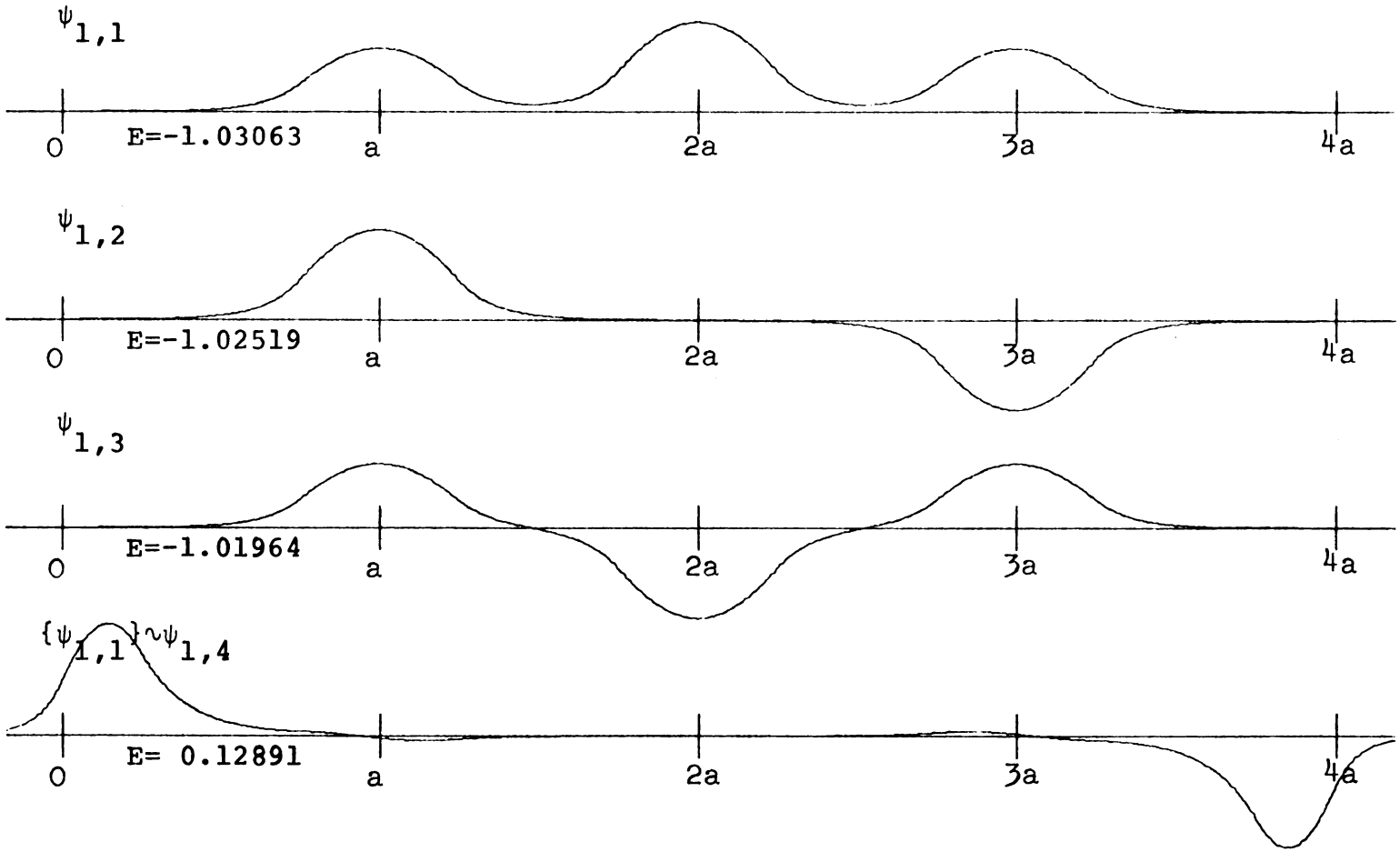

Figure 3.14a. Eigenfunctions for the first pass band and surface state eigenfunction which has emerged into the first attenuation band from the top of the first pass band (Tamm).

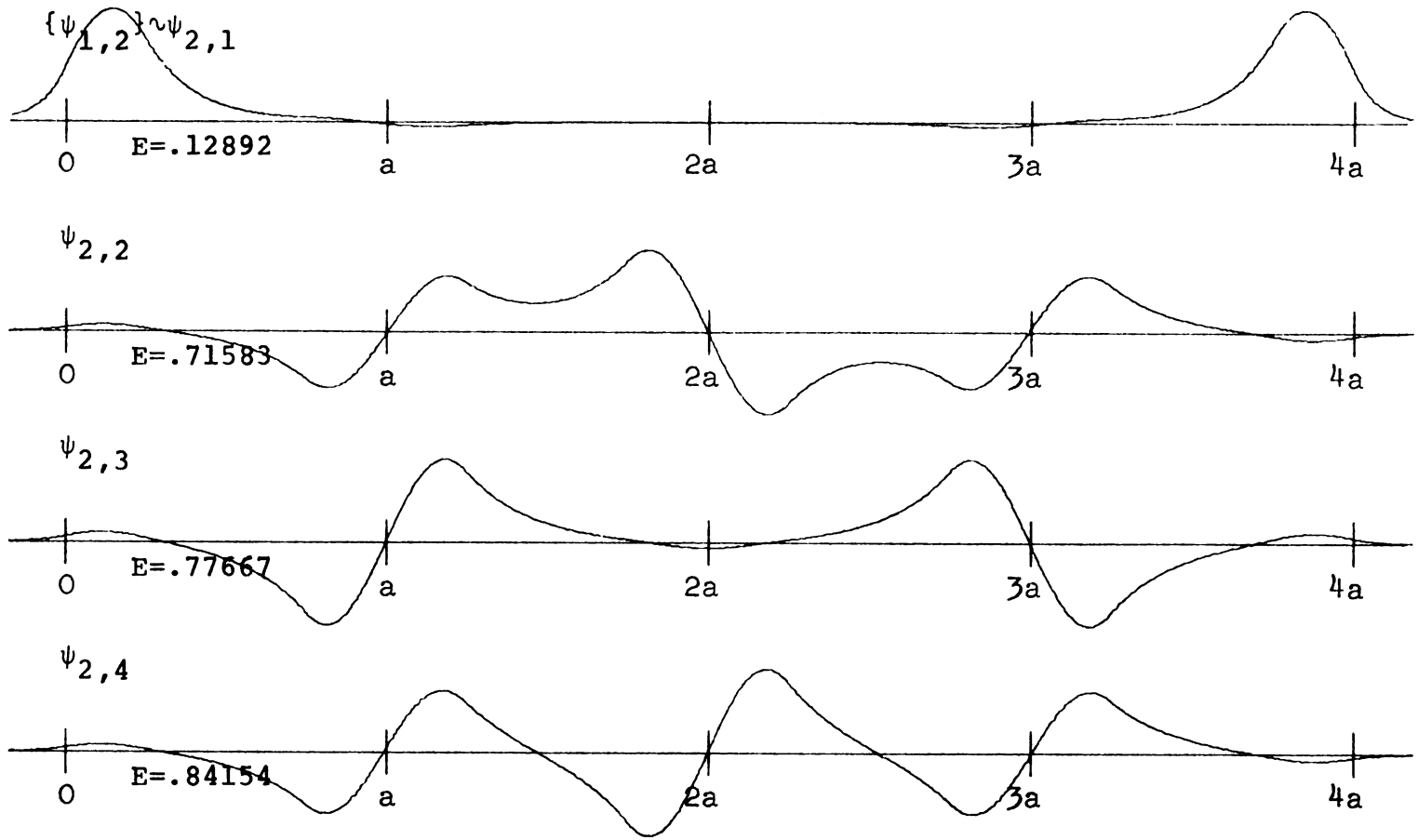

Figure 3.14b. Surface state eigenfunction which has emerged into the first attenuation band from the bottom of the second pass band and eigenfunctions of the second pass band (Tamm).

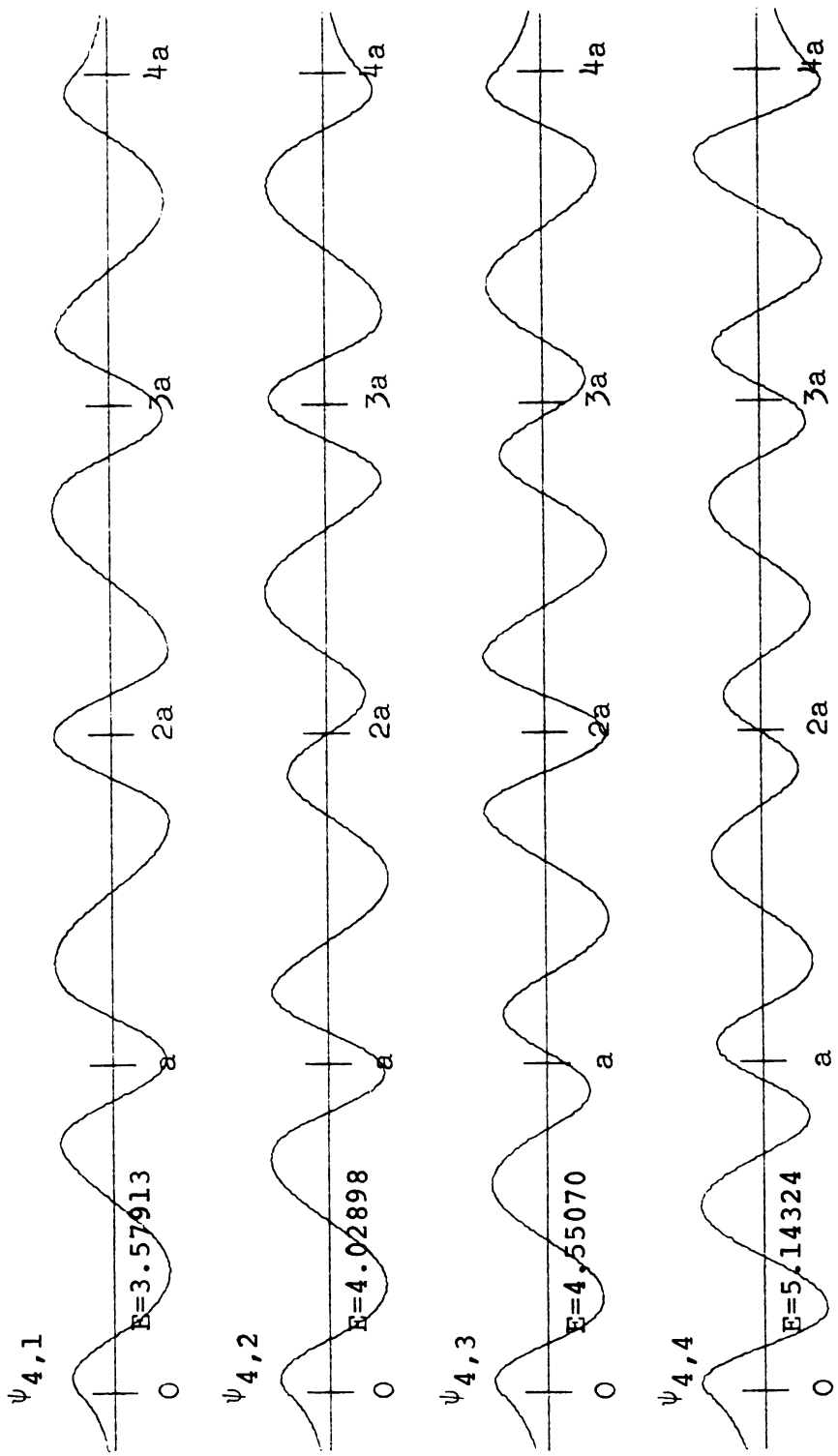

Figure 3.14d. Eigenfunctions for the fourth pass band (Tamm).

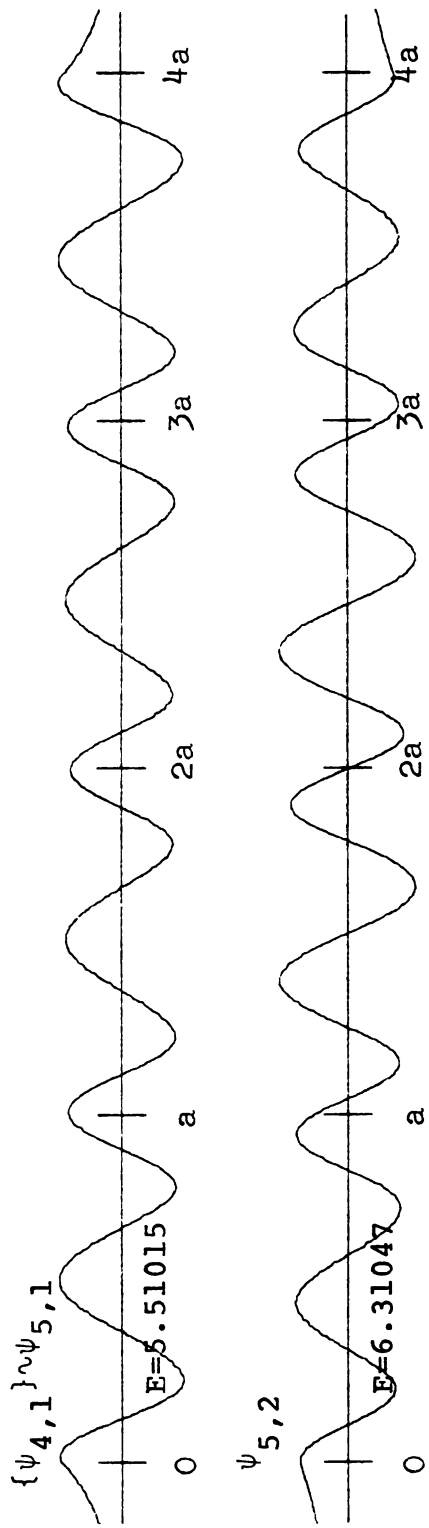

Figure 3.14e. Surface state eigenfunction which has emerged into the fourth attenuation band from the bottom of the fifth pass band and eigenfunction of the fifth partial pass band (Tamm).

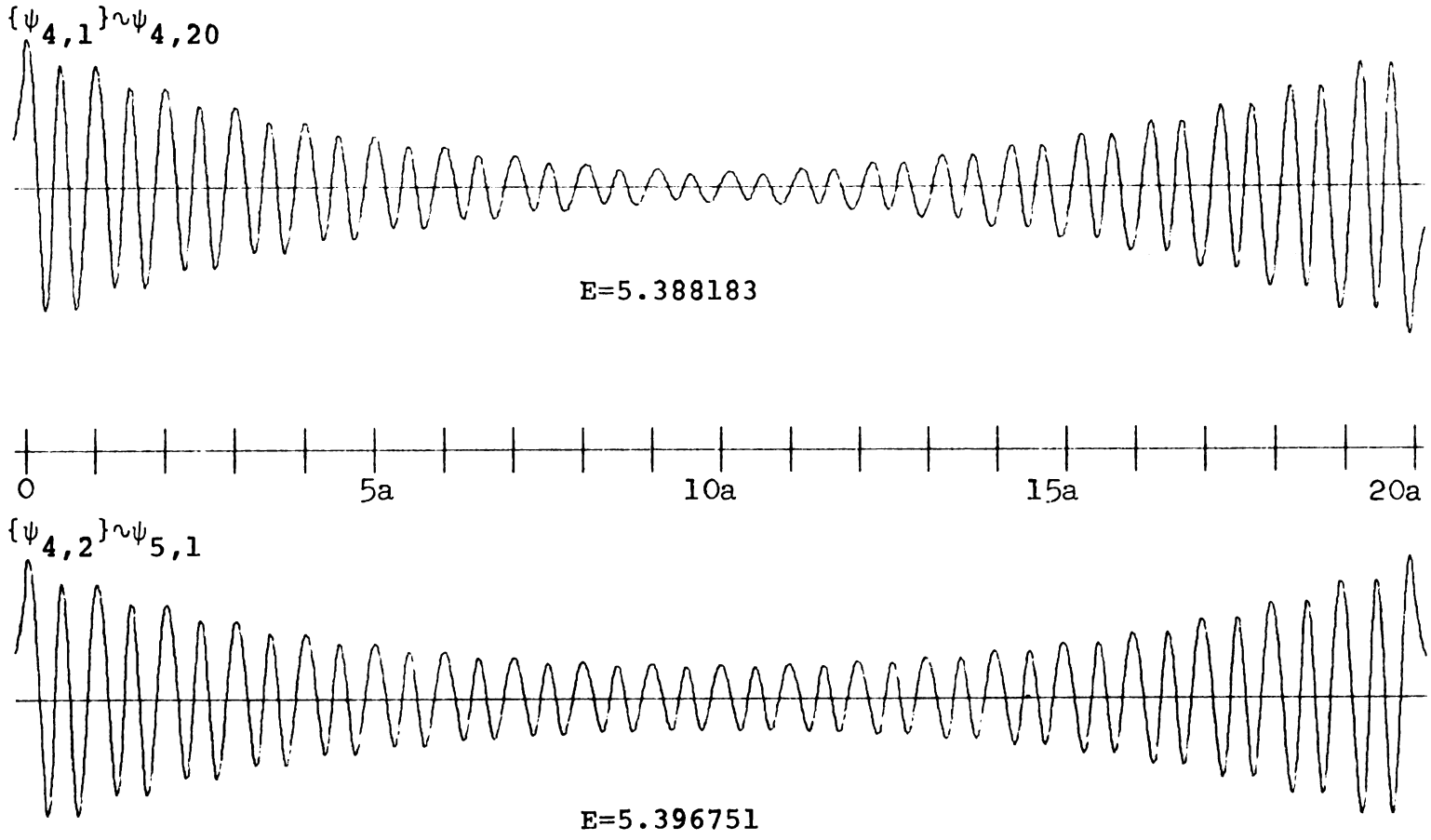

Figure 3.15. Surface state eigenfunctions in the fourth attenuation band. The eigenstates for the top of the fourth and the bottom of the fifth pass bands have moved into the fourth attenuation band to form two two surface states (Tamm).

outlined taking place internally in the computer. The total time necessary for the calculation of the band edges and 18 eigenstates to 6-figure accuracy was of the order of 10-15 seconds.

SECTION IV

ARBITRARY TERMINATION OF A FINITE PERIODIC POTENTIAL

The problem of termination of the periodic potential at an arbitrary point in the end cell will now be considered. To be more specific, we shall terminate the potential at one end by a step function at an arbitrary point in the end cell and at the other end by a step function at the potential minimum. (see Figure 4.1) Until now, with one exception, general conclusions have been drawn from symmetry arguements for crystals terminated in either a symmetric or antisymmetric manner. In the literature, the various approximation methods which have been used most extensively include the nearly-free-electron method, and the tight-binding (LCAO or MO) method. The one exception is a paper by Levine,[27] in which the problem of the arbitrary termination of a semi-infinite cosine potential is treated. We expect to find somewhat different properties for a finite crystal; consequently, we shall carry out the calculations for the above mentioned problem to determine exactly what the differences are.

This problem is made considerably more difficult by the arbitrary termination since now the wave function

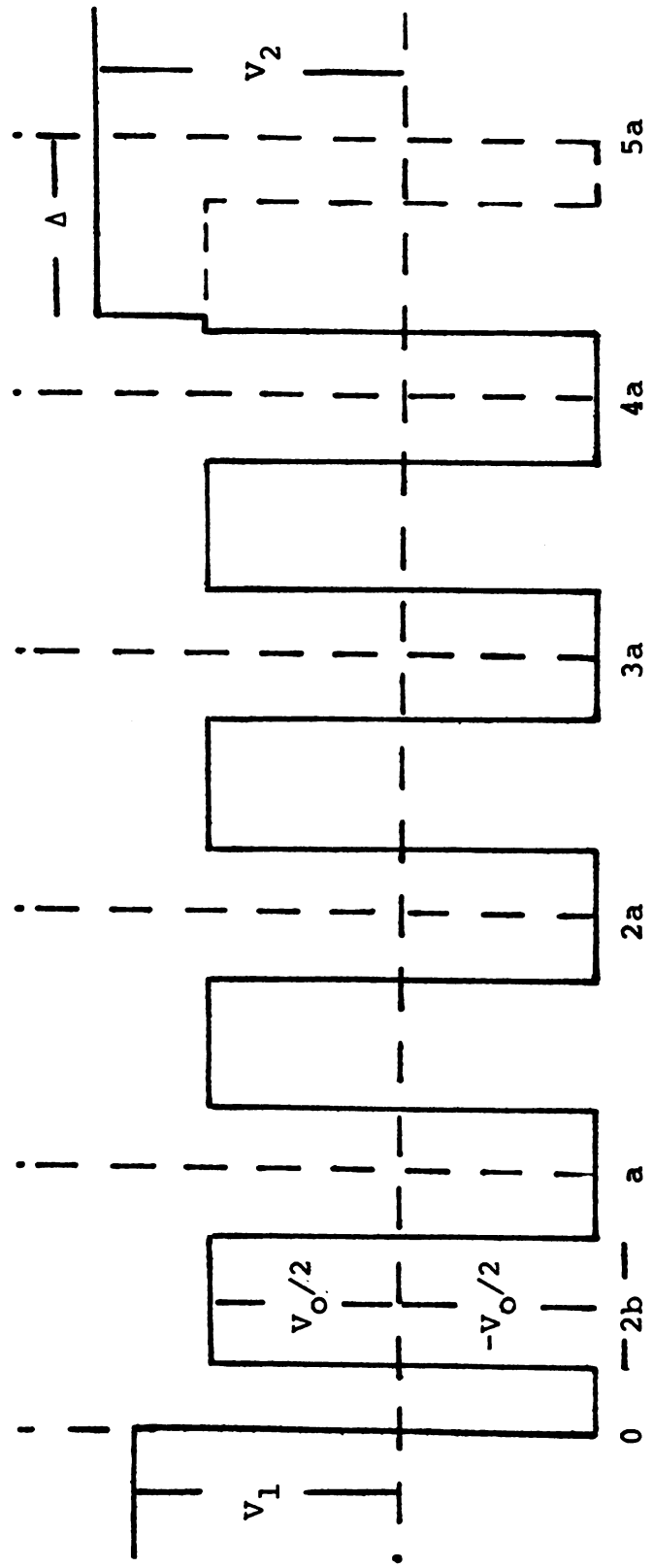

Figure 4.1. Termination of the periodic potential at an arbitrary point in the end cell.

and its derivative at the point of termination will not reduce to a simple form. From Figure 4.1, we see that the point of termination in the end cell is measured by the quantity Δ from the right edge. By continuously varying Δ through this end cell and calculating the eigenvalues for each value of Δ, we obtain a general idea of what effects an arbitrary termination has on the energy eigenstates.

Proceeding as we did in Sections II and III, we attempt to form a continuous wave function by matching the wave function and its derivative in each region to the wave function and its derivative in a neighboring region.

For $x \leq 0$, the wave function is of the form

$$\psi(x) = A e^{K_1 x} \quad , K = \sqrt{\frac{2m}{\hbar^2}(V_1 - E)}. \quad (4.1)$$

For $0 \leq x \leq Na - \Delta$, we have

$$\psi(x) = C_+ \psi_+(x) + C_- \psi_-(x), \quad (4.2)$$

where the form of ψ_+, ψ_- will depend on the energy range we are considering. For $x \geq Na - \Delta$,

$$\psi(x) = B e^{-K_1(x-(Na-\Delta))}. \quad (4.3)$$

Matching the logarithmic derivative at x = 0 yields the condition,

$$K_1 = \sigma_+\left(\frac{C_+ - C_-}{C_+ + C_-}\right), \tag{4.4}$$

while matching at x = Na- Δ yields

$$-K_1 = \left(\frac{C_+\psi_+'(Na-\Delta)+C_-\psi_-'(Na-\Delta)}{C_+\psi_+(Na-\Delta)+C_-\psi_-(Na-\Delta)}\right). \tag{4.5}$$

If we now set the right hand side of Eq. (4.4) equal to the negative of the right hand side of Eq. (4.5) and define the quantities,

$$x_1 = \psi_+'(Na-\Delta), \quad x_2 = \sigma_+\psi_+(Na-\Delta), \tag{4.6a}$$

$$y_1 = \psi_-'(Na-\Delta), \quad y_2 = \sigma_-\psi_-(Na-\Delta), \tag{4.6b}$$

we obtain

$$\left(\frac{C_+ - C_-}{C_+ + C_-}\right) = -\left(\frac{C_+x_1 + C_-y_1}{C_+x_2 - C_-y_2}\right). \tag{4.7}$$

Notice that $\sigma_+ = -\sigma_-$, and that x_1 becomes equal to x_2 and y_1 becomes equal to y_2 if Δ is equal to some integral multiple of the lattice constant. Multiplying Eq. (4.7) through by the denominators, and grouping

terms, we obtain a quadratic in C_+ and C_-,

$$C_+^2(\chi_1+\chi_2) + C_+C_-((\chi_1-\chi_2)+(y_1-y_2)) + C_-^2(y_1+y_2) = 0. \tag{4.8}$$

Factoring this equation, and using the Wronskian relation

$$W\{\psi_+, \psi_-\} = -2\alpha, \tag{4.9}$$

we find that C_+ in terms of C_- is given by

$$C_+ = \left[\frac{-[(\chi_1-\chi_2)+(y_1-y_2)] \pm \sqrt{[(\chi_1-\chi_2)-(y_1-y_2)]^2+(4\alpha)^2}}{2(\chi_1+\chi_2)}\right] C_-. \tag{4.10}$$

This equation may be simplified in form by considering the different forms of the wave function for the three regions $\rho < 0$, $0 < \rho < 1$, and $\rho > 1$. In each region, we may write the wave functions out explicitly and form the various sums and differences which are contained in Eq. (4.10). By defining new variables, we may simplify the form of Eq. (4.10) considerably. For $\rho < 0$, we define

$$\tan\phi/2 = \left(\frac{\frac{g'(a-\Delta)}{g_0'} + \frac{u(a-\Delta)}{u_0}}{\frac{u'(a-\Delta)}{u_0'} + \frac{g(a-\Delta)}{g_0}}\right)|\rho|^{\frac{1}{2}} \tag{4.11a}$$

$$R_1 = \tfrac{1}{2}\left(\frac{u'(a-\Delta)}{u_0'} + \frac{g(a-\Delta)}{g_0}\right)\cos\left(\frac{ka}{2}\right), \tag{4.11b}$$

$$R_2 = \frac{1}{2}\left(\frac{g'(a-\Delta)}{g_0'} + \frac{u(a-\Delta)}{u_0}\right)\sin(ka/2), \quad (4.11c)$$

$$\lambda_1 = \left(\frac{u'(a-\Delta)}{u_0'} - \frac{g(a-\Delta)}{g_0}\right)\cos(ka/2), \quad (4.11d)$$

$$\lambda_2 = \left(\frac{u(a-\Delta)}{u_0} - \frac{g'(a-\Delta)}{g_0'}\right)\sin(ka/2), \quad (4.11e)$$

$$T = \left(\frac{\lambda_1}{2}\right)\sin k(N-\tfrac{1}{2})a + \left(\frac{\lambda_2}{2}\right)\cos k(N-\tfrac{1}{2})a, \quad (4.11f)$$

$$r = \sqrt{R_1^2 + R_2^2}, \quad (4.11g)$$

$$\sin\beta_1 = -T/r. \quad (4.11h)$$

With these definitions, the matching condition given by Eq. (4.10) becomes

$$C_{+k} = \pm e^{-ik(N-\frac{1}{2})a + i\phi/2 \pm i\beta_1} C_{-k}. \quad (4.12)$$

For $0 < \rho < 1$, the definitions are

$$\tanh\frac{\phi_2}{2} = \left(\frac{\frac{g'(a-\Delta)}{g_0'} + \frac{u(a-\Delta)}{u_0}}{\frac{u'(a-\Delta)}{u_0'} + \frac{g(a-\Delta)}{g_0}}\right)|\rho|^{\frac{1}{2}}, \quad (4.13a)$$

$$R_1 = \frac{1}{2}\left(\frac{u'(a-\Delta)}{u_0'} + \frac{g(a-\Delta)}{g_0}\right)\cosh(ka/2), \quad (4.13b)$$

$$R_2 = \frac{1}{2}\left(\frac{g'(a-\Delta)}{g_0'} + \frac{u(a-\Delta)}{u_0}\right)\sinh(ka/2), \quad (4.13c)$$

$$\lambda_1 = \left(\frac{u'(a-\Delta)}{u_0'} - \frac{g(a-\Delta)}{g_0}\right)\cosh\left(\frac{Ka}{2}\right), \quad (4.13d)$$

$$\lambda_2 = \left(\frac{u(a-\Delta)}{u_0} - \frac{g'(a-\Delta)}{g_0'}\right)\sinh\left(\frac{Ka}{2}\right), \quad (4.13e)$$

$$T = \left(\frac{\lambda_1}{2}\right)\sinh K(N-\tfrac{1}{2})a + \left(\frac{\lambda_2}{2}\right)\cosh K(N-\tfrac{1}{2})a, \quad (4.13f)$$

$$r = \sqrt{R_1^2 - R_2^2}, \quad (4.13g)$$

$$\sinh\beta_2 = -T/r. \quad (4.13h)$$

Then Eq. (4.10) becomes

$$C_{+k} = \pm e^{-K(N-\frac{1}{2})a + \phi_2/2 \pm \beta_2} C_{-K}. \quad (4.14)$$

Similarly, for $\rho > 1$

$$\coth\phi_{3/2} = \left(\frac{\frac{u(a-\Delta)}{u_0} + \frac{g'(a-\Delta)}{g_0}}{\frac{u'(a-\Delta)}{u_0'} + \frac{g(a-\Delta)}{g_0}}\right)|\rho|^{\frac{1}{2}}, \quad (4.15a)$$

$$R_1 = \tfrac{1}{2}\left(\frac{u'(a-\Delta)}{u_0'} + \frac{g(a-\Delta)}{g_0}\right)\sinh\left(\frac{Ka}{2}\right), \quad (4.15b)$$

$$R_2 = \tfrac{1}{2}\left(\frac{u(a-\Delta)}{u_0} + \frac{g'(a-\Delta)}{g_0'}\right)\cosh\left(\frac{Ka}{2}\right), \quad (4.15c)$$

$$\lambda_1 = \left(\frac{u'(a-\Delta)}{u_0'} - \frac{g(a-\Delta)}{g_0}\right)\sinh\left(\frac{Ka}{2}\right) \quad (4.15d)$$

$$\lambda_2 = \left(\frac{u(a-\Delta)}{u_0} - \frac{g'(a-\Delta)}{g_0'}\right)\cosh\left(\frac{ka}{2}\right), \quad (4.15e)$$

$$T = \left(\frac{\lambda_1}{2}\right)\cosh k(N-\tfrac{1}{2})a + \left(\frac{\lambda_2}{2}\right)\sinh k(N-\tfrac{1}{2})a, \quad (4.15f)$$

$$r = \sqrt{R_2^2 - R_1^2}, \quad (4.15g)$$

$$\sinh\beta_3 = T/r. \quad (4.15h)$$

Eq. (4.10) then becomes

$$C_{+k} = \pm e^{-k(N-\frac{1}{2})a + \phi_3/2 \pm \beta_3} C_{-k}. \quad (4.16)$$

Substitution of Eqs. (4.12), (4.14), or (4.16) into Eq. (4.4) yields

$\underline{\rho < 0}$

$$K_1 = -i\sigma_4 \tan\left(\frac{k(N-\frac{1}{2})a - \phi_1/2 - \beta_1}{2}\right), \quad (4.17a)$$

$$K_1 = i\sigma_4 \cot\left(\frac{k(N-\frac{1}{2})a - \phi_1/2 + \beta_1}{2}\right), \quad (4.17b)$$

where $\sigma_4 = -i\left(\frac{u_0'}{u_0}\right)|\rho|^{\frac{1}{2}}$.

$\underline{0 < \rho < 1}$

$$K_1 = -\sigma_+ \tanh\left(\frac{K(N-\frac{1}{2})a - \phi_2/2 - \beta_2}{2}\right), \quad (4.18a)$$

$$K_1 = -\sigma_+ \coth\left(\frac{K(N-\frac{1}{2})a - \phi_2/2 + \beta_2}{2}\right), \quad (4.18b)$$

where $\sigma_+ = -(u_0'/u_0)\rho^{\frac{1}{2}}$.

The same formulae hold for $\rho > 1$, except that the definitions of K, ϕ_2 and β_2 are changed.

ϕ_1, ϕ_2, ϕ_3 and $\beta_1, \beta_2, \beta_3$ will, in general, exhibit quite complicated behavior as E or Δ is varied; thus is best discussed in connection with a specific potential. The procedure for finding the energy eigenvalues is the same as used before. We plot the two sides of Eq. (4.17) and Eq. (4.18) as functions of energy, and the points at which the equality is satisfied give us the eigenvalues. This is illustrated for the Kronig-Penney type potential in Figure 4.2, where we have plotted the energy eigenvalues as a function of the parameter Δ (see Figure 4.1) for N = 5 and a, b, V_0, V_1, and V_2 the same as in Section III. The lowest pass-band is not shown because it was so narrow that no details could be distinquished on the scale used to plot the graph. Figure 4.2 shows the change in the eigenvalues of the system as the crystal is continuously changed from N = 5 to N = 4 atoms.

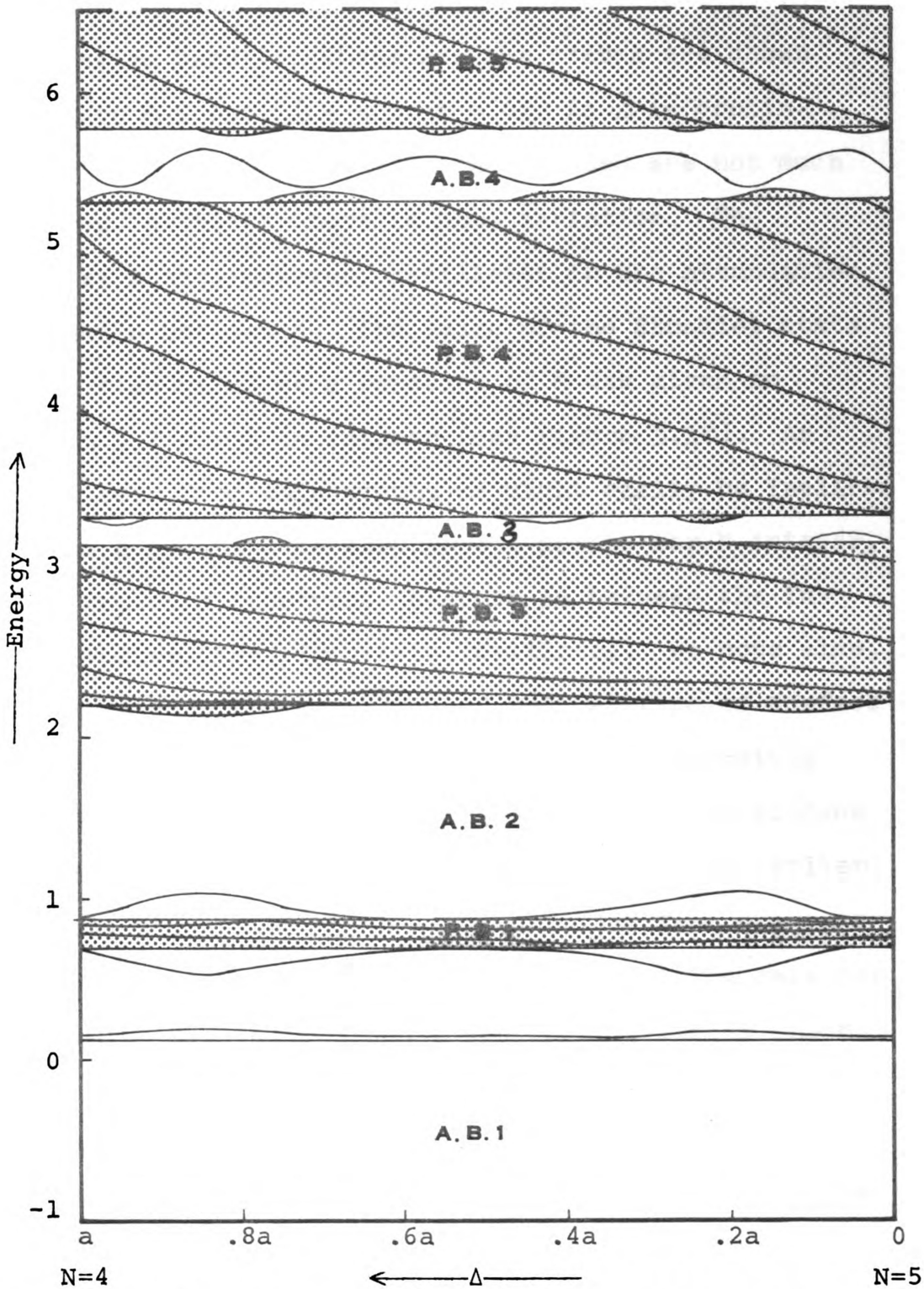

Figure 4.2 Energy eigenvalues as a function of the cell termination parameter Δ.

Upon inspecting the eigenvalue spectrum calculated for the Tamm-type terminations in Section III, we observe that there are 2 surface states of the Tamm-type in attenuation band 4. These surface states are shown in Figure 4.2 for Δ = a or N = 4. As Δ is continuously decreased the Tamm surface states are not much affected, although there is some variation. The Shockley state, however, oscillates in the attenuation band quite noticable. The value of the Shockley state energy eigenvalue as a function of N was given in Section III for N an integer (see Figure 3.10). As may be seen from this graph, we might easily be inclined to draw a smooth line through the points for N integer, which would be incorrect, because in between the integer values, the eigenstate oscillates. We note also, in Figure 4.2, the emergence of another type of surface state which is absent in symmetric or antisymmetric terminations. Levine[27] has found similar type surface states for the semi-infinite crystal mentioned earlier. However, the states which he finds cross from one pass-band into the next pass-band, which is not the case for the finite crystal. Indeed, the surface states which emerge lie very close at all times to the pass-band from which they originated and periodically disappear and reappear with decreasing Δ . The behavior of the

pass-band eigenstates is interesting but not surprising. As the crystal length increases, the number of pass-band states must increase. The new states emerge from the upper pass-band edge while some of the old states disappear into the lower pass-band edge. But the net effect of increasing the crystal by one atom is to increase the number of pass-band states by one.

The case of arbitrary termination, as may be seen from the above, leads to extra energy states. Since for real crystals we expect the termination of the crystal by the surface to be a more or less arbitrary termination, we might expect to find more states than are usually considered in the calculations which have been carried out to date for symmetric or antisymmetric terminations. These new states do not seem to be related to the bulk properties of the crystal (i.e. the number of cells, etc.) but depend only on the nature of the termination.

SECTION V

LOW ENERGY ELECTRON DIFFRACTION FROM FINITE ONE-DIMENSIONAL PERIODIC POTENTIALS

In this section, we shall study the elastic low energy electron diffraction (LEED) for electrons normally incident upon a crystal surface by calculating the reflection coefficient for a plane wave incident upon a one-dimensional periodic potential at energies greater than the vacuum level. The applicability of this model to real metallic crystals is questionable since the energies involved are high enough to ionize the core electrons, and many-body effects should be large.[29] However, if we assume that we are only interested in very low energy electrons, and that we are dealing principally with insulators, then it is probable that the main contribution to the elastic scattering is from the static potential due to the ion-cores inside the solid. This static potential should, in fact, be energy dependent as are most calculations on real crystals, but we shall assume that it is relatively constant over the energy range onsidered.

There has been much interest in recent years in the use of LEED as a tool for the study both of surfaces and the interaction of electrons with solids. Several methods

have been employed to study this problem. The method used in this thesis may be classified as a "dynamical" model calculation of which there are two different variants. The first variant is based on a generalization of Lax's multiple x-ray diffraction theory. The second, with which we shall be concerned is based on a band structure treatment. For more detail about each method, the reader is referred to the literature.[30-36] The method we shall use is essentially a matching procedure in which one matches the plane wave at the surface to the Bloch wave inside the crystal.

We proceed as follows: we consider a one-dimensional periodic potential of period a with N atoms and having either a Tamm-type or Shockley-type potential termination at either end. Our zero of energy will be at the average value of the periodic potential. The vacuum level on the left is at a height V_1 above zero energy and the vacuum level on the right is at a height V_2. For $x \leq 0$, we have a plane wave of unit amplitude incident from the left upon the periodic potential and a reflected plane wave of amplitude R going to the left. The solution of Schrodinger's equation in this region yields the wave function

$$\psi(x) = e^{ik_1 x} + R e^{-ik_1 x}, \qquad (5.1)$$

$$k_1 = \sqrt{(2m/\hbar^2)(E - V_1)}.$$

For $0 \leq x \leq Na$, there are three regions of energy in each of which the Bloch wave function assumes a different form. These are

$$\psi(x) = C_{+k} e^{ikx} P_{+k}(x) + C_{-k} e^{-ikx} P_{-k}(x); \rho < 0, \quad (5.2a)$$

$$\psi(x) = C_{+k} e^{kx} P_{+k}(x) + C_{-k} e^{-kx} P_{-k}(x); 0 < \rho < 1, \quad (5.2b)$$

$$\psi(x) = C_{+k} e^{kx} G_{+k}(x) + C_{-k} e^{-kx} G_{-k}(x); \rho > 1. \quad (5.2c)$$

As the energy of the incident plane wave is increased, we must match the appropriate Bloch function to the incident and reflected wave, depending on the band structure in the crystal. For $x \geq Na$, we have only an outgoing plane wave of the form

$$\psi(x) = T e^{ik_2(x-Na)}, \quad k_2 = \sqrt{\frac{2m}{\hbar^2}(E - V_2)}. \quad (5.3)$$

These wave functions must be matched at $x = 0$ and $x = Na$ to yield a continuous wave function throughout all space.

If the energy of the incident wave is such that $\rho < 0$ inside the crystal, then we have at $x = 0$, the matching condition

$$ik_1\left(\frac{1-R}{1+R}\right) = \sigma_1\left(\frac{C_{+k} - C_{-k}}{C_{+k} + C_{-k}}\right). \quad (5.4)$$

At x = Na, we have

$$\sigma_4\left(\frac{C_{+k}e^{ikNa}-C_{-k}e^{-ikNa}}{C_{+k}e^{ikNa}+C_{-k}e^{-ikNa}}\right)=ik_2. \qquad (5.5)$$

If we now solve Eq. (5.5) for C_{-k} in terms of C_{+k}, we obtain

$$C_{-k}=\left(\frac{\sigma_4-ik_2}{\sigma_4+ik_2}\right)e^{2ikNa}C_{+k}. \qquad (5.6)$$

Substituting this equation into Eq. (5.4), we obtain

$$\left(\frac{1-R}{1+R}\right)=\frac{\sigma_4}{ik_1}\left(\frac{1-\left(\frac{\sigma_4-ik_2}{\sigma_4+ik_2}\right)e^{2ikNa}}{1+\left(\frac{\sigma_4+ik_2}{\sigma_4+ik_2}\right)e^{2ikNa}}\right),$$

$$=\frac{\sigma_4}{ik_1}\left(\frac{ik_2-i\sigma_4\tan kNa}{\sigma_4+k_2\tan kNa}\right),$$

or

$$R=\frac{(k_1-k_2)\sigma_4+(\sigma_4^2+k_1k_2)\tan kNa}{(k_1+k_2)\sigma_4-(\sigma_4^2-k_1k_2)\tan kNa}. \qquad (5.7)$$

Since $\sigma_4=-i(\omega_0/v_0)|\rho|^{\frac{1}{2}}$, we obtain a reflection coefficient for $\rho<0$ of

$$|R|^2=\frac{(k_1-k_2)^2|\sigma_4|^2+(|\sigma_4|^2-k_1k_2)^2\tan^2kNa}{(k_1+k_2)^2|\sigma_4|^2+(|\sigma_4|^2+k_1k_2)^2\tan^2kNa}. \qquad (5.8)$$

For $0 < \rho < 1$, we simply replace k by -iK and σ_4 by $-\frac{u_6'}{u_6}\rho^{\frac{1}{2}}$ in Eq. (5.7) to obtain

$$|R|^2 = \frac{(k_1-k_2)^2|\sigma_4|^2+(|\sigma_4|^2+k_1k_2)^2\tanh^2 KNa}{(k_1+k_2)^2|\sigma_4|^2+(|\sigma_4|^2-k_1k_2)^2\tanh^2 KNa}, \quad (5.9)$$

For $\rho > 1$, instead of calculating K by the formula

$$K = -\frac{1}{a}\log\left(\frac{1-\rho^{\frac{1}{2}}}{1+\rho^{\frac{1}{2}}}\right), \quad (5.10a)$$

we use the formula

$$K = -\frac{1}{a}\log\left(\frac{\rho^{\frac{1}{2}}-1}{\rho^{\frac{1}{2}}+1}\right) \quad (5.10b)$$

and the reflection coefficient is the same as for $0 < \rho < 1$ otherwise.

For the case of a semi-infinite crystal, we need only let $N \to \infty$, to obtain

$$|R|^2 = \left(\frac{|\sigma_4|^2-k_1k_2}{|\sigma_4|^2+k_1k_2}\right)^2, \quad \rho<0; \quad (5.11)$$

$$|R|^2 = 1, \quad \rho>0. \quad (5.12)$$

If we let $V_1 = V_2$, $|R|^2$ will reduce for both $\rho < 0$ and $\rho > 0$ to

$$|R|^2 = \frac{(|\sigma_4|^2-k_1^2)^2\tan^2 kNa}{4|\sigma_4|^2k_1^2+(|\sigma_4|^2+k_1^2)^2\tan^2 kNa}, \quad \rho<0; \quad (5.13a)$$

$$|R|^2 = \frac{(|\sigma_4|^2+k_1^2)^2 \tanh^2 kNa}{4|\sigma_4|^2k_1^2+(|\sigma_4|^2-k_1^2)^2\tanh^2 kNa}, \rho>0. \quad (5.13b)$$

Notice that in this case, σ_4 always enters $|R|^2$ as a squared quantity. We saw in Section II that surface states are obtained only if $-(u_o'/u_o)|\rho|^{\frac{1}{2}}$ goes negative in an attenuation region. Since in an attenuation region σ_4 equals $-(u_o'/u_o)|\rho|^{\frac{1}{2}}$, and is squared in the formula for $|R|^2$, we do not expect to see in the reflection spectrum evidence of what would correspond to surface states with energies lying within attenuation bands. We should, however, be able to distinguish the pass region and the attenuation regions for large N.

In a pass region, k varies from 0 to π/a or from π/a to 0, so that tan(kNa) will exhibit N or N-1 zeroes, depending on the sequence of the zeroes of the functions g_o', g_o, u_o', u_o for increasing energy. In analogy with the surface states problem we find that if the band edges have crossed (i.e. if the zeroes occur out of order from the sequence g_o', g_o, u_o', u_o, g_o', g_o, u_o', u_o, . . .), then the neighboring pass regions will have (depending on how large N is or how strong the periodic potential is,) either N-1, N or N+1 zeroes. To see this, consider the form of the reflection

coefficient in a pass region. The zeroes of $|R|^2$ will occur in a pass region for either

$$\tan(kNa) = 0 \quad \text{or} \quad |\sigma_+| = k_1. \tag{5.14}$$

Considering only the tangent term, this condition implies that $k = n\pi/Na$, where n is an integer. Since $0 \leq k \leq \pi/a$, and we are restricting ourselves to only positive values for k, the possible values of n are 0, 1, 2, . . ., N. For $\rho = 0$ there is some difficulty since $k = 0$, and $|\sigma_+|$ equals zero or infinity depending on which function determines the boundary. The same difficulty arises at $\rho = \infty$. By consideration of the limiting forms for the boundaries $\rho = 0$ and $\rho = \infty$, we obtain

$$|R|^2 = \frac{k_1^2}{k_1^2 + (u_0'/u_0N)^2}, \quad g_0' = 0; \tag{5.15a}$$

$$|R|^2 = \frac{(u_0'N/u_0)^2}{(u_0'N/u_0)^2 + k_1^2}, \quad g_0 = 0; \tag{5.15b}$$

$$|R|^2 = \frac{k_1^2}{k_1^2 + (g_0'/g_0N)^2}, \quad u_0' = 0; \tag{5.15c}$$

$$|R|^2 = \frac{(g_0'N/g_0)^2}{(g_0'N/g_0)^2 + k_1^2}, \quad u_0 = 0. \tag{5.15d}$$

Thus we see that $k = 0$ and $k = (\pi/a)$ yield no zeroes of $|R|^2$. Then n is restricted to n = 1, 2, 3, . . .,

N-1. The extra zeroes may or may not occur depending on whether σ_4 becomes equal to ik_1 as k varies from 0 to π/a. Inspection of the form of $-(u_0'/u_0)|\rho|^{\frac{1}{2}}$ in Figures 2.2 and 2.3 reveals that if the functions g_0', g_0, u_0', u_0, g_0', g_0, u_0', u_0, . . . have zeroes in this sequence, there will be one value where $|\sigma_4|^2$ becomes equal to k_1^2 in each pass region, bringing the total number of zeroes for $|R|^2$ to N. For the sequence of zeroes deviating from the above order, as in Figure 2.3, we will obtain either no values or two values of $|\sigma_4|^2$ which are equal to k_1^2 in the pass region between $g_0' = 0$ and $u_0' = 0$, and either two values or no values for the next pass region between $g_0 = 0$ and $u_0 = 0$, depending on the magnitude of k_1^2. Thus in the neighboring pass regions between which the band edges have crossed, there will be either N-1 or N+1 zeroes.

For N becoming large, we see from Eq. (5.15) that $|R|^2$ approaches 1 on the band edges. For a semi-infinite crystal, the structure in the pass-band disappears because the reflection coefficient oscillates an infinite number of times, and only the envelope of the peaks remain. In the attenuation regions, the reflection is perfect.

It should be pointed out that the above analysis may also be applied to tunneling phenomena, For example,

we could let V_1 and V_2 be equal to the minimum value of the periodic potential without changing the mathematics. In this case, the calculations reduce to the solution of a particle tunneling through N identical barriers.

The above analysis also resolves a question which arises in applying the Born-von Karman boundary condition [36] to an infinite crystal. The Born-von Karman boundary condition, as usually applied, uses only one of the independent Bloch functions and requires this function to satisfy

$$e^{ikNa} = 1. \tag{5.16}$$

In this case, $k = 2n\pi/Na$ where $-N/2 \leq n \leq N/2$. There are N values of k in all, counting both positive and negative values. A better manner in which to impose periodic boundary conditions would be to require the function

$$\psi(x) = C_{+k} e^{ikx} P_{+k}(x) + C_{-k} e^{-ikx} P_{-k}(x) \tag{5.17}$$

to satisfy

$$\psi(x+Na) = \pm \psi(x). \tag{5.18}$$

In this way, one obtains twice as many values of k given by

$$k = n\pi/Na \quad , \quad -N/2 \leq n < N/2. \qquad (5.9)$$

Now there is still some doubt as whether to include N/2 or - N/2 in the values for k, and one usually picks either one or the other. However, we see by our analysis that the choice should be neither of the above, but should be such that

$$\frac{\psi_+'(na)}{\psi_+(na)} = \alpha_4 = ik_1 = \sqrt{\frac{2m}{\hbar^2}(E + V_0/2)}, \qquad (5.20)$$

where $V_o/2$ is the amplitude of the periodic potential evaluated at a lattice site. From the formula for the reflection coefficient, we see that $k = n\pi/Na$, $n = 1, 2, 3, \ldots, N-1$, and $ik = \alpha_4$ correspond to values of the energy for which the periodic potential is completely transparent to an incident electron and thus the electron is not localized to any one region of the crystal.

To illustrate the features of the above discussion, calculations were carried out on a Kronig-Penny potential for both Shockley- and Tamm-type potential terminations at either end. For comparison, we use the same values of a, b, V_o, as we used in calculating the energy states

in Section III. Figures 5.1 (a,b) show the reflection coefficients for $V_1 = V_2 = 6.5$ E.U. and $N = 4$ for both the Shockley and Tamm terminations. The vertical lines indicate the band edges, and the arrows indicate which band edges have crossed. Figures 5.2 (a,b) have the same potential configuration except now $N = 20$. Figures 5.3 (a,b) show the case of tunneling when $V_1 = V_2 = V_o/2 = -1.7$ E.U. and $N = 4$. The lowest pass-band is not shown because it is so narrow that the plotter missed it.

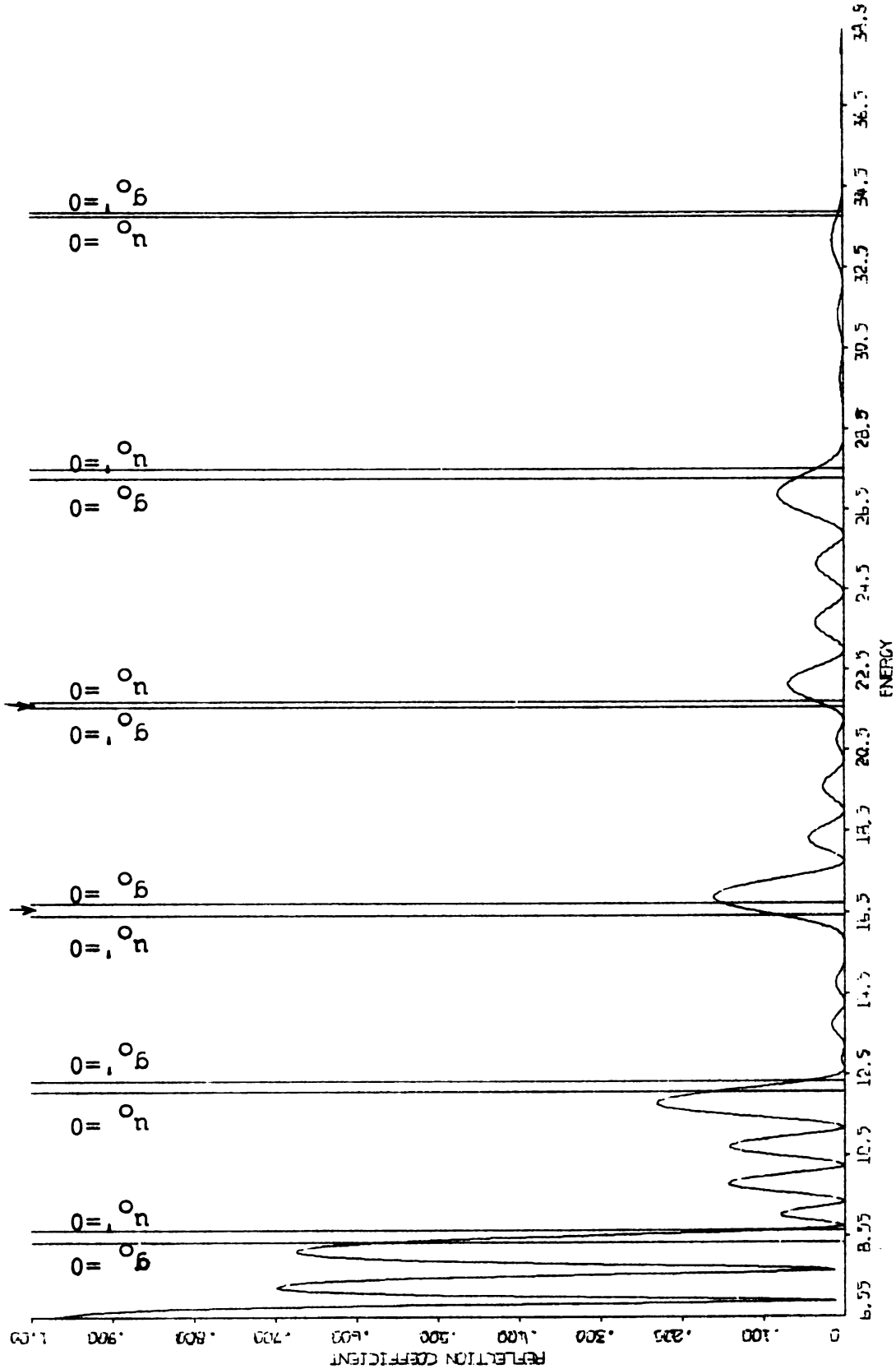

Figure 5.1a. Reflection coefficient versus energy for the Shockley-type termination of four cells.

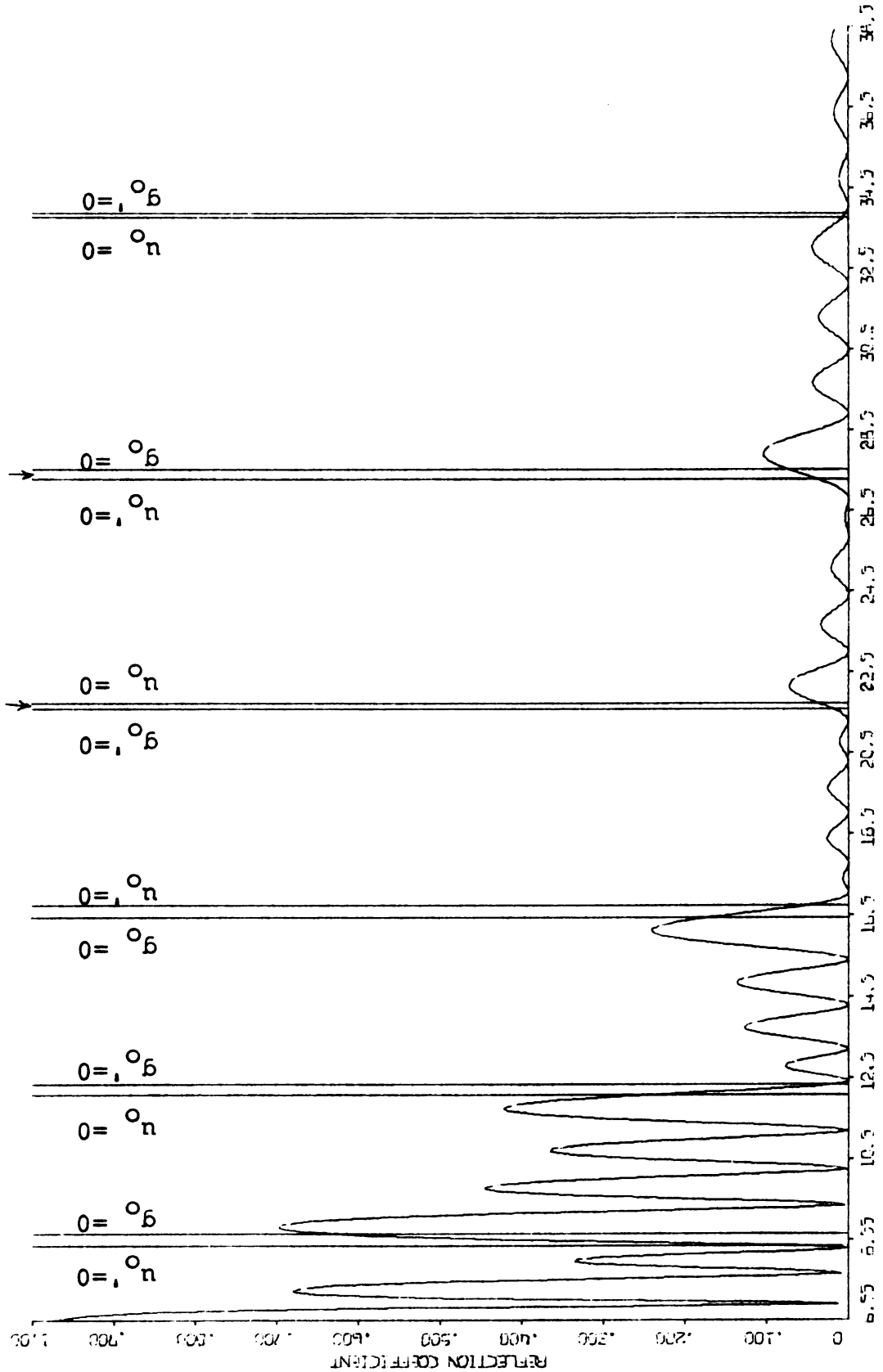

Figure 5.1b. Reflection coefficient versus energy for the Tamm-type termination of four cells.

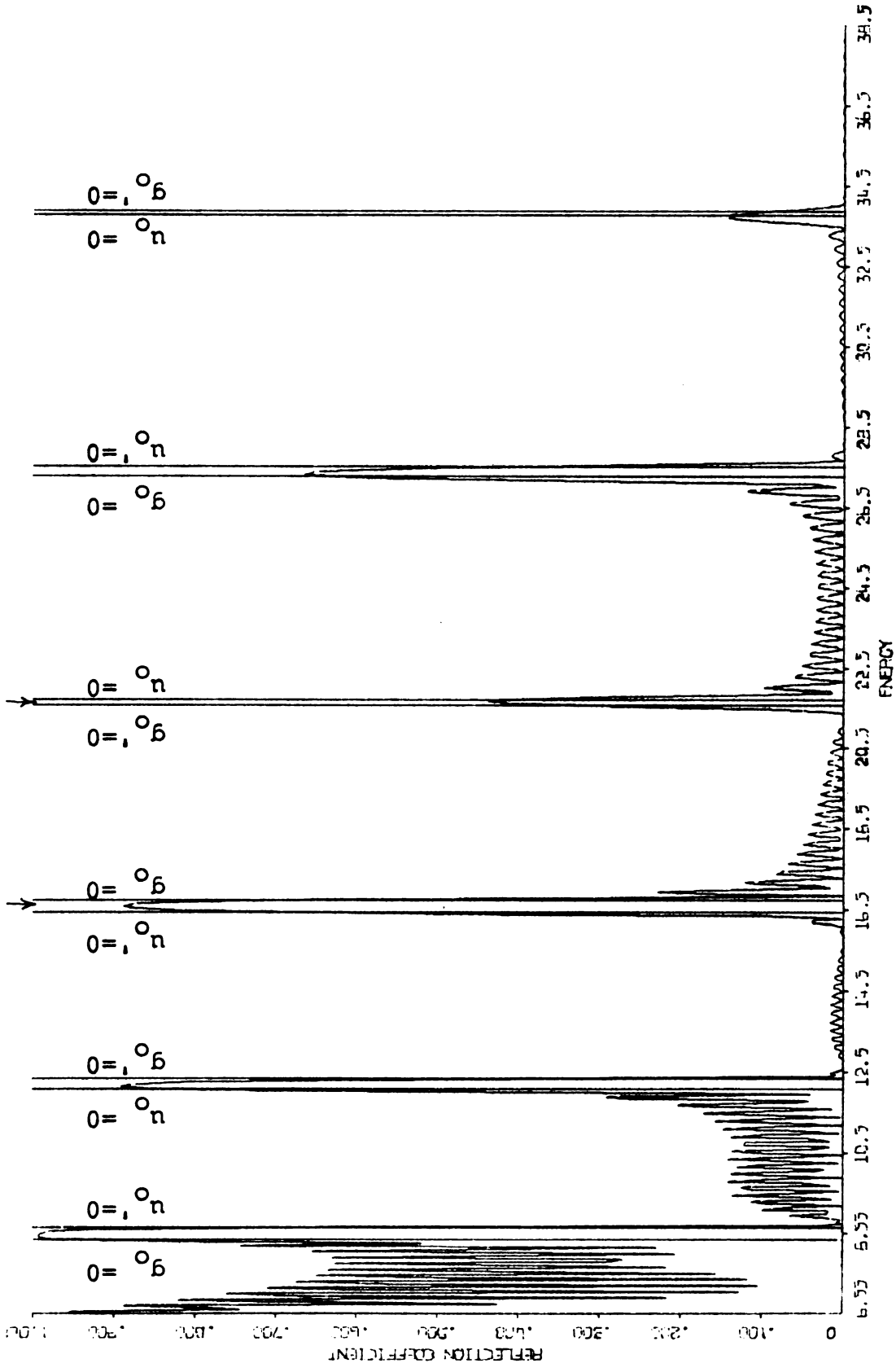

Figure 5.2a. Reflection coefficient versus energy for the Shockley-type termination of twenty cells.

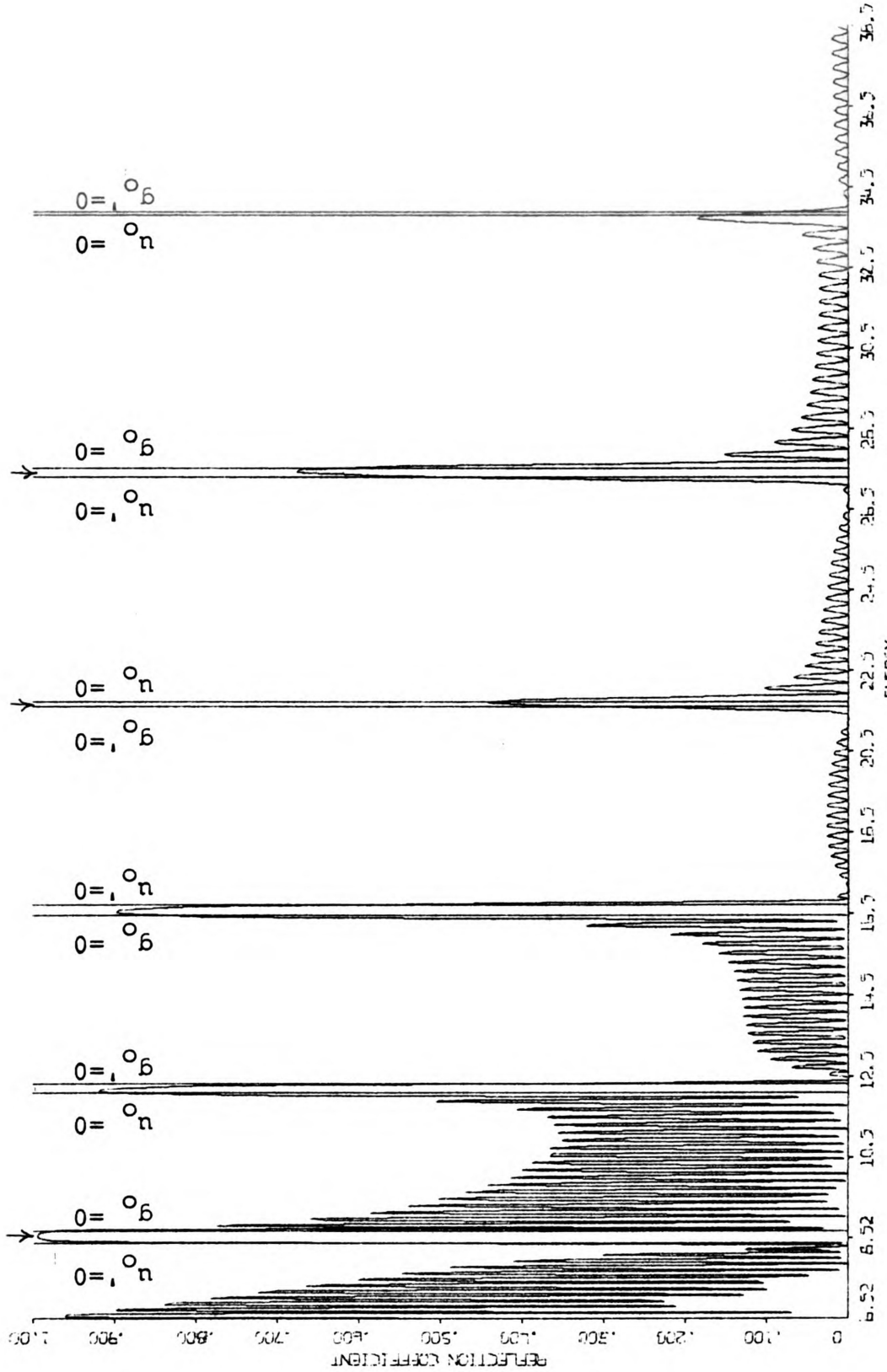

Figure 5.2b. Reflection coefficient versus energy for the Tamm-type termination of twenty cells.

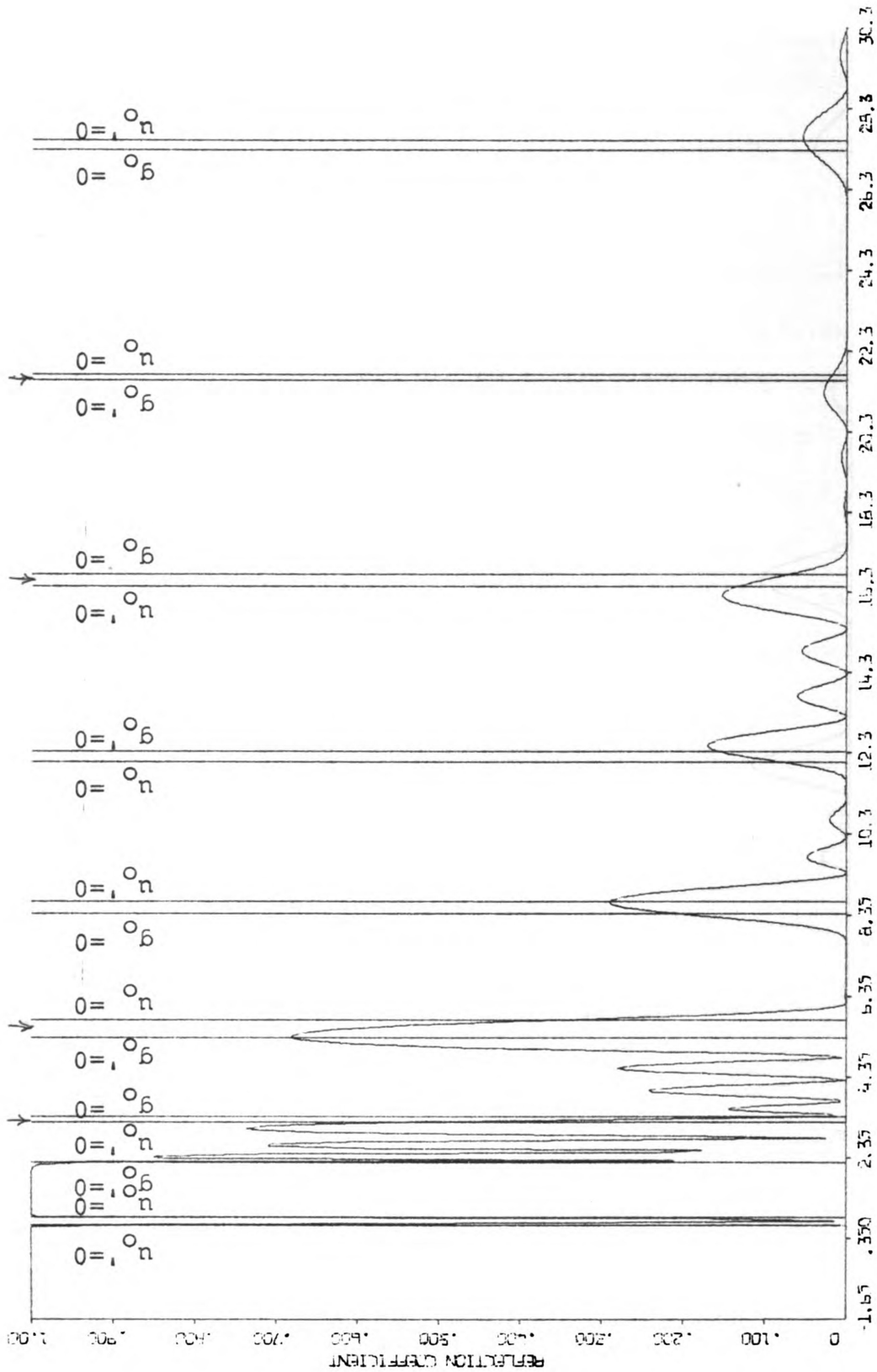

Figure 5.3a. Reflection of electrons from four identical barriers with Shockley-type terminations at both ends.

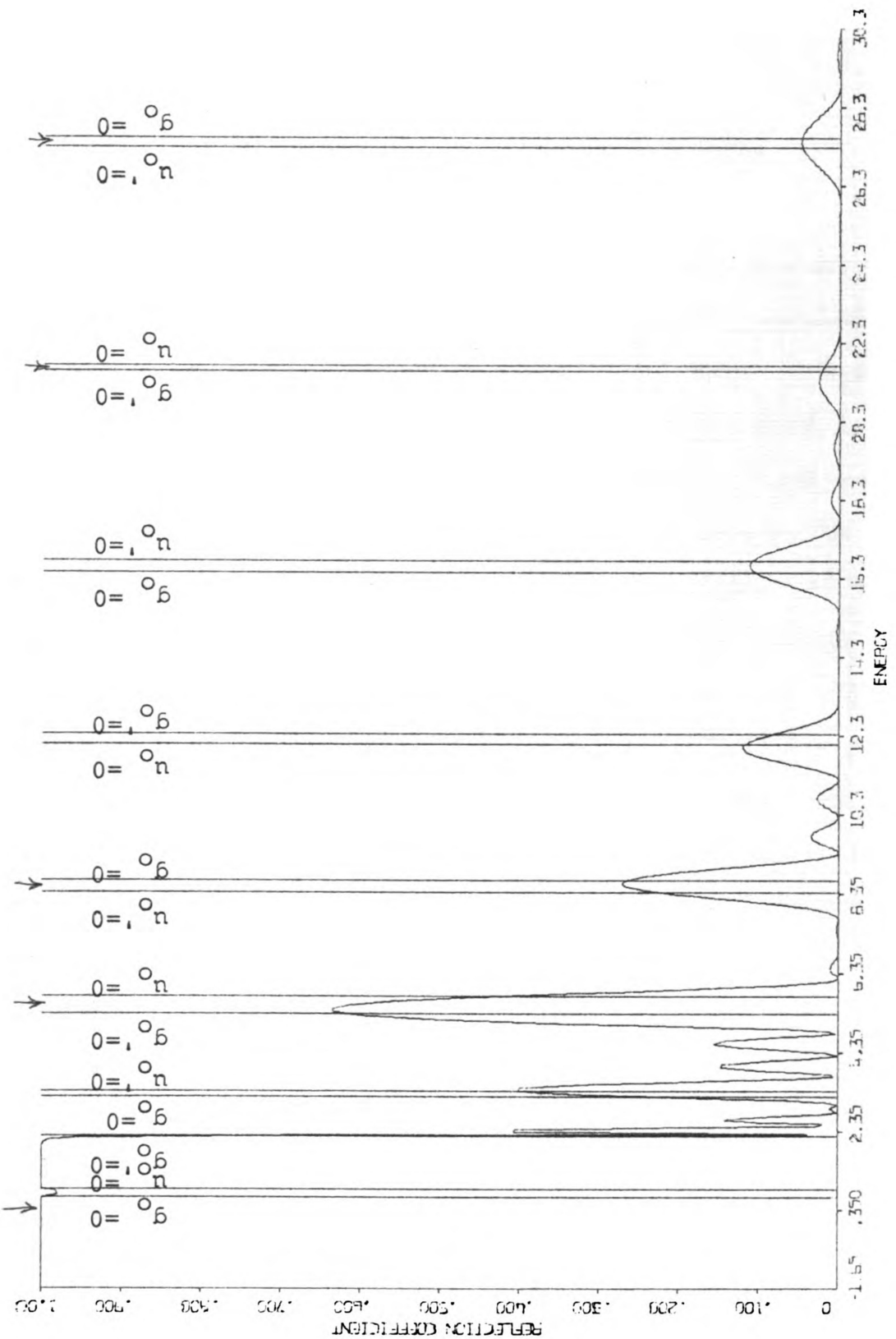

Figure 5.3b. Reflection of electrons from four identical barriers with Tamm-type terminations at both ends.

SECTION VI

RESONANCE TRANSMISSION IN ELECTRON EMISSION FROM SURFACES WITH ADSORBED ATOMS

In recent years there has been renewed interest in the role of resonance effects in the emission of electrons from a metal surface with adsorbed atoms[38-45]. Both qualitative[38] and quantitative[40] predictions indicate that structure in the total energy distribution of field emitted electrons should be related to resonance effects reflecting the atomic-like energy level spectrum of the adsorbed atoms. Gadzuk[45] has shown qualitatively that similar resonances can occur for transmission over the surface barrier in which an adsorbed atom is present. However, as we shall see later, his results are questionable in several respects. This behavior could be relevant to electron processes such as thermionic, Auger, or photoelectron emission in which a partial monolayer of an alkali metal is deposited on the surface to reduce the work function of the material. Consequently, it is interesting to try to calculate this effect.

The present section deals with a calculation which is similar in many respects to calculations performed by Gadzuk[47]. But whereas Gadzuk considered only the case of

transmission of an electron into free space from a free electron metal with a single adsorbed atom, we shall consider the more general case of transmission of an electron from one periodic potential across another periodic potential into free space. This includes the case of only one period of a periodic potential, which is just a single adsorbed atom. We may relate this type of calculation to tunneling phenomena, although there are no classically forbidden regions. However, there are quantum mechanical attenuation regions through which the electron must pass and the analogy between the classical case and the quantum-mechanical case will be clear in what follows.

A great many of the features of tunneling phenomena in solids are essentially of a one-dimensional nature. If the tunneling barrier (or effective barrier in our case) extends in the x direction the momenta in the y and z directions can usually be taken to be constants of the motion and hence are merely fixed parameters[48]. Therefore, we shall confine ourselves to one-dimension for the calculations which follow, even though such a model neglects a variety of geometrical effects.

We shall first consider the special case of electron emission from a free electron metal across several layers of foreign atoms into free space. We will not consider the

mechanisms which excite the electron into states from which it can be transmitted out of the crystal but will assume that the electron has already attained such an energy state. We shall then replace the free electron metal by a periodic potential with the same layers of foreign atoms on the surface and perform similar calculations. The model potentials we shall use for the first and second case are shown in Figures 6.1a and 6.1b.

A. ADSORBED ATOMS ON A METAL SURFACE

As a model for a metal, we assume a semi-infinite free electron region for $x < 0$, and we represent the foreign atom layers as square wells for $0 < x < Na_2$. For $x > Na_2$, the potential is zero representing free space. The three regions are labeled appropriately by I, II, and III. By using a square well for our model impurity potential, we have complicated matters considerably, since we have to deal with band-edge crossing effects also. However, real impurity potentials may be expected to have the same type of structure. In region I, the solution of Schrodinger's equation yields plane waves which we shall write (for $E > 0$) as

$$\psi(x) = e^{ik_1 x} + Re^{-ik_1 x}, \quad k_1 = \sqrt{\frac{2m}{\hbar^2}(E + V_{01})}. \tag{6.1}$$

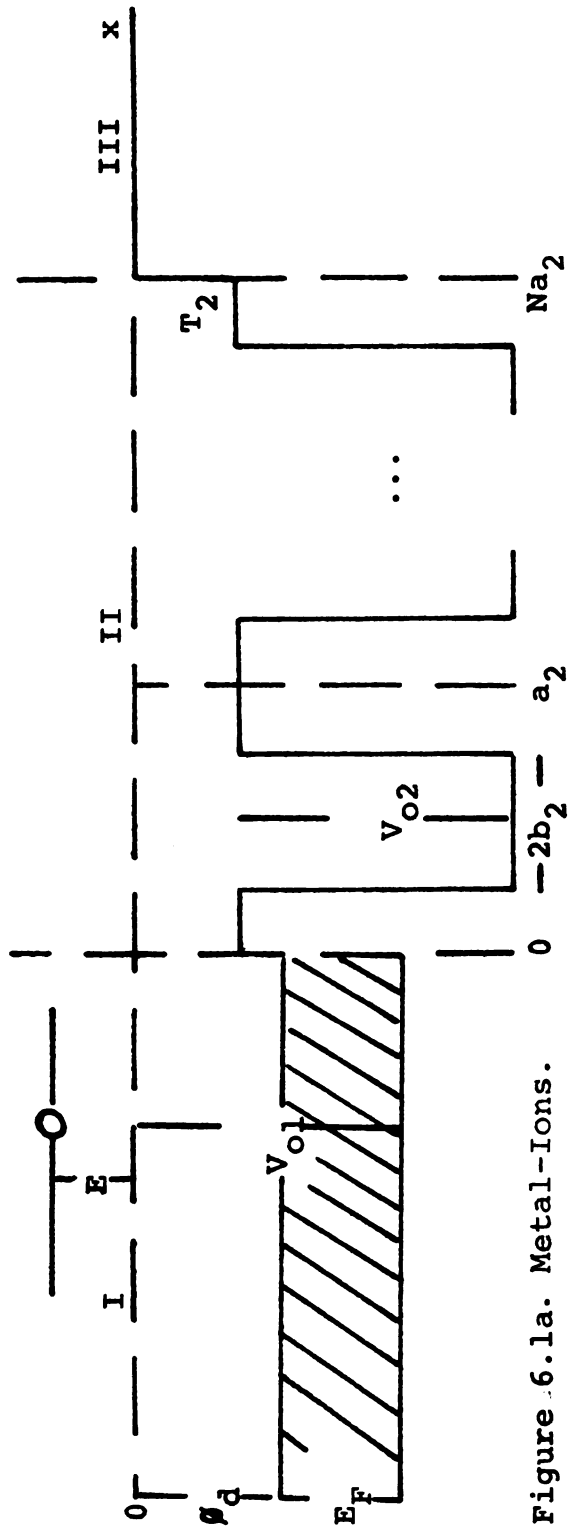

Figure 6.1a. Metal-Ions.

Figure 6.1b. Non-Metal- Ions.

We want to find the transmission coefficient of an electron incident from the left, past the foreign layers into vacuum. Consequently, we may calculate $|R|^2$, the reflection coefficient and use

$$|T|^2 = 1 - |R|^2 \tag{6.2}$$

to obtain the transmission coefficient. In region II, solution of Schrodinger's equation yields the Bloch waves

$$\psi_2 = C_+ \psi_+ + C_- \psi_- \tag{6.3}$$

the exact form of which is given in Section I. In region III, the wave function is given by the out-going plane wave

$$\psi = T e^{ik_3(x-Na_2)} \qquad k = \sqrt{\left(\frac{2m}{\hbar^2}\right)(E)}. \tag{6.4}$$

The requirement that the wave function be continuous across the three regions determines the coefficients R, C_+, C_-, and T. If we recognize that this problem is just a special case of the problem treated ir Section V with the zero of energy shifted and unequal potential terminations, we may save calculational duplication. By making the energy zero adjustment and relabeling the corresponding variables according to Figure 6.1a, we may directly carry over the calculations of Section V to this section. We wish to calculate the transmission coefficient rather than the reflection coefficient as was done in Section V; so we must use Eq. (6.2) to obtain the pertinent result.

At this point, some discussion of the choice of potentials is in order. The potential around the foreign atoms adsorbed on the surface of the metal is essentially that due to the Coulomb potential of the fractionally charged ion core. Thus, one would expect to use a strongly attractive model potential whose radius is roughly that of the ionic radius. However, if we incorporate the condition of orthogonalization to the occupied tightly bound electron as a separate, non-local term in the potential, the sum of the two potentials yields a more smoothly varying function of position. The pseudo-wave function will then be analogous to the free-electron wave function. This approach has

been used to calculate electron field emission distributions[49]. Other workers[50] dispute this approach for the following reasons. The principle of the pseudo-potential is that the exact Schrodinger equation for a system with a complicated wave function can be transformed into a pseudo-wave function equation with the same energy eigenvalue and a simple pseudo-wave function. The simple wave function has nothing to do with the real wave function. In doing transmission coefficient calculations, the form of the wave function is intimately related to the details of the potential, and the interference effects which are present in the real wave function are glossed over in the pseudo-wave function approach.

We shall adopt the latter viewpoint in calculating the wave function, so consequently, we must use strong potentials in a model of the true potential rather than weak pseudo-potentials. We shall assume the adsorbed atom is displaced to a larger lattice spacing from the end of the crystal than it would have in bulk material. As suitable parameters to use in our calculations, we take (see Figure 6.1a)

$$a_2 = 9.0\ A^o, \tag{6.5a}$$

$$b_2 = 1.5\ A^o, \tag{6.5b}$$

$$V_{o2} = 51.5\ eV = 13.28\ E.U., \tag{6.5c}$$

$$V_{o1} = 12.45 \text{ eV} = 3.20 \text{ E.U.}, \tag{6.5d}$$

$$T_2 = 3.88 \text{ eV} = 1.0 \text{ E.U.}. \tag{6.5e}$$

These are approximately the same values of the parameters as used by Gadzuk in his calculation. However, Gadzuk was mistaken in his interpretation of the units of the various parameters defined above so that when he thought he was using a well depth $V_{02} = 51.5$ eV, he was actually using a well depth $V_{o2} = 200$ eV. As a matter of fact, all of his energy units are too small by a factor of 3.88. Consequently, the transmission coefficient which he calculates has considerably more structure (i.e.the wave function has a larger number of nodes near the well) then it should. To clarify this situation, and to generalize the results for a larger number of adsorbed atoms than one, the transmission coefficient was calculated using the above parameters for the case of one, two, and three adsorbed atom layers. The results are illustrated in Figure 6.2. The solid curve represents the case of one adsorbed atom layer (N = 1), whereas the 1/16" dashed curve is for two adsorbed atom layers (N = 2), and the 1/8" dashed curve is for three adsorbed atom layers (N = 3). The range of energies in which we are interested is between zero and twenty electron volts,

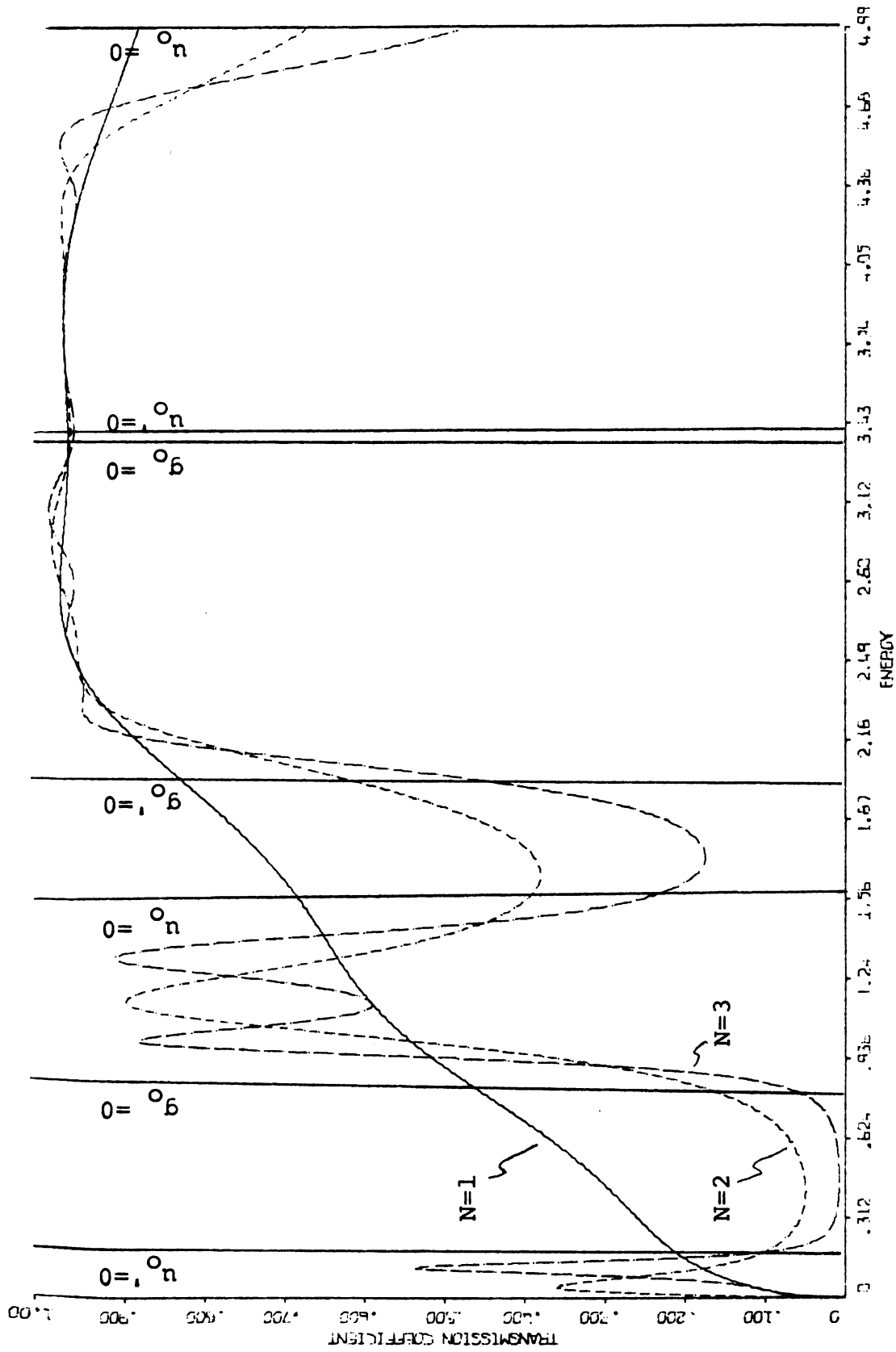

Figure 6.2. Transmission coefficient for 1, 2, 3 adsorbed atoms on a metal- Case 1.

since calculations of this type for higher values of energy are made irrelevant by inelastic effects. The most striking feature about the N = 1 case is that the transmission coefficient has very little structure, and is a slowly varying function of energy. This is in agreement with previous authors' assumptions about the nature of the transmission coefficient with regard to photoemission calculations, etc.. The small variation which does occur is a result of the attenuation bands of the adsorbed atom. The attenuation band edges are denoted by the vertical lines. For two adsorbed atom layers, the situation is quite different owing to the resonating effects between the impurity atoms. If we realize that this situation is analogous to the situation in Section V, we may apply the same reasoning to explain the structure of the transmission coefficient. The main difference between the calculations of this section and those of Section V is that we are now dealing with unequal boundary conditions at either end of the "periodic potential". The main effect which this has on the form of the transmission coefficient is that, in a pass band, instead of achieving the value one (corresponding to the reflection coefficient of Section V going to zero) at various values of k, the transmission coefficient reaches a relative maximum which may be shifted slightly from the values of

$k = n\pi/Na_2$, $n = 1, 2, \ldots N-1$. Otherwise, the two situations are analogous. The number of relative maxima which the transmission coefficient will have in a given pass-band will depend on whether the band edges which bound the pass-band have crossed. Consequently, there will be either N-1, N, or N+1 relative maxima in each pass-band. The attenuation bands, of course, tend to lower the transmission coefficient. Thus, the reason for the structure for the two cases, N=2 and N=3, becomes clear. To obtain a better understanding of what effect the potential depth of the impurity layers has on the transmission coefficient, we have performed the same calculations as above using the same values for all the parameters except V_{o2} which was reduced to half of its previous value. The results are illustrated in Figure 6.3. This should be compared with Figure 6.2. As may be seen, the transmission coefficient is enhanced in an overall manner, and the structure changes slightly due to the change in the position and widths of the pass-bands and attenuation bands. The fact that an attenuation band becomes wider as the potential becomes weaker is purely a band-edge crossing effect, as may be seen in Section III.

B. ADSORBED ATOMS ON A NON-METAL SURFACE

The situation of a non-metal with adsorbed atoms on its surface represents a more complicated problem mathema-

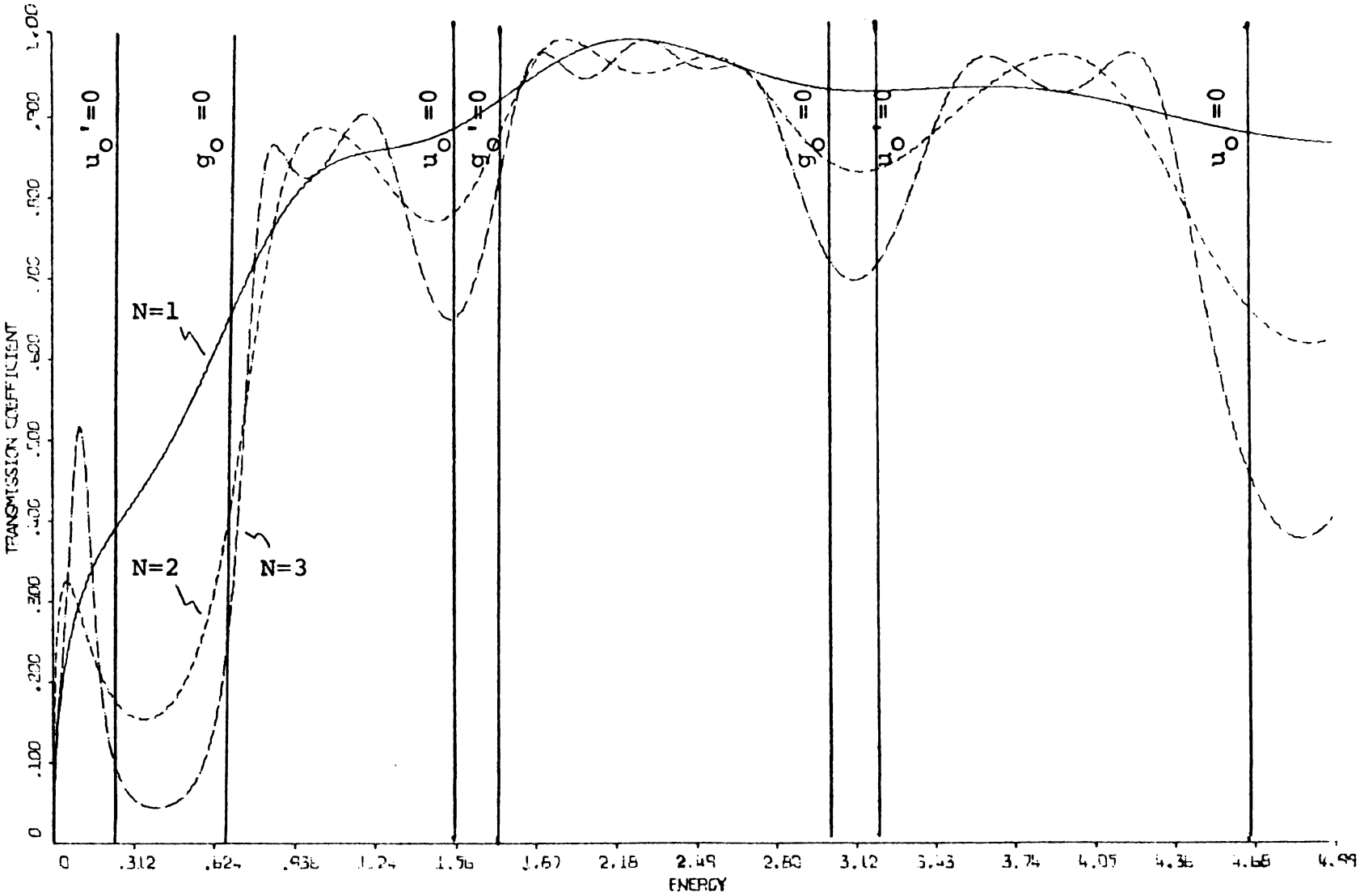

Figure 6.3. Transmission coefficient for], 2, 3 adsorbed atoms on a metal- Case 2.

tically than does the previous case, since now we must take into account the band structure of the non-metal as well as the band structure of the adsorbed atoms. The approach to solving this problem for the transmission of electrons from the non-metal into free space is, however, analogous to the previous calculation. As before, we form a continuous wave function throughout all space by joining the appropriate solutions to Schrodinger's equation at the boundaries of the regions in which they are valid. We shall denote the non-metal as region I, the adsorbed surface layers as region II, and the vacuum as region III.

Since region I is characterized by a periodic potential, the solutions to Schrodinger's equation will yield a wave function of the form

$$\psi = C_+^I \psi_+^I + C_-^I \psi_-^I, \quad x<0, \qquad (6.6)$$

where the exact form of ψ_+ , ψ_- will depend on the value of energy; i.e. on whether $\rho^I < 0$, $0 < \rho^I < 1$, $\rho^I > 1$. Region I will have a band structure which depends only on the periodic potential in region I. We want to have a wave traveling to the right (i.e. incident wave) and a wave traveling to the left (i.e. reflected wave), in order to calculate the reflection coefficient. Since the indepen-

dent solutions for an attenuation band are both real functions, they do not carry any current. To be able to obtain a current in an attenuation band, it is necessary to take a complex linear combination of the two real solutions. However, we shall not attempt to do this since the reflection coefficient would depend exponentially on the depth inside the non-metal at which the unstable state was created. Since the time required for an electron to "tunnel" out of the crystal is much larger than the time during which the electron would stay in such an unstable state, we can say that the reflection coefficient is essentially one, or that the transmission coefficient is zero. The independent solutions for the pass bands, in contrast, carry currents of

$$j_+ = \frac{ih}{2m}\left(\psi_+^I \psi_+^{I\prime *} - \psi_+^{I*}\psi_+^{I\prime}\right) = -\frac{ih\sigma_+}{m}, \quad (6.7a)$$

$$j_- = \frac{ih}{2m}\left(\psi_-^I \psi_-^{I\prime *} - \psi_-^{I*}\psi_-^{I\prime}\right) = \frac{ih\sigma_+}{m}, \quad (6.7b)$$

where $\sigma_+ = -\sigma_-$ and $\sigma_+ = i\left(-\frac{u_0'}{u_0}\right)|\rho|^{\frac{1}{2}}$.

From Section II, we know that the quantity $-(u_0'/u_0)|\rho|^{\frac{1}{2}}$ is positive for the odd numbered bands and negative for the even numbered bands. Since

$$j_+ = \frac{h}{m}\left(-\frac{u_0'^I}{u_0^I}\right)|\rho^I|^{\frac{1}{2}}, \quad (6.8a)$$

$$j_- = -j_+ , \tag{6.8b}$$

We must identify the wave traveling to the right as ψ_+^I for odd numbered pass bands and ψ_-^I for even numbered pass bands. The situation is reversed for the wave traveling to the left. Thus, the reflection coefficient is given by

$$|R|^2 = \begin{cases} \left|\frac{C_-^I}{C_+^I}\right|^2 & \text{odd pass bands,} \\ \left|\frac{C_+^I}{C_-^I}\right|^2 & \text{even pass bands.} \end{cases} \tag{6.9}$$

In region II, we will again have a band-structured situation, so we may write the wave function in this region as

$$\psi = C_+^{II}\psi_+^{II} + C_-^{II}\psi_-^{II}, \quad 0 \leq x \leq Na_2. \tag{6.10}$$

The band structure in this region will, in general, be different from that of region I.

In region III, the wave function takes the form of an

out-going wave

$$\psi = Te^{ik_3(x-Na)}, \quad k_3=\sqrt{2mE/\hbar^2}, \quad x \geq Na_2. \tag{6.11}$$

If we now require the logarithmic derivatives to be equal at the boundaries x = 0 and x = Na_2, we obtain the reflection coefficients of

$\underline{\rho^I<0,\ \rho^{II}<0}$

$$|R|^2 = \left(\frac{(\epsilon q_1-k_3)^2q_2^2+(q_2^2-\epsilon q_1k_3)^2\tan^2kNa}{(\epsilon q_1+k_3)^2q_2^2+(q_2^2+\epsilon q_1k_3)^2\tan^2kNa}\right),$$

$$q_1=-\left(\frac{u_0'^I}{u_0^I}\right)|\rho^I|^{\frac{1}{2}},$$
$$q_2=-\left(\frac{u_0'^{II}}{u_0^{II}}\right)|\rho^{II}|^{\frac{1}{2}}, \tag{6.12}$$
$$\epsilon = \begin{cases} +1 & \text{odd bands,} \\ -1 & \text{even bands.} \end{cases}$$

$\underline{\rho^I<0,\ \rho^{II}>0}$

$$|R|^2 = \left(\frac{(\epsilon q_1-k_3)^2q_2^2+(q_2^2+\epsilon q_1k_3)^2\tanh^2kNa}{(\epsilon q_1+k_3)^2q_2^2+(q_2^2-\epsilon q_1k_3)^2\tanh^2kNa}\right). \tag{6.13}$$

$\rho^I > 0$, ρ^{II} arbitrary

$$|R|^2 = 1. \tag{6.14}$$

The transmission coefficient is just

$$|T|^2 = 1 - |R|^2. \tag{6.15}$$

Notice that ϵq_1 is always positive and could be replaced by $|q_1|$. As the periodic potential in region I goes to zero, $|q_1|$ goes to k_1, where k_1 was defined earlier in Eq. 6.1, and we recover the results of the earlier subsection.

In order to be able to draw comparisons between this calculation and the calculation done earlier, we let a_2, b_2, V_{o2}, and T_2 have the same values as used before, and let a_1, b_1. V_{o1}. and T_1 be such that the average value of the periodic potential is the same as the V_{o1} chosen earlier. Thus, we let

$$a_1 = 3.0\ A^o \tag{6.15a}$$

$$b_1 = .75\ A^o, \tag{6.15b}$$

$$V_{o1} = 2.0\ E.U., \tag{6.15c}$$

$$T_1 = 1.2\ E.U.. \tag{6.15d}$$

Using the above parameters for region I, and the two sets of parameters for region II, the transmission coefficient was calculated for the range $0 < E < 20$ eV, and is illustrated in Figures 6.4 and 6.5. As before, the vertical lines represent the band edges for region II. The band edges for region I can clearly be distinguished by the fact that the transmission coefficient goes to zero. These graphs should be compared with Figures 6.2 and 6.3 and the differences noted. There is only one attenuation band occurring in region I for the range of energies considered. It occurs more or less in the middle of a pass band of region II.

The structure in the transmission coefficient is enhanced in the pass band regions, as is readily seen by comparison. The various relative peaks in the transmission coefficient may be explained by previous considerations.

To summarize, we have seen that for the case of one layer of adsorbed atoms on the surface of a metal or non-metal, the transmission coefficient is a slowly varying function of energy, except near a band edge for a non-metal. With the introduction of more than one layer, resonance effects predominate, leading to considerable structure in the transmission coefficient. Hence, we would expect to observe this type of effect in the total energy distribution of electrons emitted from metals or non-metals with more than one layer of foreign atoms deposited on the surface.

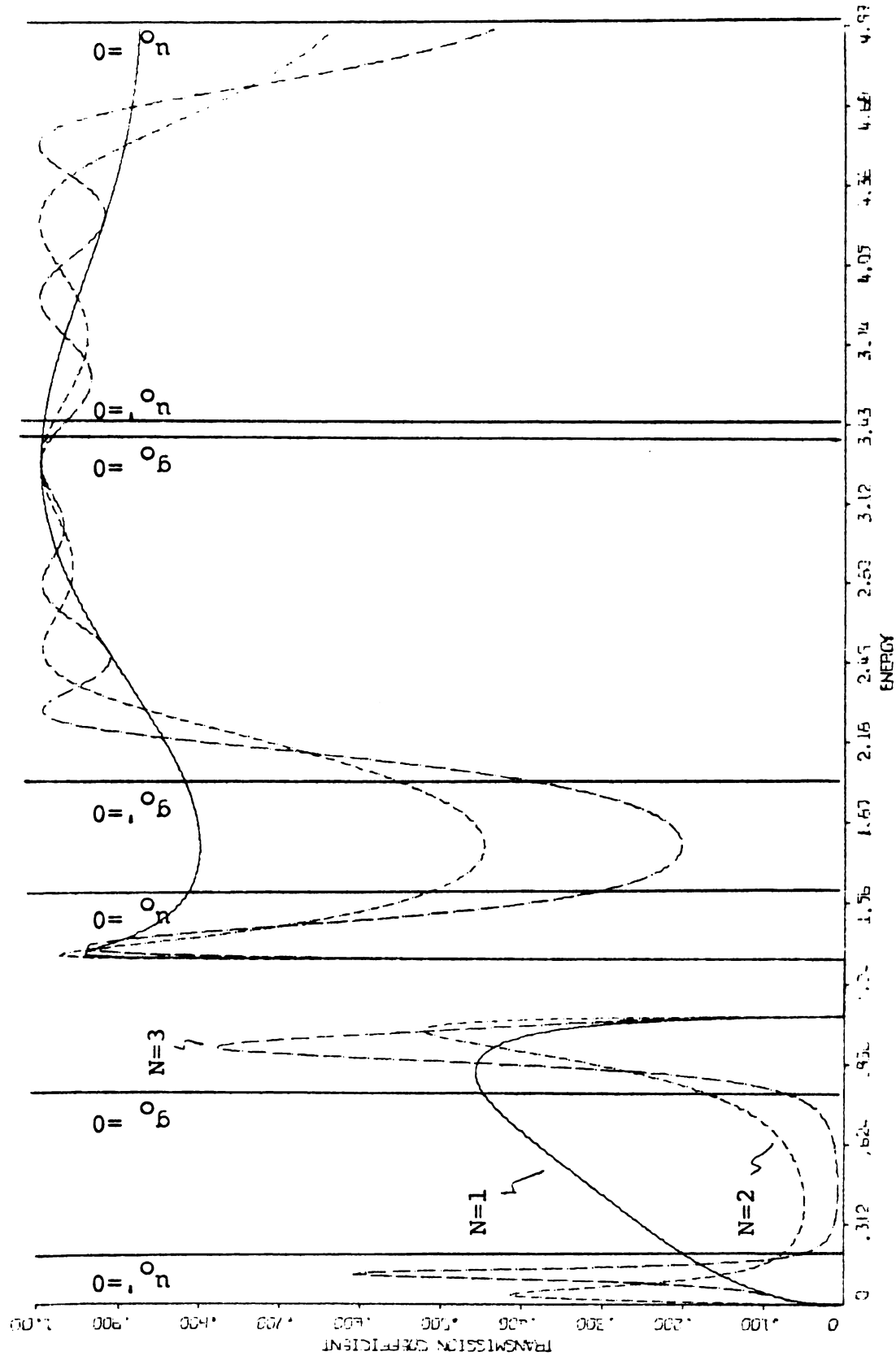

Figure 6.4. Transmission coefficient for 1, 2, 3 adsorbed atoms on a non-metal--Case 1.

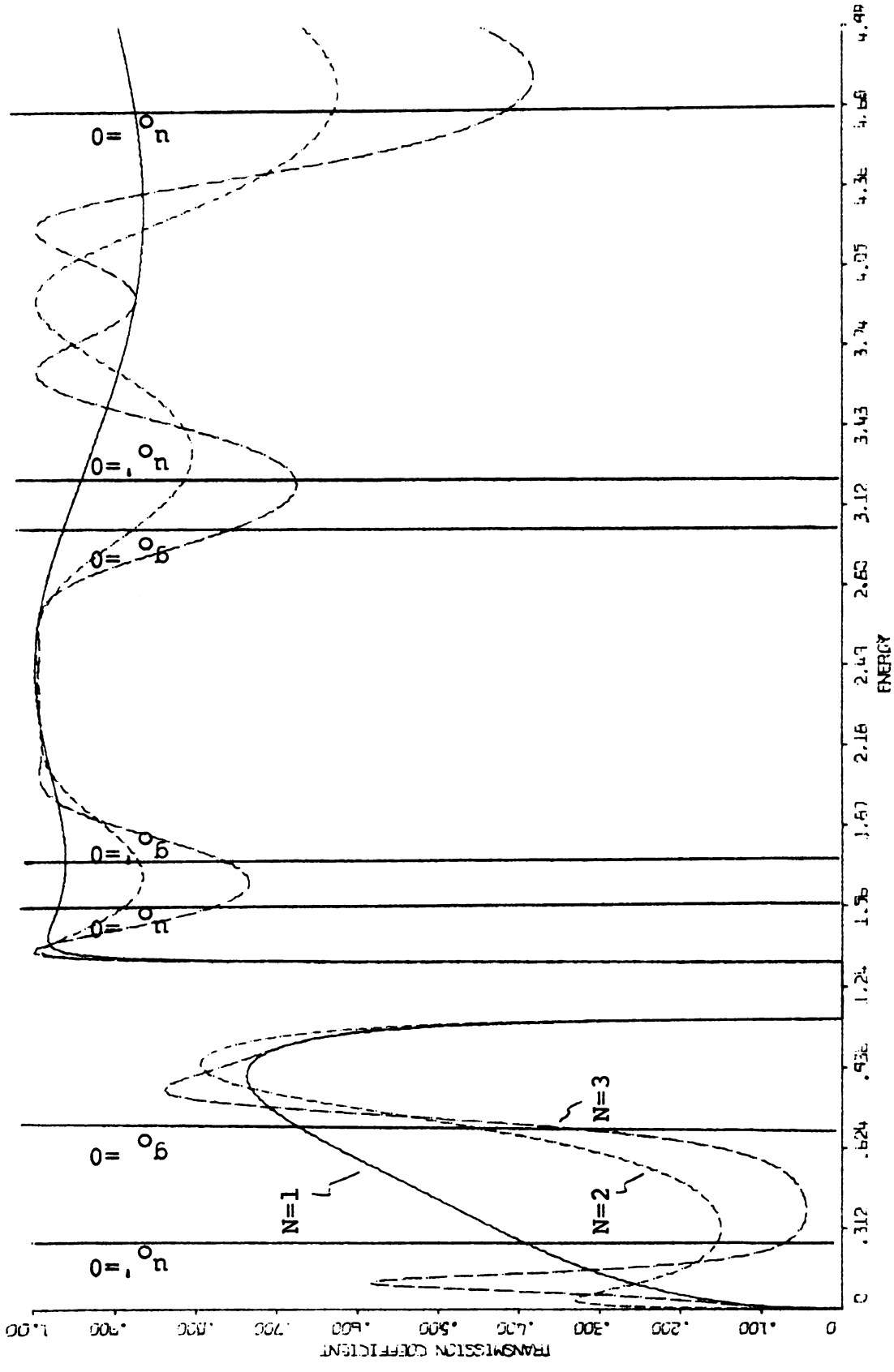

Figure 6.5. Transmission coefficient for 1, 2, 3 adsorbed atoms on a non-metal--Case 2.

SUMMARY

By constructing the total wave function for a one-dimensional potential from individual cell solutions, we have found that such wave functions may assume three forms, depending on whether the parameter ρ (defined in Section I) is less than zero, between zero and one, or greater than one. All three forms are of the Bloch-function type; there is no restriction as to the form or magnitude of the periodic potential. Via the parameter ρ, a band structure may be associated with a single period of the periodic potential. By applying Tamm and Shockley type potential terminations at either end of the periodic potential, we have found that the emergence of surface states is dependent on whether the parameter $-(u_0'/u_0)|\rho|^{\frac{1}{2}}$ (defined in Section I ; it corresponds to an effective wave number) goes negative in an attenuation region. The number of surface states in an attenuation region was found to depend on the number of cells in the periodic potential considered and the width of the attenuation band. Using a Kronig-Penney type periodic potential as an illustration, we have seen quite graphically the effects which the two different types of potential terminations have on the energy states and the

dependence of these states on the parameters which specify the potential. For potentials terminated at an arbitrary point in the end cell, we have found the emergence of a new type of surface state which is not found for terminations which are symmetric. The band structure above the vacuum level was investigated by considering the reflection of free electrons from a finite periodic potential with the Tamm and Shockley type terminations. It was found that the presence of surface states for energies below the vacuum level may be inferred from the structure of the curves giving the reflection coefficient versus electron energy. For the emission of electrons from crystals with from one to a few layers of adsorbed atoms on the surface, resonance transmission effects were found to be significant only for the case of more than one layer of adsorbed atoms.

BIBLIOGRAPHY

BIBLIOGRAPHY

1. I. Tamm, Phys. Z. Sowjet. 1, 733 (1932); Z. Phys. 76, 849 (1932).
2. W. Shockley, Phys. Rev. 56, 317 (1939).
3. S. G. Davison and J. D. Levine, to appear in Solid State Physics (Academic Press, New York, Vol. 21, 1968) ed. by F. Seitz, D. Turnbull and H. Ehrenreich.
4. E. T. Goodwin, Proc. Cam. Phil. Soc. 35, 205, 221, 232 (1939).
5. M. Born and J. R. Oppenheimer, Ann. Physik 84, 457 (1927).
6. H. M. James, Phys. Rev. 76, 1602 (1949).
7. Ibid.
8. All definitions of James have been changed by a sign (i.e. our α_+ corresponds to his σ_-, our γ_+ corresponds to his γ_-, etc.).
9. D. S. Boudreux and V. Heine, Surf. Sci. 8, 426 (1967).
10. W. Shockley, op. cit.
11. I. Tamm, op. cit.
12. R. L. Kronig and W. G. Penney, Proc. Roy. Soc. A130, 499 (1931).
13. Ibid.
14. A. W. Maue, Z. Physik 94, 717 (1935).
15. H. Statz, Z. Naturforschg. 5a, 534 (1950).
16. J. Koutecky, J. Phys. Chem. Solids 14, 233 (1960).
17. G. Allen, Phys. Rev. 91, 531 (1953).
18. Ibid.
19. B. A. Lippmann, Ann. Phys. 2, 16 (1957).
20. F. Herman, Rev. Mod. Phys. 30, 102 (1958).
21. T. O. Woodruff, Phys. Rev. 103, 1159 (1956).

22. S. G. Davison and J. D. Levine, op. cit.
23. E. Antoncik, J. Phys. Chem. Solids 21, 137 (1961).
24. V. Heine, Surf. Sci. 2, 1 (1964).
25. Ibid.
26. W. Shockley, op. cit.
27. J. D. Levine, Phys. Rev. 171, 701 (1968).
28. Ibid.
29. C. B. Duke and C. W. Tucker, Jr., Surf. Sci. 15, 231 (1969).
30. E. G. McRae, J. Chem. Phys. 45, 3258 (1969); Surf. Sci. 8, 14 (1967).
31. K. Hirabayashi and Y. Takeishi, Surf. Sci. 4, 150 (1966).
32. F. Hofmann and H. P. Smith,Jr., Phys. Rev. Letters 19, 1492 (1967).
33. P. M. Marcus and D. W. Jepsen, Phys. Rev. Letters 20, 925 (1967).
34. J. S. Plaskett, Proc. Roy. Soc. (London) A301, 363 (1967).
35. R. M. Stern, H. Traub and A. Gervais, J. Vacuum Sci. Tech. 5, 182 (1968).
36. R. M. Stern, J. J. Perry and D. S. Boudreux, Phys. Rev. 41, 275 (1969).
37. see, for example, J. M. Ziman, Principles of the Theory of Solids (Cambridge University Press, 1965), p. 25.
38. C. B. Duke and M. E. Alferieff, J. Chem. Phys. 46, 923 (1967).
39. E. W. Plummer, J. W. Gadzuk and R. D. Young, Solid State Commun. 7, 487 (1969).
40. J. W. Gadzuk, Phys. Rev. 182, 416 (1969).
41. R. Gomer and L. W. Swanson, J. Chem. Phys. 38, 1613 (1963).

42. L. D. Schmidt and R. Gomer, J. Chem. Phys. 45, 1605 (1966).
43. A. J. Bennett and L. M. Falicov, Phys. Rev. 151, 512 (1966).
44. J. W. Gadzuk, Surf. Sci. 6, 133 (1967).
45. H. D. Hagstrum, Phys. Rev. 150, 495 (1966).
46. J. W. Gadzuk, Surf. Sci. 18, 193 (1969).
47. Ibid.
48. E. O. Kane, in Tunneling Phenomena in Solids, ed. by E. Burstein and S. Lundquist (Plenum Press, New York, 1969) pp. 1-12.
49. C. B. Duke and M. E. Alferieff, op. cit.
50. see reference 46.